

**Functional and Structural Analysis of the  
*Yersinia enterocolitica* Type III Secretion  
Translocon**

**Inauguraldissertation**

zur

Erlangung der Würde eines Doktors der Philosophie

vorgelegt der

Philosophisch-Naturwissenschaftlichen Fakultät

Der Universität Basel

von

**Petr Broz**

aus

Rheinfelden, Schweiz

Basel, 2006

Genehmigt von der Philosophisch-Naturwissenschaftlichen Fakultät auf  
Antrag von

- Prof. Dr. Guy Cornelis
- Prof. Dr. Urs Jenal
- Prof. Dr. Andreas Engel

Basel, den 19.9.2006

Prof. Dr. Hans-Jakob Wirz

## Abstract

Many pathogenic bacteria use type III secretion systems (TTSS) to deliver effector proteins into the cytosol of target cells to subvert host cell functions. The actual secretion apparatus, called injectisome, consist of a basal body embedded in the bacterial membranes and a needle. The needle is thought to serve as a conduit for protein secretion. However, to cross the target cell membrane an additional translocation step is necessary. This translocation involves the formation of a pore in the target cell membrane, which is presumably connected to the needle. Three proteins are required for the assembly of this pore. In *Yersinia*, the three “translocators” are YopB and YopD, two putative membrane proteins, and LcrV a hydrophilic protein. LcrV is also known, since the mid-fifties, to represent the major protective antigen against plague infections. The aim of my thesis was to characterize the structure and function of the translocators.

Infection of erythrocytes with wildtype *Yersiniae* causes hemolysis due to the formation of the translocation pore in the red blood cell membrane. We showed that the isolated membranes of these erythrocytes contain the hydrophobic translocators YopB and YopD, but not LcrV. Bacteria deprived of LcrV did not assemble a functional pore, but were still able to insert reduced amounts of YopB and YopD into the target cell membrane. This is in agreement with reports showing that purified YopB and YopD can oligomerize and insert into artificial membranes independently of LcrV. We showed further that polyclonal antibodies directed against LcrV interfere with the formation of a functional translocation pore by live bacteria. Based on these results, we hypothesized that LcrV acts as a platform or scaffold onto which the YopBD translocation pore assembles (Goure, Broz et al. 2005, **Journal of Infectious Diseases** 192:218-25).

We purified needles and detected LcrV as well as YscF, the needle subunit, in these preparations. In parallel we analyzed these purified needles by STEM (scanning transmission electron microscopy) and found that the needle ends with a defined tip complex, that comprises a head, a neck and a base. We then showed that the tip complex is missing in *lcrV* mutant bacteria and can be restored after the mutation is complemented in *trans*. These results indicated that LcrV is involved in the formation of the tip complex. In addition, crosslinking of purified needles indicated that LcrV and YscF interact and thus the V-antigen might form the tip complex. Immunolabelling of wildtype needles with anti-LcrV antibodies showed a strong binding to the tip complex, anti-YscF antibodies bound to the bottom of the needle. Together these results demonstrate that LcrV forms the observed tip complex and explain why anti-LcrV antibodies can inhibit pore formation. In addition, these data reinforce the assembly platform hypothesis (Mueller, Broz et al. 2005, **Science** 310: 674-676).

*P. aeruginosa* and *A. salmonicida* possess an injectisome closely related to that of *Yersinia*. Their respective LcrV orthologs, PcrV (32.3 kDa) and AcrV (40.2 kDa) are slightly different in size to LcrV (37.6 kDa). We demonstrated that PcrV as well as AcrV can functionally complement a *lcrV* deletion in *Y. enterocolitica*. The needles exhibited distinct tip complexes similar to those of wildtype needles but they were smaller in the case of PcrV and larger with AcrV (Mueller, Broz et al. 2005, **Science** 310: 674-676). Hybrids between the three proteins LcrV, PcrV and AcrV could complement an *lcrV* deletion in *Y. enterocolitica* in the hemolysis assay, but the level of complementation varied. The amino-terminus seemed to play an important role in the function of the protein. STEM analysis of tip complexes formed by different hybrid proteins allowed us to show that the aminoterminal domain of LcrV forms the base while the second globular domain forms the head of the tip complex. In addition we determined the stoichiometry of YscF and LcrV in purified needles and found that between three to six molecules of LcrV form the tip complex. Together, these results allowed us to propose an atomic modeling of the LcrV tip complex on top of the injectisome needle.

# Table of contents

<b>1 Introduction.....</b>	<b>2</b>
1.1 Type III secretion systems .....	3
1.2 The concept of translocation.....	6
1.3 The triplet of translocators .....	6
1.4 The role of the translocators during infection .....	9
1.5 Evidence for a pore formed by the translocators.....	10
1.6 Structure of the translocation pore .....	11
1.7 The role of the needle in the translocation process .....	14
1.8 How is the injectisome coupled to the translocation pore?.....	15
<b>Accessory .....</b>	<b>18</b>
1.9 The chaperone of the hydrophobic translocators.....	18
1.9.1 Role as chaperone .....	18
1.9.2 Role in regulation .....	20
1.10 The LcrG-LcrV complex regulates the secretion of effector Yops.....	22
1.11 Requirements on the membrane side .....	25
1.12 Other needle extensions .....	27
1.13 Double function as translocator and effector .....	31
<b>2 Aim of the thesis.....</b>	<b>32</b>
<b>3 Results.....</b>	<b>34</b>
3.1 The Needle Length of Bacterial Injectisomes is Determined by a Molecular Ruler .....	34
3.2 Protective Anti-V Antibodies Inhibit Pseudomonas and Yersinia Translocon Assembly within Host Membranes .....	36
3.3 The V-antigen of Yersinia Forms a Distinct Structure at the Tip of Injectisome Needles .....	38
3.4 Unpublished results .....	41
3.4.1 The orientation of the LcrV molecule in the tip complex .....	42
3.4.2 Production of antibodies directed against PcrV and AcrV .....	53
3.4.3 Determination of the Stoichiometry of needle components.....	54
3.4.4 Estimation of the size of pores made by LcrV and its orthologs .....	56
3.4.5 The translocators YopB and YopD interact with liposomes <i>in vitro</i> .....	58
3.4.6 Purification of the TTS translocation pore using tagged translocators.....	66
<b>4 Discussion.....</b>	<b>71</b>
<b>5 Outlooks .....</b>	<b>81</b>
<b>Appendix .....</b>	<b>83</b>
A List of constructs .....	84
B References .....	86
C Acknowledgments.....	91
D Curriculum vitae .....	92



# 1 Introduction

# 1 Introduction

## 1.1 Type III secretion systems

Interaction of bacterial pathogens or symbionts with host cells is mediated by factors that are located on the bacterial surface or are secreted into the extracellular space. Although these proteins are numerous and diverse, exhibiting a wide variety of functions that include proteolysis, hemolysis, cytotoxicity, protein phosphorylation and dephosphorylation, only a few pathways exist by which these proteins are transported from the bacterial cytoplasm to the extracellular space. Such secretion systems are classified into four major types: I-IV.

Type III secretion, the subject of this work, is probably the most sophisticated export apparatus described so far and is found in many gram-negative bacteria, pathogenic for animals and plants, as well as in endosymbionts. The discovery of type III secretion (TTS) was made in the early 1990s, when a few groups, studying *Yersinia*, were trying to understand the mysterious phenomenon of Calcium-dependency: When incubated at 37°C in the absence of Ca<sup>2+</sup>-ions, *Yersinia* bacteria stop growing and start to release large amounts of proteins, called Yops, into the culture medium (Michiels *et al.*, 1990). Amino-terminal sequence analysis revealed that these Yop proteins must be secreted in a *sec*-independent manner and hence by a new pathway.

This release, generally referred to as Yop secretion, is rather a massive leakage resulting from an artificial opening of an otherwise tightly controlled secretion apparatus. Despite the fact that this leakage is presumably artefactual, this observation turned out to be of great importance because it allowed to carry out genetic analysis that lead to the identification of more than 25 genes involved in the process of Yop secretion. These genes, encoded together with the *yop* genes on the 70 kb *Yersinia* virulence plasmid (pYV), were called *ysc* for Yop secretion (**Fig. 1**). Interestingly most of the inner membrane Ysc proteins are homologous to components of the flagellar biosynthesis apparatus, suggesting a common evolutionary origin with the flagellum. These similarities prompted the research groups led by J. Galan and S.I. Aizawa to apply extraction and visualization techniques of the flagellum basal body to the *Salmonella enterica* serovar Typhimurium TTS system, which allowed them to visualize the secretion apparatus (**Fig. 2A**, Kubori *et al.*, 1998). This structure, called needle-complex (NC) or injectisome, is composed of a needle like portion that projects outward from the surface of the bacterial cell and a cylindrical basal body that anchors the structure to the inner and outer membranes. Since then electron micrographs of NCs from *Shigella flexneri* and enteropathogenic *Escherichia coli* (EPEC) have been produced (**Fig. 2B-D**; Blocker *et al.*, 1999; Sekiya *et al.*, 2001; Tamano *et al.*, 2000; Kimbrough and Miller, 2000; Daniell *et al.*, 2001; Blocker *et al.*, 2001; Ogino *et al.*, 2006; Morita-Ishihara *et al.*, 2006).

Lately a model of the NC from *S. Typhimurium* has been presented at a resolution of 1.7 nm (Fig. 2F; Marlovits *et al.*, 2004).

Little is known about the actual mechanism of export, but the structure of the injectisome implies that it serves as a hollow conduit across both bacterial membranes for the exported proteins.

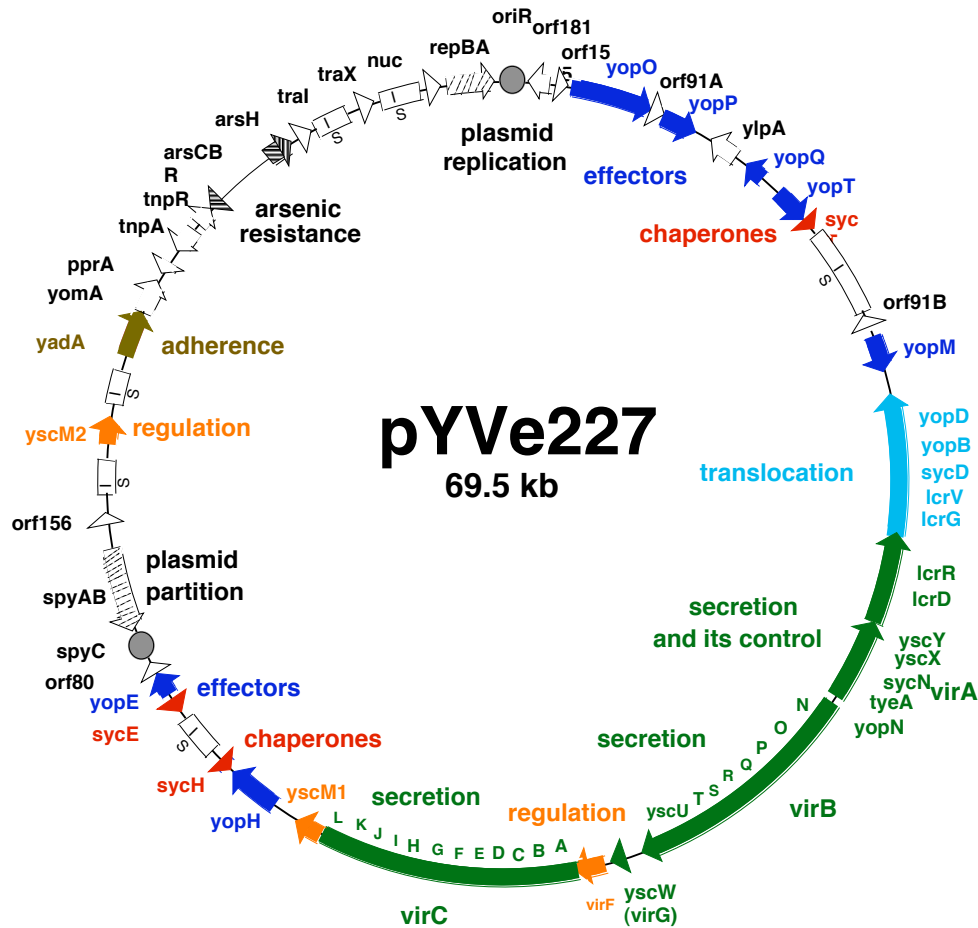


**Fig. 1. The *Y. enterocolitica* pYV plasmid.** Taken from "The 70-Kilobase Virulence Plasmid of *Yersinia*", Iriarte M. and Guy R. Cornelis, in "Pathogenicity Islands and Other Mobile Virulence Elements", ASM press 1999.

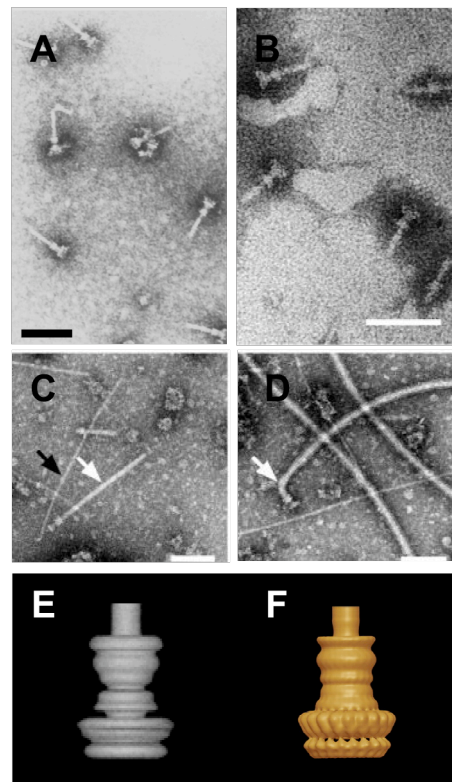


**Fig. 2. Electron micrographs of the flagellum and the needle complexes from different bacteria.** (A) Purified needle complexes from *S. Typhimurium* (Kubori *et al.*, 1998). (B) Purified needle complexes from *S. flexneri* (Tamano *et al.*, 2000). (C) Purified needle complexes from EPEC (Sekiya *et al.*, 2001). (D) Isolated flagella from EPEC (Sekiya *et al.*, 2001). (E) Surface rendering of the needle complex from *S. flexneri* assuming cylindrical symmetry (Blocker *et al.*, 2001) (F) Surface rendering of the needle complex from *S. Typhimurium* (Marlovits *et al.*, 2004). Scale bar represent 100 nm in (A, B, D) and 50 nm in (C).

## 1.2 The concept of translocation

The actual destination of effector proteins secreted by type III secretion systems is not the extracellular medium but the cytosol of eukaryotic cells, where they affect signaling or control pathways. Surprisingly the secreted Yop proteins have no cytotoxic effects on cultured cells, although live *Yersiniae* have such an activity. Cytotoxicity was found to depend on the capacity of the bacterium to secrete both YopE and YopD (Rosqvist *et al.*, 1991). Moreover YopE alone was shown to be cytotoxic when microinjected into the cells. This suggested that YopD somehow helps the injection of the cytotoxin YopE into the target cell. In 1994, this hypothesis was demonstrated by two different methods, immunofluorescence and a reporter enzyme based strategy (Rosqvist *et al.*, 1994; Sory and Cornelis, 1994) that allowed the detection of Yop-proteins in target cells. Thus, extracellular *Yersinia* bacteria do not only secrete YopE, but they also inject YopE into the cytosol of eukaryotic cells by a mechanism that involves at least one other protein, YopD. Later, YopB was shown to be required for the delivery of YopE and YopH (Boland *et al.*, 1996; Hakansson *et al.*, 1996). Finally, LcrV was shown to be also involved (Fields *et al.*, 1999; Marenne *et al.*, 2003; Pettersson *et al.*, 1999).

These observations and others lead to the present concept that the secreted Yop proteins consist of two groups, a collection of intracellular effectors and proteins that are required for the translocation of these effectors across the plasma membrane of the target cells. This general principle: secretion machinery, “effectors” and “translocators” (**Fig. 1**), applies to all type III secretion systems studied so far. While the secretion machinery is more or less conserved, the effectors vary considerably, depending on the particular needs of the bacteria. Among the animal pathogens, type III secretion systems have been most intensely studied in *Yersinia* spp., *Shigella* spp., *Salmonella* spp., *Pseudomonas aeruginosa*, EPEC and enterohemorrhagic *E. coli*. The best-studied system of a plant pathogen is the one of *Pseudomonas syringae* (for a review see, Mota *et al.*, 2005b).

## 1.3 The triplet of translocators

As the concept of type III secretion evolved and more proteins were studied, it became evident that the group of the translocators generally consists of three proteins (YopB, YopD and LcrV in *Yersinia*). They have in common that knockout mutants in these proteins completely lose the ability to translocate effector proteins into target cells, while the secretion process itself is not affected (for a review see, Buttner and Bonas, 2002). Another general feature of the three translocators is that two have hydrophobic domains (YopB and YopD) while the third is clearly hydrophilic (LcrV) (**Fig. 3**). This applies to the type III secretion

translocators from *P. aeruginosa* (PopB, PopD and PcrV), *Aeromonas salmonicida* (AopB, AopD and AcrV), *S. flexneri* (IpaB, IpaC and IpaD), *S. Typhimurium* SPI-1 (SipB, SipC and SipD), EPEC (EspB, EspD and EspA) and *S. Typhimurium* SPI-2 (SseD, SseC and SseB). In several systems, the three translocators were reported to interact with each other (Chiu and Syu, 2005; Menard *et al.*, 1994; Sarker *et al.*, 1998a; Schoehn *et al.*, 2003; Tucker and Galan, 2000) and most translocators even contain coiled-coil domains, known to be involved in protein-protein interactions (**Fig. 3**).

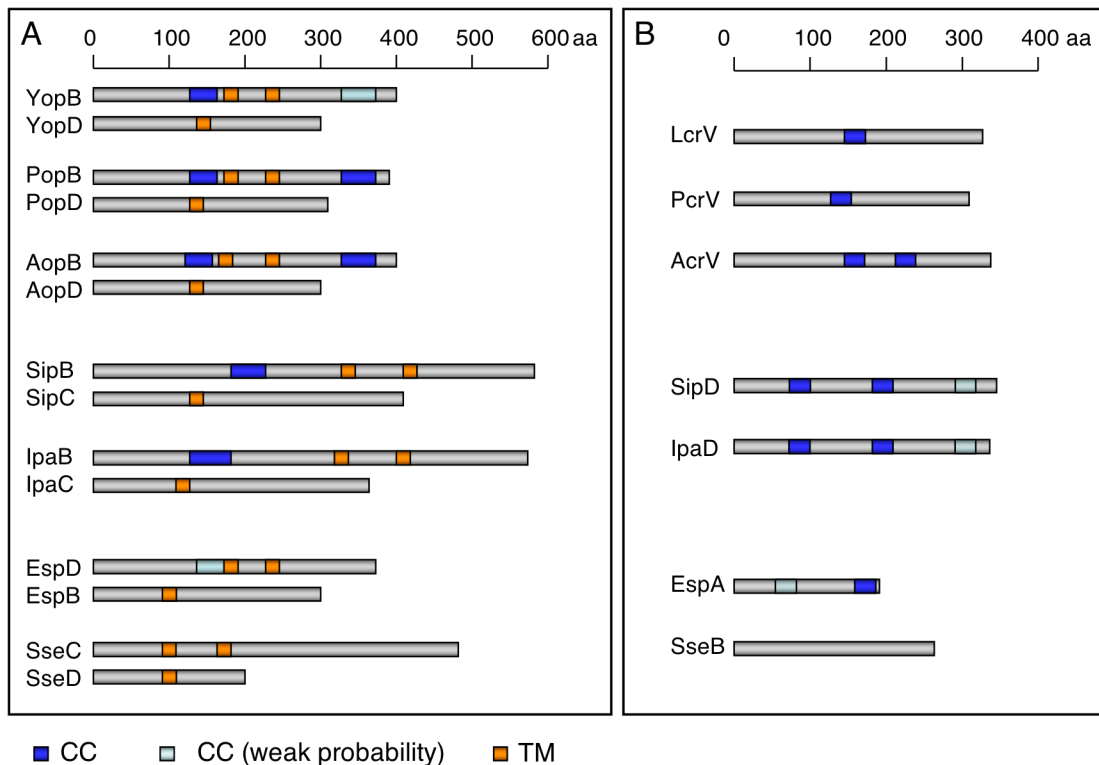


**Fig. 3. Structural organization of the three type III secretion translocators found in different pathogenic bacteria.** Schematic representation of putative transmembrane (TM) regions and coiled-coil (CC) regions in the hydrophobic translocators (**A**) and the hydrophilic translocators (**B**). TM regions were predicted with the TM-PRED program ([http://www.ch.embnet.org/software/TMPRED\\_form.html](http://www.ch.embnet.org/software/TMPRED_form.html); 17-33 residues, scores >1000). CC regions were predicted with the MULTICOIL program (<http://multicoil.lcs.mit.edu/cgi-bin/multicoil>; probabilities >80%) or the COILS program ([http://www.ch.embnet.org/software/COILS\\_form.html](http://www.ch.embnet.org/software/COILS_form.html)).

In all type III secretion systems studied so far the three translocators were found to be encoded together in one large operon (**Fig. 4**). In addition to the translocators, this operon contains genes coding for proteins involved in the regulation of type III secretion and for small proteins that serve as chaperones for the hydrophobic translocators (see chapters 1.9 and 1.10)

The similarities between the translocators are not restricted to their function and genetic localization, but also extend to their sequence (Buttner and Bonas, 2002). The most closely

related homologs of YopB/YopD are PopB/PopD of *P. aeruginosa* and AopB/AopD of *A. salmonicida*. The homology goes so far that *popB/popD* can complement a mutation of the *yopB/yopD* genes in *Yersinia* when expressed from its native operon (Broms *et al.*, 2003; Frithz-Lindsten *et al.*, 1998). IpaB/IpaC from *Shigella* and SipB/SipC from *Salmonella* SPI-1 also share homologies to YopB/YopB, especially in the hydrophobic domains (Hakansson *et al.*, 1993).

The hydrophilic translocators seem to be more diverse. The only sequence homologs of LcrV are PcrV of *P. aeruginosa* and AcrV of *A. salmonicida*. These proteins are so closely related that PcrV and AcrV complement a *Yersinia lcrV* mutation (Holmstrom *et al.*, 2001; Mueller, Broz *et al.*, 2005). Others, like IpaD, SipD, EspA and SseB, exhibit only low sequence homology to LcrV and should be rather considered as functional homologs.

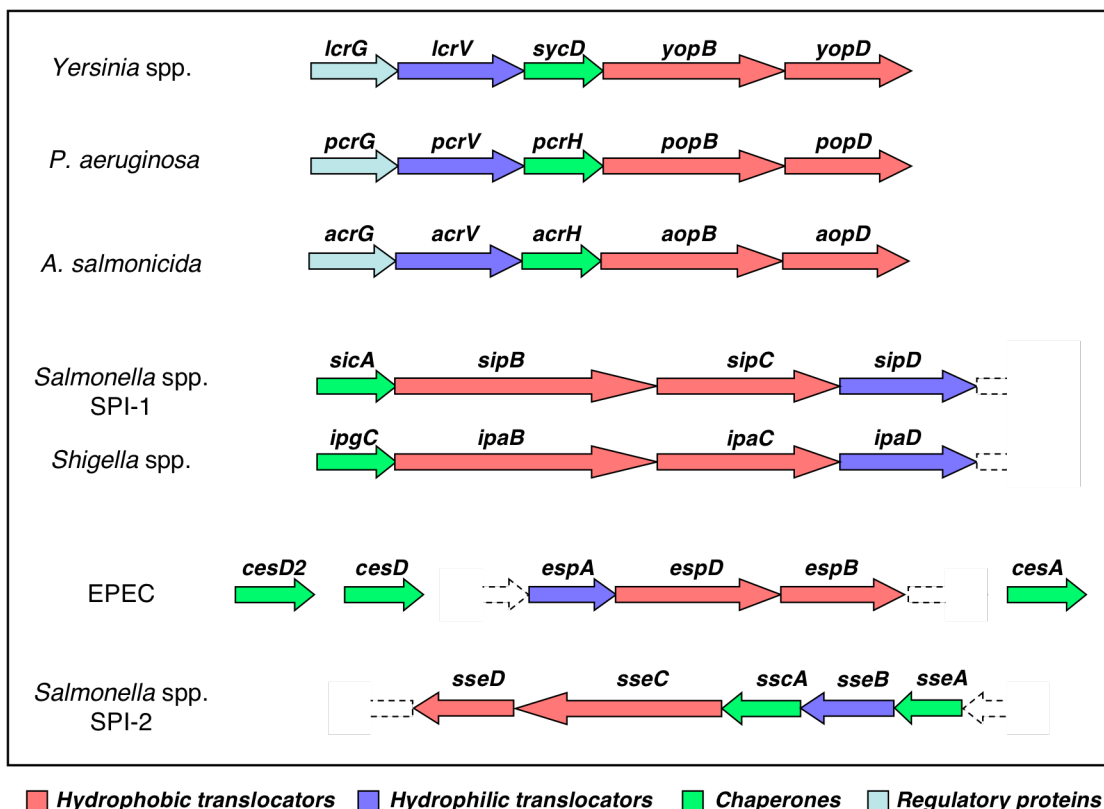


Fig. 4. Organization of the translocator operons from different TTS systems.

## 1.4 The role of the translocators during infection

As mentioned above two of the translocators have hydrophobic domains. It was hypothesized that they could act as some kind of transmembrane proteins (Hakansson *et al.*, 1993). Early reports mentioned that YopB has a membrane disturbing activity (Hakansson *et al.*, 1996) suggesting that the translocators may destabilize the membranes and thus allow translocation. Consistent with this YopB/YopD, PopB/PopD, IpaB/IpaC and EspB/EspD were found to be inserted in the membranes of erythrocytes after infection (Blocker *et al.*, 1999; Goure *et al.*, 2004; Goure, Broz *et al.*, 2005; Ide *et al.*, 2001). In addition YopB and YopD were reported to bind to artificial liposomes that were incubated with secreting *Yersinia* spp. (Tardy *et al.*, 1999). Several *in vitro* studies were done with purified translocators to analyze their properties. It was shown that purified IpaB and SipB are able to bind membranes, lead to release of Calcein from liposomes and have membrane fusion activity (De Geyter *et al.*, 2000; Hayward *et al.*, 2000; Hume *et al.*, 2003). Other translocators, PopB/PopD and YopB/YopD, were also shown to bind to liposomes and insert into liposome membranes *in vitro* (Faudry *et al.*, 2006; Schoehn *et al.*, 2003), P. Broz unpublished data). On the basis of these results it was hypothesized that the hydrophobic translocators form the transmembrane part of the type III secretion translocon.

To understand the role of the hydrophilic translocator was more difficult. The best-studied example is LcrV. This protein was described already in the nineteen fifties as a soluble antigen involved in the virulence of *Yersinia* spp. (hence named V antigen) long before the concept of type III secretion was shaped (Burrows, 1956). Early studies reported that it was a protective antigen against plague infections (Lawton *et al.*, 1963) and antibodies directed against LcrV protect cultured cells from *Yersinia* infections (Pettersson *et al.*, 1999). In 1999 it was shown by immunogold electron microscopy that LcrV is exposed on the surface of *Yersinia* spp. before contact to target cells (Pettersson *et al.*, 1999). Its functional counterparts IpaD and SipD are probably surface exposed as well (Turbyfill *et al.*, 1998), but this was not formally demonstrated so far. These results suggested that the hydrophilic translocator is part of a structure that is preassembled on the bacterial surface.



## 1.5 Evidence for a pore formed by the translocators

A feature, observed for most bacteria employing type III secretion systems is a contact-dependent lytic activity on red blood cells. Erythrocyte lysis was reported for *Yersinia spp.*, *P. aeruginosa*, *S. flexneri*, *Salmonella spp.* and EPEC and was dependent on the presence of the translocators (Blocker *et al.*, 1999; Dacheux *et al.*, 2001; Hakansson *et al.*, 1996; Holmstrom *et al.*, 2001; Ide *et al.*, 2001; Miki *et al.*, 2004; Neyt and Cornelis, 1999a; Shaw *et al.*, 2001). This suggests that the translocation apparatus involves some kind of a pore in the eukaryotic cell membrane by which the effectors are injected into the target cell. For *Yersinia*, the hemolytic activity is higher when the effectors are deleted suggesting that the pore is normally filled with trafficking effectors (Hakansson *et al.*, 1996). Osmoprotection experiments allowed the estimation of the size of this translocation pore, which is around 2-3 nm in diameter (**Table 1**; Blocker *et al.*, 1999; Dacheux *et al.*, 2001; Holmstrom *et al.*, 2001; Ide *et al.*, 2001; Miki *et al.*, 2004; Shaw *et al.*, 2001). The idea of a translocation pore is further supported by the observation that the membrane of macrophage-like cells infected with an effector polymutant *Y. enterocolitica* becomes permeable to small dyes (Neyt and Cornelis, 1999a). If the macrophages are preloaded with a low-molecular-weight fluorescent marker, they release the marker but no cytosolic proteins, indicating that there is no membrane lysis but rather the insertion of a small pore into the macrophage plasma membrane (Neyt and Cornelis, 1999a). Finally the hypothesis of a channel was reinforced by the observation that artificial liposomes that have been incubated with *Yersinia spp.* contained channels, detectable by electrophysiology (Tardy *et al.*, 1999).

The formation of the translocation pore and the translocation of effector proteins are in all cases dependent on the presence of the three translocators. This suggests that the translocators form a pore in the target cell membrane. But, it could not be formally proved so far that the two events, translocation of effectors and formation of a channel, are linked.

Pathogen	Pore size	System	Method	Reference
<i>Yersinia</i>	1.2-3.5 nm	erythrocytes	osmoprotection	(Hakansson <i>et al.</i> , 1996)
	2.2-3.5 nm	erythrocytes	osmoprotection	(Holmstrom <i>et al.</i> , 2001)
	2.4-3.2 nm	erythrocytes	osmoprotection	P.Broz, unpublished data
	1.6-2.3 nm	macrophages	dye release	(Neyt and Cornelis, 1999a)
<i>P. aeruginosa</i>	2.8-3.5 nm	erythrocytes	osmoprotection	(Dacheux <i>et al.</i> , 2001)
<i>S. flexneri</i>	~2.5 nm	erythrocytes	osmoprotection	(Blocker <i>et al.</i> , 1999)
<i>S. Typhimurium</i> SPI-1	~3.5 nm	erythrocytes	osmoprotection	(Miki <i>et al.</i> , 2004)
EPEC	2.2-5 nm	erythrocytes	osmoprotection	(Ide <i>et al.</i> , 2001)
	2-3.2 nm	erythrocytes	osmoprotection	(Shaw <i>et al.</i> , 2001)

**Table 1.** Estimated sizes of the translocation pore from different type III secretion systems

## 1.6 Structure of the translocation pore

As mentioned above it was hypothesized that the three translocators constitute a pore that mediates translocation. In agreement with their hydrophobic nature, two of the translocators would form the transmembrane part of the pore. How the third, hydrophilic translocator is involved, remained unclear. It was proposed that it could form the core of a membrane channel, stabilized by YopB and YopD (Holmstrom *et al.*, 2001).

The first study trying to visualize the translocation pore and analyze its components was published in 2001 (Ide *et al.*, 2001). The authors incubated erythrocytes with concentrated culture supernatant from wildtype DA-EPEC bacteria and from a mutant deficient for type III secretion. They examined the membranes of these erythrocytes by negative stain TEM and observed segmented, pore like structures in the sample incubated with SN from wildtype bacteria (**Fig. 5**). These big rings had an outer diameter of 55-65 nm and rose up to 20 nm from the membrane plane. The inner diameter was estimated to be at least 8 nm, which is considerably bigger than the diameter of the translocation pore determined by osmoprotection. In addition, the authors demonstrated that EspD and EspB are associated to the membranes of the erythrocytes after incubation with SN from wildtype bacteria. They concluded that the observed structures might be the type III secretion translocon of EPEC, formed by EspD and EspB. The major drawback of this study was that it could not be shown that the observed rings are composed of the translocators EspD and EspB. Furthermore the inner diameter of the observed rings was far too big to be the translocation pore and the overall dimensions of these rings suggest that the authors had rather purified some porin-like structures.

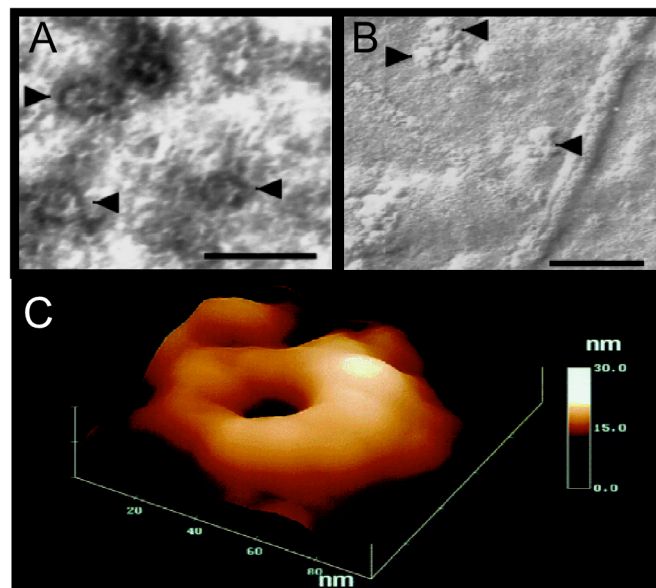


**Fig. 5. Electron micrographs of red blood cell membranes incubated with concentrated supernatant from wildtype EPEC bacteria (Ide *et al.*, 2001).** Transmission electron micrographs (A) and etched replicas (B) viewed by electron microscopy. Ring-like structures are indicated (black arrowheads). Scale bar is 100 nm in (A) and 200 nm in (B). Three-dimensional image of a representative single pore-like structure (C) after Atomic Force Microscopy (AFM) analysis.

The next study, using an *in vitro* approach to analyze the structure of the translocon, was published two years later (Schoehn *et al.*, 2003). The authors expressed and purified the translocators PopB and PopD of *P. aeruginosa* together with their native chaperone PcrH. They found that at acidic pH the translocators could bind and disrupt artificial liposomes. Electron microscopy revealed ring-like structure on and next to these liposomes with an internal diameter of 4 nm and an external diameter of 8 nm (Fig. 6). What was puzzling was the observation that the incubation with PopB alone, PopD alone and an equimolar mix of PopB and PopD lead to the formation of comparable ring-like structures. The authors concluded that upon secretion the translocators PopB and PopD oligomerise, form ring-like structures and insert into the target cell membranes (Fig. 7). Even though the approach was new and ingenious, this study was incomplete and opened more new questions than it could answer. First, it was reported that purified PcrV had no influence on the ring-formation, even though PcrV is absolutely required for pore formation *in vivo*. Second, PopB alone, PopD alone and a mix of both formed similar ring-like structures. Third, the authors did not show that the rings represented functional pores. And finally, there is no evidence that the translocation pores formed by bacteria *in vivo* are the same as those formed by the translocators *in vitro*.

A recent follow-up paper from the same group (Faudry *et al.*, 2006) showed that liposomes incubated with purified PopB and PopD are permeabilized due to the formation of

pores. These pores were estimated to have a rather wide range of diameter from 3.4 to 6.1 nm, which is in contrast to native pores formed by *P. aeruginosa* that have a defined size from 2.8-3.4 nm (Dacheux *et al.*, 2001). This suggests that the pores formed *in vitro* are a heterogeneous mix of pore-like structures with different diameters as observed for *Yersinia* (*P. Broz*, unpublished data), possibly due to the lack of LcrV/PcrV.

Even though it is by now generally accepted that the hydrophobic translocators form the translocation pore, it could not be convincingly visualized so far. Therefore the structure and composition of the translocation pore remains one of the big mysteries of type III secretion.

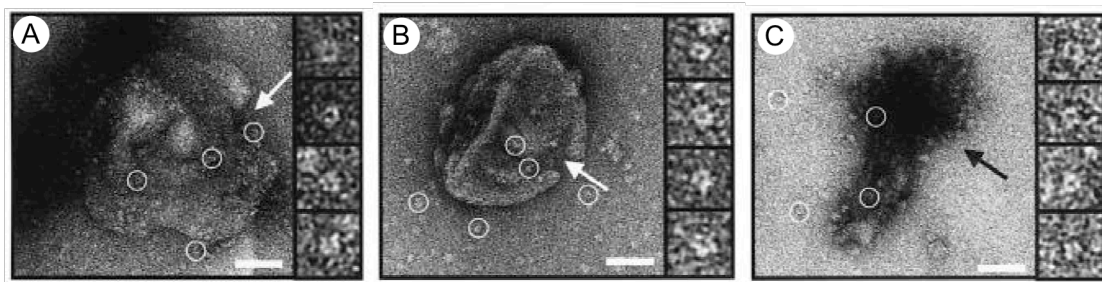


**Fig. 6. Negative staining electron micrographs showing ring-like structures formed by the *P. aeruginosa* translocators upon interaction with liposomes at acidic pH (Schoehn *et al.*, 2003). (A) PopB incubated with liposomes at pH 5.3, stained with uranyl acetate. (B) PopD incubated with liposomes at pH 5.3, stained with uranyl acetate. (C) Equimolar mixture of PopB and PopD incubated with liposomes at pH 5.3, stained with uranyl acetate. Scale bars are 50 nm.**

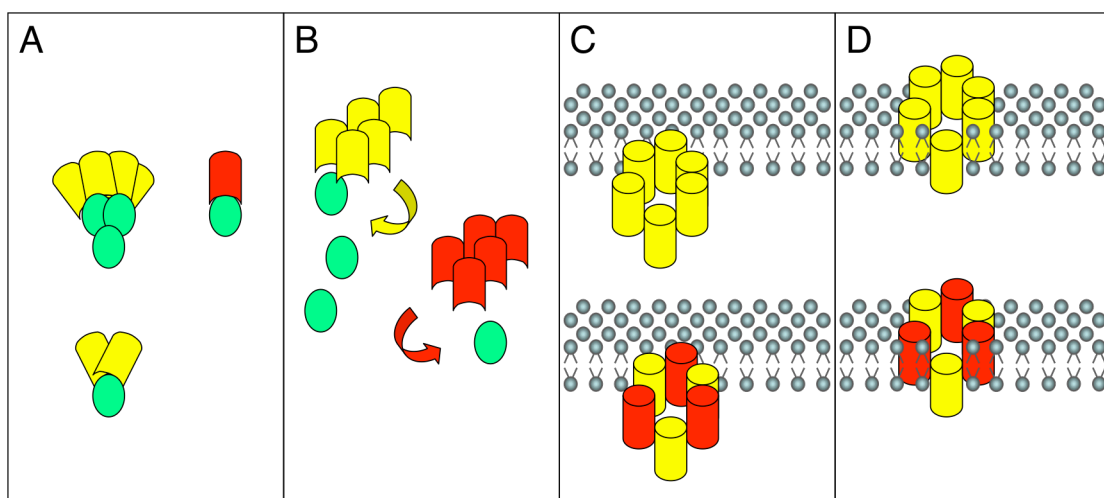


**Fig. 7. Model of translocon formation by PopB and PopD in *P. aeruginosa* (Schoehn *et al.*, 2003). (A) PcrH associates to both PopB and PopD while they remain in the bacterial cytosol preventing aggregation and/or activation. (B) The “*in vivo* switch”, which *in vitro* is mimicked by a decrease in pH leads to the formation of metastable oligomers. (C) PopB and PopD may associate into a homomeric and/or heteromeric ring-like structures that bind to membranes. (D) The rings insert into the membranes.**

## 1.7 The role of the needle in the translocation process

As mentioned above the secretion apparatus consists of a basal body, embedded in the bacterial membranes, topped by a needle-like structure. Electron micrographs of purified needle-complexes show that a central channel of 2-3 nm extends from the bottom set of rings all the way to the tip of the needle. This suggests that the secreted proteins have to travel in a partially unfolded way through this channel and emerge at the tip of the needle. Hoiczky and Blobel proposed that the needle itself, powered by the oligomerization of the needle subunit YscF, would punch a hole in the target cell membrane thus placing its tip inside the host cell and thereby deliver the effector proteins (Hoiczky and Blobel, 2001). Attractive as this model is, it neglected the fact that the translocators are essential for the delivery of the effector proteins. Still one could imagine that the hydrophobic translocators interact with the host cell membrane, destabilize it and hereby allow the needle to pierce into the target cell. The observed “translocation pores” might in fact just be needles that have been broken off, stay inserted in the membranes and thus allow the passage of molecules through a 2-3 nm wide channel.

The *Yersinia* injectisome needle has a remarkably constant length of around 60 nm (+/- 10 %) suggesting that it is genetically controlled. Journet et al. proposed that YscP acts as a molecular ruler, the length of the protein determining the length of the needle (Journet *et al.*, 2003). This opened the question, why it has to be controlled. Structures like the adhesin YadA and/or the LPS, found on the bacterial surface, determine the distance between the bacterium and the target cell, which have to be bridged by the needle. Indeed, it seems that the precise length of the needle has been evolutionary adjusted relative to the dimensions of the adhesin YadA (Mota *et al.*, 2005a) and the LPS (West *et al.*, 2005). If the needle is too short to bridge the distance between the bacterium and the target cell, the effector proteins cannot be translocated.

Surprisingly, when the needle is too short the effectors are not lost in the extracellular space. Rather, they are not exported, meaning that the needle itself acts as a sensor to trigger export (Mota *et al.*, 2005a). This suggests that the secretion and translocation of effectors is only triggered when the needle is long enough to reach the target cell membrane and the translocation pore is assembled. Furthermore it can be assumed that the pore is somehow connected to the needle, as no leakage of effectors can be observed during the infection.

## 1.8 How is the injectisome coupled to the translocation pore?

One central question is how the pore, presumably consisting of the hydrophobic translocators, is connected to the needle of the injectisome. First clues to answer this question were provided, when the membranes of erythrocytes, infected with *Yersinia*, were analyzed. Wild type bacteria (*lcrV*<sup>+</sup>) formed functional pores and inserted YopB and YopD, but no LcrV into the erythrocyte membranes. On the other hand,  $\Delta$ *lcrV* bacteria did not form pores, but still inserted YopB and YopD into the erythrocyte membranes. This suggested that LcrV mediates the assembly of the YopB/YopD translocation pore (Goure, Broz *et al.*, 2005). In addition, protective antibodies directed against LcrV inhibited pore formation in infected erythrocytes, but not the insertion of the hydrophobic translocators YopB and YopD into the erythrocyte membranes (Goure, Broz *et al.*, 2005). Similar observations were made with the LcrV orthologs, IpaD from *S. flexneri* (Picking *et al.*, 2005) and PcrV from *P. aeruginosa* (Goure *et al.*, 2004). These data support a model in which the hydrophilic translocator, acting as an extracellular chaperone or assembly scaffold, helps the hydrophobic translocators to integrate into the eukaryotic cell membrane and to form a functional pore (Goure, Broz *et al.*, 2005). Protective antibodies inhibit the translocation by blocking the function of LcrV and thus prevent the assembly of the translocation pore.

According to this model, the obvious localization of LcrV would be at the tip of the injectisome needle, where the secreted proteins are thought to exit the secretion machinery. This prompted Mueller, Broz and coworkers to closely analyze the needles of *Y. enterocolitica* (Mueller, Broz *et al.*, 2005). They reported a novel structure, called the tip complex, at the distal end of wildtype needles (**Fig. 8**). Needles of *lcrV* mutant bacteria lacked this tip structure and it was restored when the mutation was complemented in *trans*. When the mutation was complemented with the LcrV orthologs, PcrV from *P. aeruginosa* or AcrV from *A. salmonicida*, the tip complex was brought back, resembling that formed by LcrV. As a final proof that the tip complex is composed of LcrV the authors showed that anti-LcrV antibodies bound specifically to the tip complex. This led to the present model, in which the LcrV tip complex, localized at the tip of the needle, assists the assembly of the translocation pore, formed by the secreted translocators YopB and YopD (**Fig. 9**). At a later stage LcrV presumably connects the pore to the needle, forming a continuous channel from the bacterium to the cytoplasm of the eukaryotic cell.

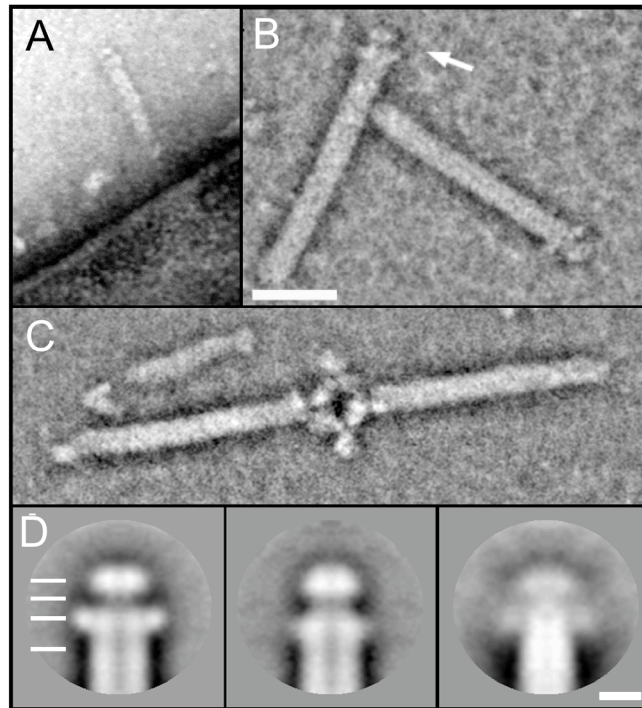


**Fig. 8. LcrV forms a structure at the tip of the injectisome needle (Mueller, Broz *et al.*, 2005).** (A) Transmission electron micrograph of *Y. enterocolitica* negatively stained with 2 % uranyl acetate. Needles protrude from the cell surface and have a distinct structure at their distal end. Scale bar is 40 nm. (B) Scanning Transmission Electron Microscopy (STEM) images of negatively stained wt needles. The characteristic tip complex (white arrow) comprises a head, a neck and a base. Scale bar is 20 nm. (C) STEM images of wt needles incubated with anti-LcrV antibodies and negatively stained. The antibodies generally attached to the “head” domain of the tip complex. Scale bar is 20 nm. (D) Projection averages of the complexes formed by LcrV, PcrV and AcrV at the tip of the injectisome needle of *Y. enterocolitica* E40 (resolution 1.5 nm). A central channel permeates both the needle and the tip complex. Scale bar is 5 nm.



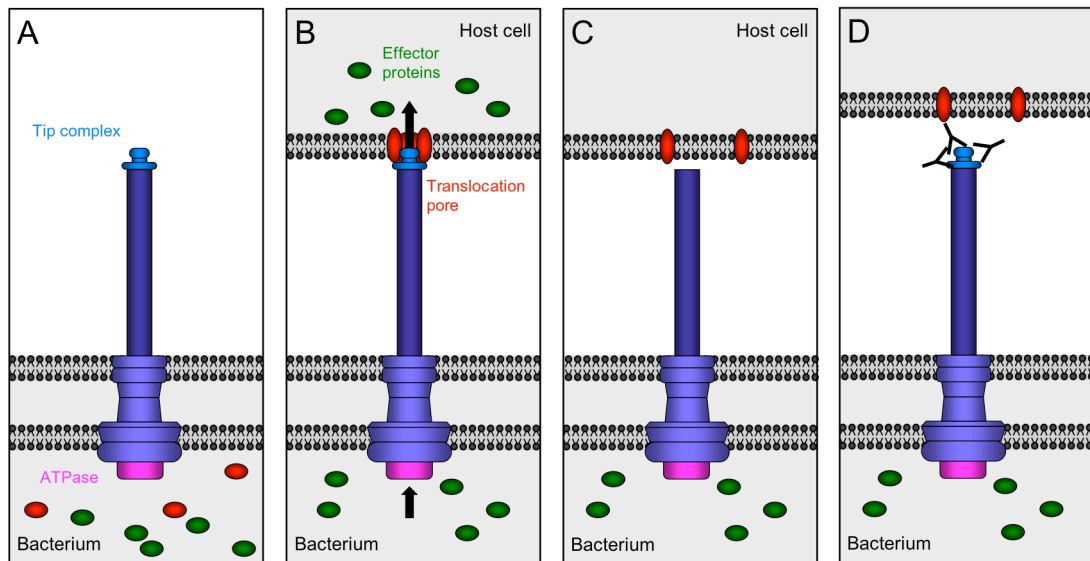


**Fig. 9. Hypothetical model for the function of the LcrV tip structure in the assembly of the translocation pore formed by the translocators YopB and YopD (Mueller, Broz *et al.*, 2005). (A)** Before contact to a target cell. The injectisome is assembled and LcrV forms the tip complex on the distal end of the needle. **(B)** Contact to target cell. The translocation pore is assembled, forming a continuous channel from the bacterium to the host cell cytosol and allowing translocation of effector proteins. The LcrV tip complex serves as an assembly platform. **(C)** Situation in *lcrV* deletion mutant. The translocators YopB and YopD are secreted and insert into the target cell membrane. No translocation pore is formed due to the lack of the tip complex. **(D)** Presence of protective antibodies. The translocators are secreted and insert into the target cell membrane. No functional pore can be assembled, because anti-LcrV antibodies bind to the tip complex and block its function.



## Accessory

### 1.9 The chaperone of the hydrophobic translocators

A hallmark of type III secretion is that efficient secretion or translocation of some substrate proteins requires the presence of small cytosolic chaperones. They are divided into three distinct classes: I, II and III. Chaperones of the hydrophobic translocators constitute the class II. The archetype of this chaperone class is SycD, the specific chaperone of both YopB and YopD from *Yersinia* (Neyt and Cornelis, 1999b; Wattiau *et al.*, 1994). Homologs of SycD in other type III secretion systems usually serve as chaperone for two hydrophobic translocators as well (**Fig. 4**): PcrH for PopB and PopD (Allmond *et al.*, 2003; Schoehn *et al.*, 2003), SicA for SipB and SipC (Kaniga *et al.*, 1995; Tucker and Galan, 2000) and IpgC for IpaB and IpaC (Menard *et al.*, 1994). In EPEC the situation seems to be more complex: Initially, CesD was reported to be the chaperone for the translocators EspB and EspD (Wainwright and Kaper, 1998). Meanwhile, a second chaperone for EspD, called CesD2, was discovered (Neves *et al.*, 2003). In the SPI-2 system of *S. Typhimurium*, the *sscA* gene shares homology to *sycD* of *Yersinia*, but the protein has not been analyzed so far.

#### 1.9.1 Role as chaperone

Immunoprecipitation experiments have shown that, in the cytoplasm of *S. flexneri*, IpgC is associated either with IpaB or IpaC (Menard *et al.*, 1994). As IpaB and IpaC have been shown to form a complex after secretion it was proposed that the chaperone prevents the premature association of the two translocators (Menard *et al.*, 1994). The same role has been attributed to SicA, the homolog of IpgC, in *S. Typhimurium* (Tucker and Galan, 2000). Consistent with this it could be shown that in *Yersinia* and *P. aeruginosa*, SycD/PcrH also associates independently with YopB or YopD, PopB or PopD respectively (Anderson *et al.*, 2002; Schoehn *et al.*, 2003). In contrast to chaperones of the effectors (class I), chaperones of the translocators might not bind to a unique region on their substrates. YopD possesses two distinct SycD binding domains, one spanning the N-terminus and one encompassing the C-terminal amphipathic domain (Francis *et al.*, 2000), while several binding sites were identified in YopB (Neyt and Cornelis, 1999b). In *S. flexneri*, however, a unique binding site for IpgC has been identified in the N-terminal part of both IpaB and IpaC (Page *et al.*, 2001). So far no similarities between these regions could be identified. Only the crystallization of the chaperones together with their substrates will determine the nature of this interaction.

When expressed in *E. coli*, IpaB is degraded in the absence of the chaperone IpgC, while IpaC is stable (Menard *et al.*, 1994). When IpaB and IpaC are co-expressed both proteins are degraded but this can be prevented by the expression of IpgC. Thus in the

absence of IpgC the unstable IpaB associates to IpaC and leads to its degradation. In *Salmonella*, SipB is degraded in a *sicA* mutant, but not in a *sicAsipC* mutant, suggesting that, in the absence of SicA, SipC interacts with SipB and leads to its degradation (Tucker and Galan, 2000). In *Yersinia* also YopB and, to a lesser degree YopD, require SycD for its stability (Edqvist *et al.*, 2006; Francis *et al.*, 2000; Neyt and Cornelis, 1999b). In addition, if YopB is expressed in *E. coli* without the chaperone it leads to lysis of the bacteria, probably due to the interaction with membranes (Neyt and Cornelis, 1999b). Similar observations were reported for PopB and PopD from *P. aeruginosa* (Schoehn *et al.*, 2003). No toxic effects are observed when the translocators are expressed with their chaperone.

Altogether these results suggest that the function of class II chaperones is to prevent premature association of the translocators and also to stabilize their substrates. Because some of the translocators might have a deleterious effect on the bacteria, they are rapidly degraded if they are not bound to the chaperone.

Structurally, class II chaperones are characterized by the possession of three tandem tetratricopeptide repeats (TPR's), which are otherwise only found in eukaryotic molecular chaperones (Pallen *et al.*, 2003). No class II chaperone has been crystallized so far, but the TPR's allowed a homology modeling of SycD based on human protein phosphatase 5 (Fig. 10, (Pallen *et al.*, 2003). According to this, class II chaperones would have an all-alpha-helical domain structure in contrast to class I chaperones, which comprise alpha-helical and beta-strand structures (Parsot *et al.*, 2003). The mapping of residues critical for the interaction with the translocators revealed two distinct interaction interfaces in SycD, one for YopD and one for YopB (Fig. 10, (Edqvist *et al.*, 2006).

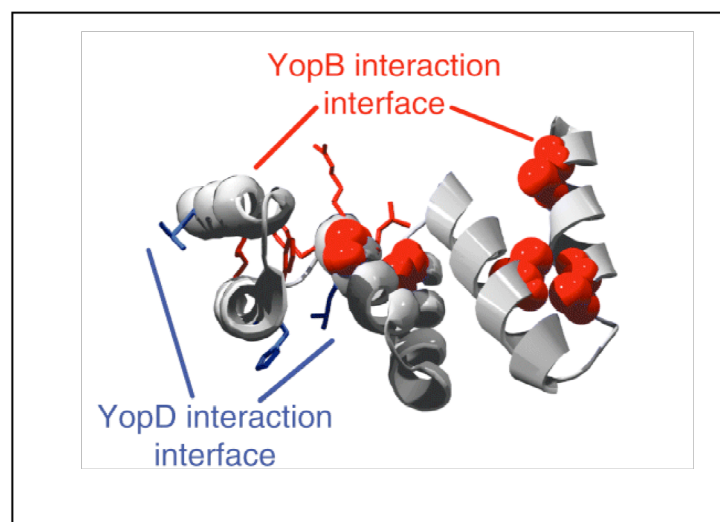


**Fig. 10. Homology modeling of the hypothetical structure of the translocator chaperone SycD (Edqvist *et al.*, 2006).** The modeling is based on the TPR's of the human protein phosphatase 5. Interaction interfaces with YopB and YopD were determined by mutagenesis and are indicated.

### 1.9.2 Role in regulation

Initially, SycD was discovered as a negative regulator because a *sycD* mutation leads to increased *yop* gene expression and reduced growth in high calcium conditions; hence it is also called LcrH for “low Calcium response H” (Bergman *et al.*, 1991; Price *et al.*, 1989). Overexpression of SycD in *Yersinia* causes a decrease in Yop synthesis. Deletion of the *yopD* gene results in a constitutive production of Yops, similar to a *sycD* mutation. It was shown that the formation of a complex between YopD and SycD is necessary for the regulation of *yop* gene expression (Anderson *et al.*, 2002; Francis *et al.*, 2000). Mutants that could not form the complex could no longer regulate *yop* gene expression, even though YopD and SycD were both produced. Therefore it has been proposed that together with YopD, SycD/LcrH establishes a negative regulatory loop for the control of Yop synthesis (Francis *et al.*, 2000).

Homologs of SycD/LcrH from other system have been shown to be involved in regulation as well. In *S. Typhimurium* the chaperone SicA is necessary for the activation of the *sicA*, *sigDE* and *sopE* operons, which also depends on the presence InvF, a transcriptional activator of the AraC family (Darwin and Miller, 2001; Tucker and Galan, 2000). Co-expression of SicA and InvF is sufficient to activate the promoters of these operons in *E. coli* (Darwin and Miller, 2001). In addition both proteins were shown to interact in *E. coli*, suggesting that SicA could act as co-activator of InvF. In *S. flexneri*, IpgC and MxiE, the homologs of SicA and InvF, are involved in the activation of effector genes, like *ipaH* (Mavris *et al.*, 2002). Co-expression of both proteins in *E. coli* is sufficient to activate transcription from regulated promoters. Furthermore, overexpression of IpgC in wildtype *S. flexneri* leads to the activation of the regulated genes. Similar observations were made for SycB and YsaA from the *Yersinia* Ysa-Ysp system (Walker and Miller, 2004). The model proposed for this family of TTSSs states that, in non-secreting conditions, the chaperone is associated with the translocators and is not available for the AraC-like activator (**Fig. 11**). Upon secretion of the translocators the chaperone is released and can act as co-activator for the transcription of regulated promoters. This imposes a level of hierarchy between the translocators and the effectors. One could therefore speculate that the class II chaperones not only serve as chaperones for the hydrophobic translocators but also might ensure the secretion of the translocators at the right time, before the effectors.

According to this model, the translocators have to be secreted before the effectors can be produced. However, it is known that effectors are synthesized and stored in the cytosol already before the system is triggered. Upon activation they are supposed to be secreted post-translationally. This implies that the translocators have to be detached from the chaperone already before the secretion is triggered. This suggest that, during the assembly of the injectisome, the translocators are secreted and/or stored somewhere in the injectisome. It could be possible that the needle is filled with the translocators. Purified needle preparations

from *Yersinia* contain YopD (Mueller, Broz *et al.*, 2005) and recently it was reported for *S. flexneri* that IpaB is present in purified needle preparations (Espina *et al.*, 2006). If these proteins are only contaminants of the needle preparations or indeed the needles were preloaded with translocators remains to be determined.

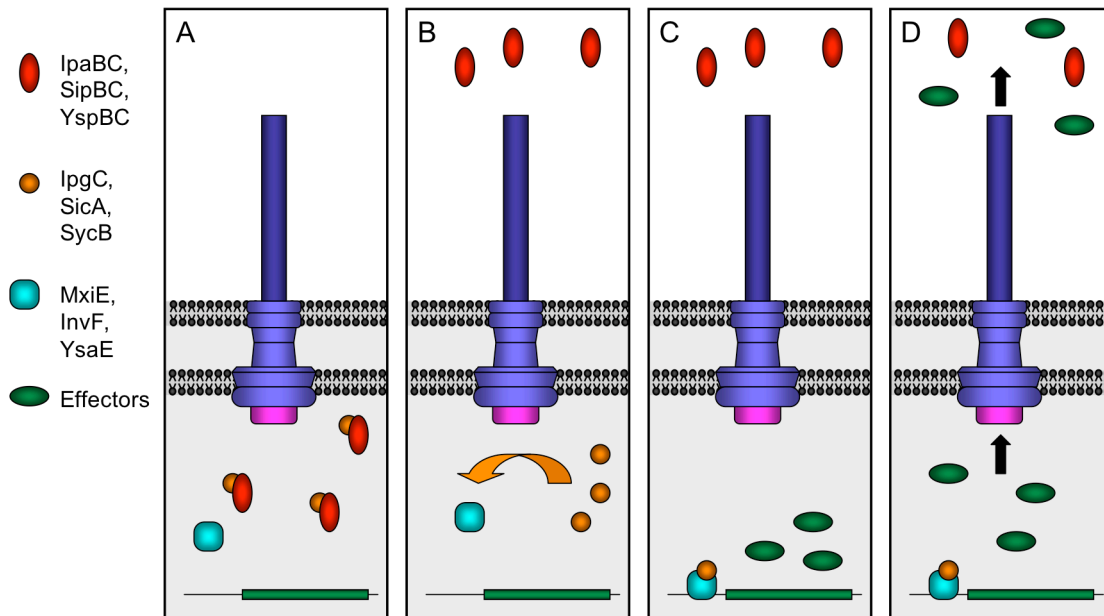


**Fig. 11. Simplified model of regulation of transcription by TTS apparatus activity in *S. flexneri*, *S. Typhimurium* SPI-1 and *Y. enterocolitica* Ysa-Ysp system. (A) Inactive secretion apparatus. The translocators (red) are bound to their chaperone (orange). The AraC-like activator (turquoise) cannot activate the transcription of effector genes. (B) Active secretion apparatus. Secretion of the translocators leads to the release of the chaperone. (C) The chaperone interacts with the AraC-like activator. This allows the transcription of effector genes (green). (D) The effectors are secreted.**

## 1.10 The LcrG-LcrV complex regulates the secretion of effector Yops

As mentioned above the operon encoding the translocators and SycD also encodes LcrG, a small cytosolic protein, which is also involved in the low Calcium response (LCR) of *Yersinia*. A mutant in *lcrG* exhibits a Calcium-blind phenotype, expressing and secreting Yop proteins independently of the presence of Calcium at 37°C (Perry *et al.*, 1986; Price *et al.*, 1991; Skrzypek and Straley, 1993). LcrV, encoded in the same operon, is also involved in the LCR of *Yersinia*. But in contrast to *lcrG* mutants, *lcrV* mutants express and secrete severely reduced amounts of effectors and translocators and also do not show any growth inhibition when deprived of Calcium at 37° (Marenne *et al.*, 2003; Skrzypek and Straley, 1995).

LcrG and LcrV form a stable heterodimeric complex in the cytosol (Nilles *et al.*, 1997). This complex-formation prompted the analysis of an *lcrGV* double mutant (Matson and Nilles, 2001; Nilles *et al.*, 1998) and it appeared that this mutant exhibited the same phenotype as an *lcrG* mutant, expressing and secreting Yop proteins independently of the presence of Calcium at 37°C. Providing *lcrV* in *trans* had no effect on the phenotype. On the other hand, complementation of the double mutant with *lcrG* completely abolished secretion and decreased expression of Yops at 37°C in the presence and the absence of Calcium. This indicated that LcrG could act as a negative regulator for Yop secretion. If the mutant was complemented with both genes (*lcrG* and *lcrV*) the wildtype phenotype was restored. These results lead to the so-called LcrG titration model for the regulation of Yop secretion that was first proposed by Nilles *et al.* (**Fig. 12**; Nilles *et al.*, 1998). This model states that, before the machinery is active, LcrG is expressed and directly or indirectly blocks the secretion machinery, acting from within the bacterial cytoplasm. Contact with the target cell or Calcium chelation (*in vitro*) would lead to increased expression of LCR-regulated genes, including the positive regulator LcrV. Increasing levels of LcrV would lead to complex formation between LcrV and LcrG, thus removing LcrG from its secretion-blocking function. In agreement with this, mutant LcrG proteins that cannot longer interact with LcrV block secretion, mimicking an *lcrV* phenotype (Matson and Nilles, 2001). Although the titration model is appealing, it is hard to imagine how contact to the target cell increases the expression of LcrV and not of LcrG as both of them are in the same operon. It is also unknown how the LcrG-LcrV plug is connected to the YopN plug, which also controls secretion.

Interestingly, it was shown that LcrG is also necessary for the efficient translocation of effectors into target cells, because when HeLa cell were infected with an *lcrG* mutant for 2 h, no cytotoxicity was observed (Sarker *et al.*, 1998b). Only after prolonged infection (4 h) cytotoxic effects were observed (Nilles *et al.*, 1998), suggesting that LcrG is not essential for translocation, but has a facilitating effect. This is consistent with the observation that LcrG might be required for maximal or efficient secretion of LcrV (Fields *et al.*, 1999). These results

indicate that LcrG has a facilitating role in Yop targeting by promoting LcrV secretion, which is necessary to form the translocation pore.

Based on these observation it has also been proposed that LcrG could be the chaperone of LcrV (Lee *et al.*, 2000). This idea is in addition supported by the facts that LcrG is small and primarily cytosolic. Purified LcrV forms dimers and to a certain extend also multimers (Lawton *et al.*, 2002). Upon addition of LcrG the LcrV-dimer is dissociated and LcrG-LcrV heterodimers are formed. This suggests that LcrG prevents the polymerization of LcrV. The observation that LcrV forms the tip complex, implies that it has to polymerize (Mueller, Broz *et al.*, 2005). In addition crosslinking of purified needles indicates close interaction between LcrV molecules (Mueller, Broz *et al.*, 2005).

EspA, the ortholog of LcrV in EPEC, requires the chaperone CsaA that keeps it in a monomeric form and prevents polymerization in the bacterial cytoplasm (Yip *et al.*, 2005). Both LcrG and CsaA have a basic pI, unlike class I chaperones that have an acidic pI. In contrast to EspA, LcrV does not require LcrG for its stability and secretion. The interaction between CsaA and EspA is mediated via a coiled-coil motif, made of long alpha helices (**Fig. 13**). LcrV is much bigger than EspA but also has two long alpha helices that form a coiled-coil, similar to EspA. Comparably, in the *S. Typhimurium* SPI-2 system the interaction of SseB and its chaperone SseA is mediated by a putative coiled-coil motif (Zurawski and Stein, 2004). Indeed it has been reported that the interaction between LcrG and LcrV is also mediated by coiled-coil domains (Lawton *et al.*, 2002). These coiled-coils are formed by the two long alpha helices that connect the globular domains of LcrV (**Fig. 13**). It is possible that these hydrophilic translocators need the chaperone to prevent their polymerization by masking their coiled-coil motifs.

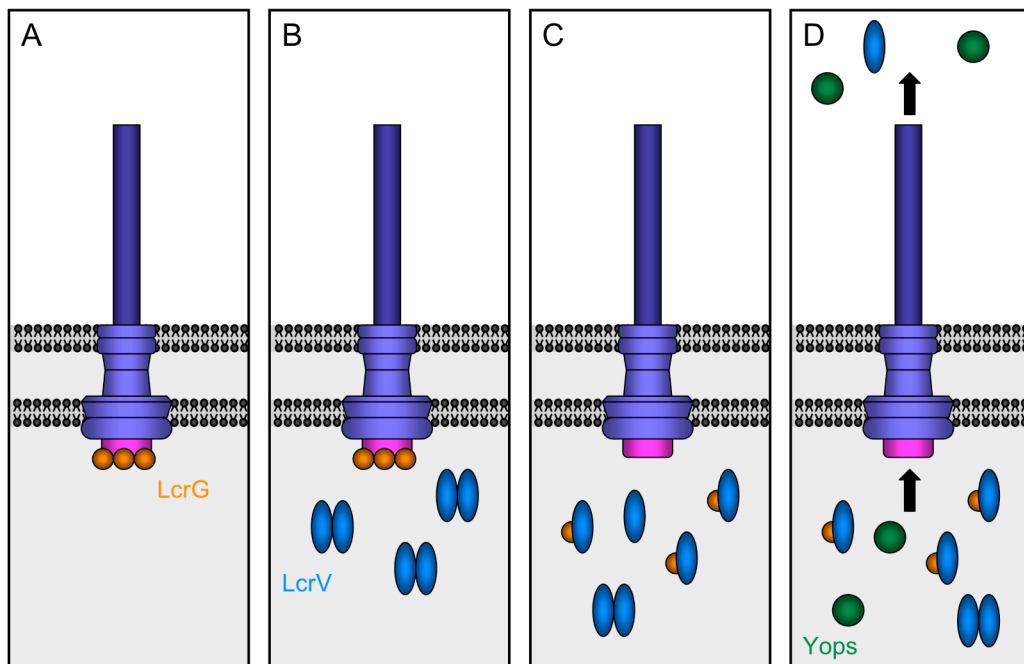


**Fig. 12. The LcrG titration model (Nilles *et al.*, 1998).** (A) Non secreting condition: LcrG is expressed and blocks the secretion apparatus from within the bacterial cytosol. (B) Contact with the target cell membrane or Calcium chelation leads to increased LcrV synthesis. (C) Formation of LcrG-LcrV dimers. Removal of gating. (D) The channel is open and secretion of effectors is possible.

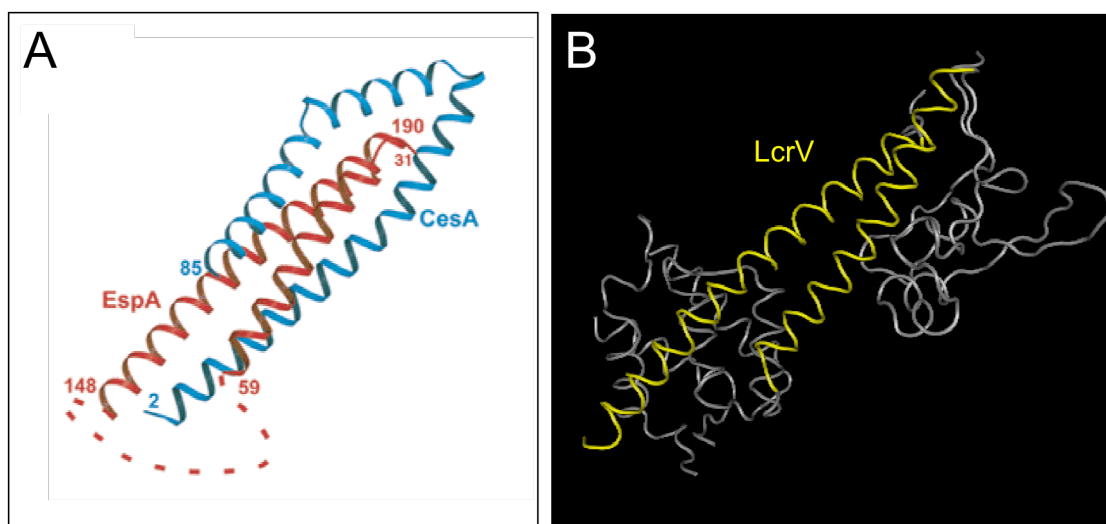


**Fig. 13. The coiled-coil motifs in EspA and LcrV.** (A) Structure of CesA (blue) in complex with EspA (red) (Yip *et al.*, 2005). The flexible central region of EspA is drawn as a dashed red line. Two extensive alpha helices of EspA (coiled-coil) interact closely with CesA in the protein complex. (B) Structure of LcrV (gray) as reported by Derewenda *et al.*, 2004. The two long alpha helices that connect the globular domains and that are involved in the formation of coiled-coils and the interaction with LcrG are arranged in front (yellow).



## 1.11 Requirements on the membrane side

Many pathogenic bacteria have been found to interact with specialized domains of the host membrane that are rich in cholesterol and sphingolipids and that are termed rafts. Cholesterol rich microdomains have been found to be necessary for type III secretion mediated uptake of *S. Typhimurium* (Garner *et al.*, 2002) and *S. flexneri* (Lafont *et al.*, 2002) (for a review see, Lafont and van der Goot, 2005). Cellular receptors that partition into microdomains cluster during *Salmonella* and *Shigella* entry and upon initial EPEC-host contact (Garcia-del Portillo *et al.*, 1994; Lafont *et al.*, 2002; Zobiack *et al.*, 2002). As the translocators insert directly into host cell membranes it was speculated that the formation of the translocation pore could depend on the presence of certain lipids in the host cell membrane. Indeed it could be shown recently that cholesterol is required for the translocation of effector proteins into host cells by *Salmonella*, *Shigella* and EPEC (Hayward *et al.*, 2005). In addition the authors show that purified *Salmonella* SipB and *Shigella* IpaB are cholesterol-binding proteins and that cholesterol is the main binding determinant of purified SipB/IpaB to host cells (Hayward *et al.*, 2005).

In vitro, liposome fusion induced by purified SipB protein is enhanced when target liposomes contain cholesterol (Hayward *et al.*, 2000). Cholesterol-containing liposomes have also been shown to weakly stimulate the *Shigella* TTSS, suggesting that raft-like lipids may trigger effector release (van der Goot *et al.*, 2004).

No cholesterol dependence has been reported for infections with *P. aeruginosa* so far, but the interaction of the *P. aeruginosa* translocators with artificial membranes has been studied (Schoehn *et al.*, 2003). It was reported that purified PopB and PopD only bind to liposomes containing negatively charged phospholipids (phosphatidylserine) and that PopB and PopD can lyse liposomes containing cholesterol (Schoehn *et al.*, 2003). The latter observation had to be revised in a later study (Faudry *et al.*, 2006), as no lysis could be observed any more, even with liposomes containing cholesterol. Similar experiments with purified translocators from *Yersinia* suggested that negatively charged phospholipids (DOPS) are required for the association of YopB and YopD with liposomes and for their insertion into membranes, while cholesterol is dispensable (P. Broz, unpublished results). *In vivo* studies with *Yersinia* showed that the depletion of cholesterol has no influence on the infection of cells (L. J. Mota, unpublished results).

Taken together, there is strong evidence that the interaction of several pathogens employing type III secretion systems, like *Shigella*, *Salmonella* and EPEC, is dependent on lipid rafts in the host cell membrane. Although some raft- or cholesterol-dependent events have been identified, the exact mechanisms at the molecular level remain obscure and will require further studies. However, not all type III secretion systems need to be triggered by the



same kind of lipids. Some bacteria have to act in seconds to escape macrophages, while others have more time to find the right spot to enter a target cell.

## 1.12 Other needle extensions

As mentioned before the LcrV tip complex forms an extension of the needle structure and possibly connects the translocation pore to the needle. Another type of extension is the EspA filament found in EPEC (**Fig. 14**; Knutton *et al.*, 1998). This filament is a polymer made of multiple copies of a single hydrophilic protein, EspA. This protein, together with the hydrophobic proteins EspD and EspB is necessary for translocation of effectors and the formation of the translocation pore. EM analysis of purified injectisomes of EPEC show that the EspA filament is firmly attached to a very short needle made by EscF (**Fig. 14**; Daniell *et al.*, 2001; Sekiya *et al.*, 2001), which is similar to needles observed in other type III secretion systems. So far it was not defined whether EspA polymerizes around or on top of the EscF needle. The length of the EspA-filament varies considerably and can reach up to 600 nm. The 3D structure of EspA filaments at a resolution of 26 Å revealed that the structure comprises a helical tube with a diameter of 120 Å enclosing a central channel of 25 Å diameter (Daniell *et al.*, 2003), which is similar to the diameter of the injectisome needle (25 Å). Furthermore the helical parameters of the EspA filament (5.6 subunits per turn, 4.6 Å axial rise per subunit, Daniell *et al.*, 2003) resemble that of the needle (5.6 subunits per turn, 4.3 Å axial rise per subunit, Cordes *et al.*, 2003) and the R-type straight flagellar filament of *Salmonella* (5.47 subunits per turn, 4.69 Å axial rise per subunit, Mimori *et al.*, 1995). In addition all three structures have five-fold symmetry.

The EspA filament is thought to be a necessary adaptation to enable the pathogen to penetrate the thick glycocalyx layer and to reach the cells of the intestinal. The EspA filament would serve as a hollow conduit connecting the injectisome of EPEC with the translocation pore, formed by EspD and EspB.

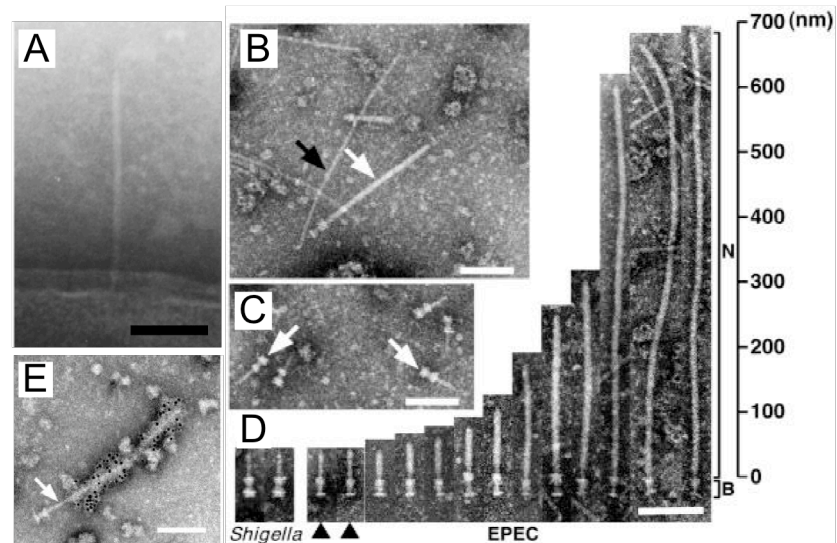


**Fig. 14. EspA forms a long filament, attached to the needle of the injectisome from EPEC.** (A) Electron micrographs of osmotically shocked EPEC stained with 1 % PTA (Daniell *et al.*, 2001). (B) Electron micrographs of negatively stained purified NCs from EPEC. The white arrow indicates NCs and black arrow indicates pilus-like structures (Sekiya *et al.*, 2001). (C) Electron micrographs of negatively stained purified NCs from *S. flexneri*. The white arrows indicate NCs (Sekiya *et al.*, 2001). (D) Alignment of EPEC NCs and comparisons to *S. flexneri* NCs. N and B indicate the needle and basal body of EPEC NCs (Sekiya *et al.*, 2001). (E) Immunogold labeling of purified NCs from EPEC with anti-EspA antibodies. Only the filament is decorated with gold particles while the basal body and the thinner needle part is not labeled. Scale bars are 100 nm (Sekiya *et al.*, 2001).

A similar structure could exist in the SPI-2, the second T3SS of *S. Typhimurium* (Chakravorty *et al.*, 2005). The three translocators of this system are SseB, SseC and SseD (Nikolaus *et al.*, 2001). TEM analysis of *S. Typhimurium* grown *in vitro* revealed novel surface appendages (Fig. 15). These appendages are composed of a needle, 150 nm long, sheathed with an irregular proteinaceous structure. Immunogold analysis revealed that this sheath contains the translocators SseB and SseC. It is likely that these sheath structures, observed *in vitro*, are the result of prolonged secretion in the absence of contact to a target cell membrane. But, ultrathin section analysis of intracellular *S. Typhimurium* in macrophages revealed that *in vivo* similar needles are formed and have also a sheath-like structure but only at their distal end. This sheath contains SseB, the hydrophilic translocator of the SPI-2 type III secretion system. It still remains to be elucidated, how the sheath structure looks in detail, what is its function and whether the sheaths, formed *in vivo*, are not also just an artifact resulting from prolonged secretion.

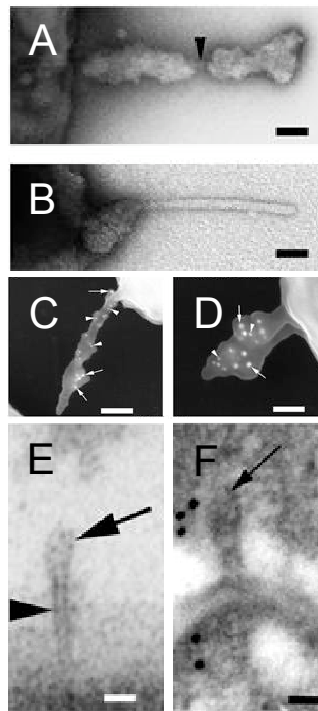


**Fig. 15. Electron micrographs of surface structures encoded by the *S. Typhimurium* SPI-2 system (Chakravorty *et al.*, 2005).** (A, B) High magnification electron micrographs of surface appendages present on wildtype *S. Typhimurium*, grown in secreting conditions. The appendages consist of an inner cylindrical needle (black arrowhead) and different extends of a proteinaceous structure. (C, D) Double immunogold labeling with antibodies directed against the translocators SseB (arrowheads) and SseC (arrows) of the surface appendages on *S. Typhimurium* grown *in vitro*. The antibodies were detected with protein A coated gold-particles of 10 nm for SseB and 15 nm for SseC. Both translocators are part of the sheath-like structure. (E, F) Ultrathin section analysis of intracellular *S. Typhimurium* bacteria. Structures consisting of needle-like stem and a sheathed distal end can be seen (E). Immunogold labeling for SseB (F) of surface appendages formed *in vivo* stains the sheath structure. Scale bars are 25 nm in (A, B, E), 100 nm in (C, D) and 50 nm in (F).

Recently, IpaD the functional ortholog of LcrV in *S. flexneri*, has been shown to be localized at the tip of the *S. flexneri* needle by immunogold electron microscopy (Espina *et al.*, 2006). What kind of structure it forms there could not be defined yet.

The EspA filament and the putative SPI-2 needle sheath resemble, at a functional level, the LcrV tip structure of *Yersinia*. It can be hypothesized that the tip protein would have evolved to polymerize as a filament rather than a simple ring structure, but that it has probably kept its scaffolding property for the hydrophobic translocators (Fig. 16).

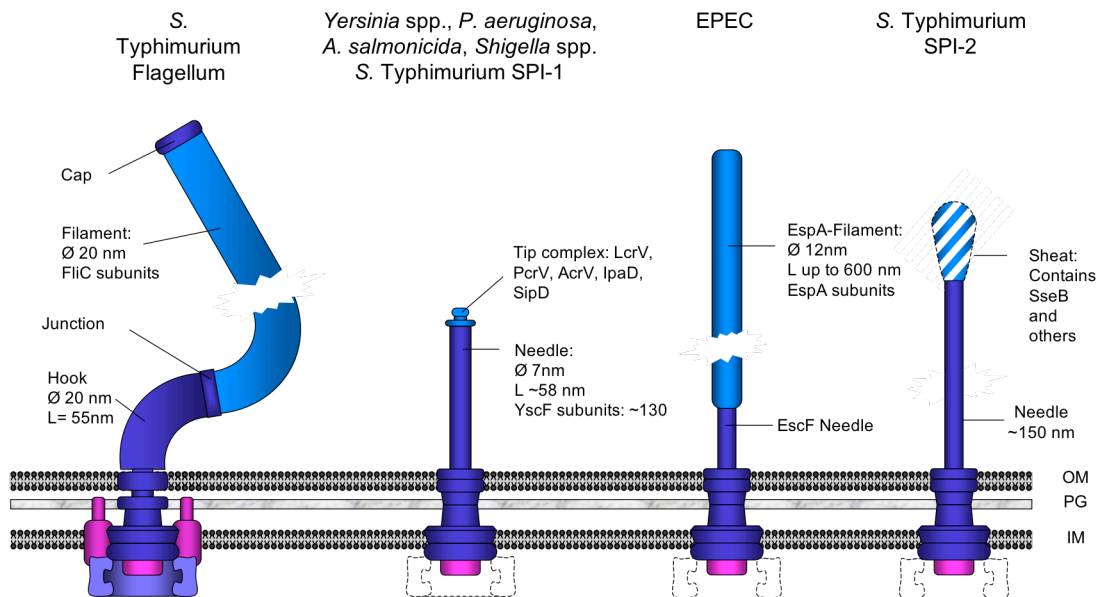


**Fig. 16. Schematic representations of the flagellum (A) and different kinds of injectisomes (B, C, D).** The flagellar hook, counterpart of the injectisome needle, is extended with a long filament made of FliC. The injectisomes of different species vary in the form of their needle extension. The needles of *Yersinia* spp., *P. aeruginosa* and *A. salmonicida* have a distinct tip complex at their distal end formed by LcrV, PcrV or AcrV respectively (B). The same is probably true for *S. Typhimurium* and *S. flexneri* (SipD and IpaD). The needle from EPEC is extended by the long EspA filament (C). The needle from the *S. Typhimurium* SPI-2 TTS system (D) is likely to be topped with an yet undefined sheath-like structure, containing SseB.

### 1.13 Double function as translocator and effector

Type III secretion effectors are proteins that are injected into the eukaryotic cell, where they act on cellular signaling and control pathways. It appears that, in addition to the known effectors, some of translocators, namely IpaB, SipB, EspB and YopD are delivered into the eukaryotic cell.

A feature of *Shigella* and *Salmonella* infections is the induction of the inflammatory response. It has been shown that IpaB as well as SipB activate the ICE cysteine protease, which converts pro-IL-1 to the mature proinflammatory cytokine IL-1 (Hersh *et al.*, 1999; Tran Van Nhieu *et al.*, 1997). In addition, IpaB leads to the activation of NF- $\kappa$ B, which is followed by the release of proinflammatory cytokines, such as IL-8 (Hobbie *et al.*, 1997). Because ICE is also a caspase (casp-1), interaction with IpaB or SipB leads to apoptosis of macrophages. Inhibition of Casp-1 activity by a specific inhibitor blocks macrophage cytotoxicity, and macrophages lacking casp-1 are not susceptible to *Salmonella* induced apoptosis (Chen *et al.*, 1996; Hersh *et al.*, 1999; Hilbi *et al.*, 1998). *Shigella*- and *Salmonella*-induced apoptosis is thus distinct from other forms of apoptosis, including that induced by *Yersinia*, in that it is uniquely dependant on Casp-1.

The host cell cytoskeleton is a major target of effector proteins injected by pathogenic bacteria. The translocators IpaC from *Shigella* and SipC from *Salmonella* were shown to act on cytoskeletal dynamics and promote the entry of the bacteria into nonphagocytic cells. IpaC induces rearrangements of the subcortical cytoskeleton via small GTPases of the Rho family, leading to the formation of protrusions and membrane ruffling at the bacterial entry site (Tran Van Nhieu *et al.*, 1999). Purified SipC nucleates actin polymerization and bundles actin into cables (Hayward and Koronakis, 1999).

EspB, one of the translocators from EPEC, is as well targeted to the host cell cytosol (Taylor *et al.*, 1998; Wolff *et al.*, 1998), where it modulates the cell actin cytoskeleton (Taylor *et al.*, 1999). Also YopD from *Yersinia* was shown to be localized in eukaryotic cells after infection (Francis and Wolf-Watz, 1998), but no function as effector could be attributed yet. As the translocators are probably internalized during the recycling of membranes, this may explain why YopD is found in the eukaryotic cell, even though it is no effector.

Taken together, these observations indicate that depending on the system, the translocators are not necessarily restricted to the contact area between the bacteria and eukaryotic cells, but that they may traffic inside the target cell and act themselves as effectors, possibly in association with membranes.

## 2 Aim of the thesis

## 2 Aim of the thesis

The three proteins YopB, YopD and LcrV have been shown to be necessary for the translocation of effectors into target cells by the TTSS of *Yersinia*. It has been hypothesized that the translocators form a pore in the target cell membrane, but this pore has not been visualized so far. The role of the different translocators YopB, YopD and LcrV in the assembly of the translocon was unknown. The hydrophobic domains found in YopB and YopD suggested that they might be transmembrane proteins, facilitating the translocation. In addition, the role of LcrV, the major protective antigen, remained mysterious. The aim of my thesis was to characterize the type III secretion translocon of *Y. enterocolitica* in different aspects.

First the role of the hydrophilic LcrV had to be clarified. Second we wanted to find a way to isolate the translocation pore formed by the translocators, analyze its composition and visualize it by electron microscopy. And third we wanted to determine if certain lipids of the target cell membrane, in particular those found in lipid rafts, play a role during the formation of the translocation pore from *Y. enterocolitica*.



## 3 Results

### 3.1 The Needle Length of Bacterial Injectisomes is Determined by a Molecular Ruler

Journet L., Agrain C., Broz P., and Cornelis G.R.

**Science** 302: 1757-60 (2003)

## Summary

The *Yersinia* injectisome needle has a remarkably constant length of around 60 nm suggesting that it is genetically controlled. Mutants affected in the *yscP* gene display abnormally long needles, indicating that the needle length is indeed regulated and that YscP is involved in this process, as it is the case for its counterparts in other TTSS. To determine how YscP is exerting its length control function, we engineered a set of deletions and insertions in the protein. Deletions affecting either the extreme N-or C-term lead to needles of deregulated lengths suggesting that they are required for the length-control of the needles. In contrast, the central part can be shortened or lengthened without the loss of function. Moreover, deletions or insertions in this central part give rise to shorter or longer needles, respectively and a strict linear relationship between the number of residues of YscP and the needle length can be observed. Analysis of purified needles indicated that YscP is found in the purified needle fraction in non-secreting conditions but not any more in secreting conditions. Altogether these results demonstrate that YscP is acting during the assembly of the injectisome as a molecular ruler to determine needle length.

## Statement of my work

I contributed to this paper by providing the electron micrographs of the *yscP* mutant strain, the needle purification protocol and the analysis of purified needles. I also contributed by preparing figures (Fig. 1, 3 and 4) and I was involved in the writing of the manuscript.

lines was 1.23 and 1.26 mm, whereas it was 1.23 mm for the *ds2<sup>M</sup>* line (Wilcoxon rank-sum test  $P > 0.1$  for all comparisons, sample sizes  $N = 18$ ). If anything, one of the *ds2<sup>Z</sup>* lines shows an effect in the wrong direction.

Lack of sex specificity of the influence of *ds2* on both starvation and cold tolerance suggests that this effect is not due to differences in cuticular hydrocarbons per se. Perhaps it is due to an influence of *ds2* on phospholipid composition, as in many other organisms (22). Whatever the exact mechanism of *ds2* action, our results strongly suggest that it is involved in stress resistance. Note, however, that the *ds2<sup>M</sup>* allele appears to be the derived one (6). Consequently, we have restored the ancestral state at the *ds2* locus of the Cosmopolitan line, whereas the actual adaptation involved the loss of the *ds2<sup>Z</sup>* allele from the African population.

The possibility that ecologically driven adaptation at the *ds2* locus results in sexual isolation as a pleiotropic by-product is certainly intriguing. The role *ds2* may play in Z-M sexual isolation is being debated. The genetic basis of Z behavior is complex (12, 39). Thus, *ds2* cannot be the only gene involved and, because the Caribbean flies carry the African *ds2<sup>Z</sup>* allele but exhibit M-type behavior, the locus has initially been excluded as a candidate sexual isolation gene (4). However, this lack of association across genetic backgrounds is inconclusive. A comparison within populations, in which the genetic background is randomized, is more informative. Indeed, when three African populations polymorphic for both Z behavior and *ds2* were tested, a positive correlation between the presence of *ds2<sup>Z</sup>* and the strength of female Z behavior was found in all of them (11). Thus, loss of *ds2<sup>Z</sup>* from the average African background may reduce Z-M sexual isolation.

Although the role of *ds2* in premating isolation remains to be firmly established, we have identified a potential ecological basis for the maintenance of pheromone polymorphism as a result of strong geographical differentiation at the *ds2* locus. Our ability to detect the role of *ds2* in differential adaptation depended crucially on manipulating the gene at its locus while leaving the rest of the genome intact. The phenotypic differences associated with *ds2* allele replacement are small enough to be drowned out by the noise introduced by the genetic background in conventional genetic analyses. Precise allele substitution thus promises to lead to insights into the molecular and evolutionary mechanism of adaptation and speciation.

References and Notes

1. D. Schluter, *The Ecology of Adaptive Radiation* (Oxford Univ. Press, 2000).
2. C.-I. Wu, *J. Evol. Biol.* **14**, 851 (2001).
3. D. Presgraves, L. Balagopalan, S. Abmayr, H. Orr, *Nature* **423**, 715 (2003).

4. J. A. Coyne, C. Wicker-Thomas, J. M. Jallon, *Genet. Res.* **73**, 189 (1999).
5. R. Dallerac et al., *Proc. Natl. Acad. Sci. U.S.A.* **97**, 9449 (2000).
6. A. Takahashi, S. C. Tsaur, J. A. Coyne, C.-I. Wu, *Proc. Natl. Acad. Sci. U.S.A.* **98**, 3920 (2001).
7. J. M. Jallon, *Behav. Genet.* **14**, 441 (1984).
8. J. Tillman, S. Seybold, R. Jurenka, G. Blomquist, *Insect Biochem. Mol. Biol.* **29**, 481 (1999).
9. J. A. Coyne, A. P. Crittenden, K. Mah, *Science* **265**, 1461 (1994).
10. J. Coyne, *Genetics* **143**, 353 (1996).
11. S. Fang, A. Takahashi, C.-I. Wu, *Genetics* **162**, 781 (2002).
12. H. Hollocher, C. T. Ting, M. L. Wu, C.-I. Wu, *Genetics* **147**, 1191 (1997).
13. H. Hollocher, C. T. Ting, F. Pollack, C.-I. Wu, *Evolution* **51**, 1175 (1997).
14. C.-I. Wu et al., *Proc. Natl. Acad. Sci. U.S.A.* **92**, 2519 (1995).
15. C. C. Laurie-Ahlberg, L. F. Stam, *Genetics* **115**, 129 (1987).
16. D. J. Hawthorne, S. Via, *Nature* **412**, 904 (2001).
17. M. Doi, M. Matsuda, M. Tomaru, H. Matsubayashi, Y. Oguma, *Proc. Natl. Acad. Sci. U.S.A.* **98**, 6714 (2001).
18. Y. S. Rong, K. G. Golic, *Genetics* **157**, 1307 (2001).
19. Y. Rong et al., *Genes Dev.* **16**, 1568 (2002).
20. A detailed description of allele substitution line construction can be found in the "Gene Targeting" section of Materials and Methods on Science Online.
21. J. Hazel, E. Williams, *Prog. Lipid. Res.* **29**, 167 (1990).
22. A. R. Cossins, Ed., *Temperature Adaptation of Biological Membranes* (Portland Press, London, 1994).
23. T. Ohtsu, M. Kimura, C. Katagiri, *Eur. J. Biochem.* **252**, 608 (1998).
24. P. Tikku, A. Gracey, A. Macartney, R. Beynon, A. Cossins, *Science* **271**, 815 (1996).
25. M. T. Kimura, *Evolution* **42**, 1288 (1988).
26. P. Gibert, B. Moreteau, G. Petavy, D. Karan, J. David, *Evolution* **55**, 1063 (2001).
27. P. Gibert, R. Huey, *Physiol. Biochem. Zool.* **74**, 429 (2001).
28. A. A. Hoffmann, A. Anderson, R. Hallas, *Ecol. Lett.* **5**, 614 (2002).

29. A. A. Hoffmann, J. G. Sørensen, V. Loeschcke, *J. Therm. Biol.* **28**, 175 (2003).
30. D. Knipple, C. Rosenfield, R. Nielsen, K. You, S. Jeong, *Genetics* **162**, 1737 (2002).
31. J. David, P. Capy, *Trends Genet.* **4**, 106 (1988).
32. A detailed description of fly rearing and stress tolerance experimental conditions can be found in the "Fly Rearing and Stress Tolerance Assays" section of Materials and Methods on Science Online.
33. D. Karan, J. David, *J. Therm. Biol.* **25**, 345 (2000).
34. R. Parkash, A. K. Munjal, *Evol. Ecol. Res.* **2**, 685 (2000).
35. A. A. Hoffmann, R. Hallas, C. Sinclair, P. Mitrovski, *Evolution* **55**, 1621 (2001).
36. K. Lockey, *Comp. Biochem. Physiol. B-Biochem. Mol. Biol.* **89**, 595 (1988).
37. L. Partridge, B. Barrie, K. Fowler, V. French, *Evolution* **48**, 1269 (1994).
38. J. Coyne, *Evolution* **37**, 1101 (1983).
39. C. T. Ting, A. Takahashi, C.-I. Wu, *Proc. Natl. Acad. Sci. U.S.A.* **98**, 6709 (2001).
40. Statistical tests were performed with the R package, version 1.6.1. To assess significance levels, survival curves were treated as cumulative distributions and compared with the two-sample Kolmogorov-Smirnov test.
41. Funding for this work was provided by NIH grants for C.-I.W. and J.A.C. and an NIH Ruth L. Kirschstein National Research Service Award fellowship to A.J.G. We thank K. Golic and Y. Rong for advice and materials, S. Fang and A. Takahashi for information on *desaturase2* sequence and primers, J. Huie and J. Fay for comments on the manuscript, J. Shapiro for help with the production and injection of some of the constructs, and M.-L. Wu, V. I. and E. Chang for help with fly work.

Supporting Online Material

www.sciencemag.org/cgi/content/full/302/5651/1754/DC1  
Materials and Methods

14 August 2003; accepted 16 October 2003

# The Needle Length of Bacterial Injectisomes Is Determined by a Molecular Ruler

Laure Journet, Céline Agrain, Petr Broz, Guy R. Cornelis\*

Size determination represents a fundamental requirement for multicomponent biological structures. Some pathogenic bacteria possess a weapon derived from the flagellum. Like the flagellum, this type-III secretion apparatus, called the injectisome, has a transmembrane basal body, but the external component is a needle-like structure instead of a hook and a filament. Here, we provide evidence that the length of this needle is determined by the size of a protein, YscP, acting as a molecular ruler.

*Yersinia pestis* and *Y. enterocolitica*, the infectious agents of bubonic plague and gastroenteritis, respectively, share a common plasmid-encoded type-III secretion system consisting of the Ysc (Yop secretion) injectisome and the Yops (*Yersinia* outer proteins) that are secreted by this apparatus (1). The injectisome, made of 27 Ysc proteins, is thought to resemble those of *Salmonella enterica* and *Shigella flexneri*. These injectisomes, or "needle complexes," appear as two pairs of rings that are anchored to the inner and

outer membranes of the bacterial envelope, joined by a central rod and supporting a hollow needle about 10 nm thick and 60 nm long (2–4). It is thought that the injectisome serves as a hollow conduit through which the secreted proteins travel across the two bacterial membranes and the peptidoglycan in one step.

Several Ysc proteins that are anchored in the inner membrane and form the core of the secretion apparatus are similar to proteins from the basal body of the flagellum, suggesting a common evolutionary origin (5). Not surprisingly, the *Salmonella* and *Shigella* injectisomes resemble the flagellar basal body (6) except that they are topped by a

Biozentrum, Universität Basel, 4056 Basel, Switzerland.

\*To whom correspondence should be addressed: E-mail: guy.cornelis@unibas.ch

## REPORTS

needle instead of a hook and a flexible filament. The length of the flagellar hook (55 nm) is genetically controlled. Mutations in the gene *fliK* give rise to hooks of indefinite length (7), but it is unclear how FliK exerts its control. The fact that all truncated FliK proteins engineered so far lead to longer hooks rather than shorter hooks is presented as an argument that FliK cannot act as a simple molecular ruler (8). In addition, certain mutations in genes that encode the cytoplasmic ring lead to shorter hooks (8), supporting an elegant model in which this structure controls the hook length by acting as "a quantized measuring cup," storing the subunits before their export (8). In this mod-

el, the role of FliK would be to terminate hook elongation by changing the secretion mode from hook-monomer to flagellin-monomer secretion (8). As for the injectisome of *Salmonella* and *Shigella*, mutants affected in a gene called *invJ* or *spa32*, respectively, display needles of various lengths, ranging from normal (60 nm) to as long as 1  $\mu\text{m}$  (2, 9, 10). Thus, InvJ and Spa32 behave as FliK homologs, although they do not share any substantial sequence homology with FliK.

Here, we address the question of what controls the injectisome needle length in *Yersinia*. We first examined by electron microscopy *Y. enterocolitica* E40 bacteria incubated

under conditions that artificially induce secretion of the Yops (11). We observed many needle-like structures that were about 6 to 7 nm thick and 60 nm long (12). Many of these needles were detached from the bacterial body (Fig. 1). We purified these detached needles and confirmed that they were made of the 6-kD YscF protein (12). Because it is difficult to define the exact insertion point of needles on bacteria, we measured only the detached needles. The length was distributed with an average of  $58 \pm 10$  nm (Fig. 1), suggesting that the needles either detached or broke at a precise point close to the bacterial surface. Next, we examined *Y. enterocolitica* with a large deletion (codons 97 to 465 out of 515) in *yscP* (*yscP* $_{\Delta 97-465}$ ) (13). This gene is synthetic to *spa32* and *invJ*, but its product has no substantial sequence identity with Spa32, InvJ, or FliK. The *yscP* $_{\Delta 97-465}$  mutant bacteria produced needle-like structures with an indefinite length ranging from 45 nm up to 1570 nm (Fig. 1). When the *yscP* $_{\Delta 97-465}$  mutation was complemented with the *yscP* $^+$  allele, control of the length was restored ( $55 \pm 8$  nm), indicating that YscP played an essential role in length control.

YscP from *Y. enterocolitica* E40 (YscP $_{\text{entero}}$ ) carries a duplication of 60 central residues (13) (Fig. 2). YscP from *Y. pestis* KIM5 (YscP $_{\text{pestitisKIM5}}$ ) is 90% identical in sequence to YscP $_{\text{entero}}$ , but it is shorter (455 residues) because of the lack of such repetition (14). To explore whether the two proteins lead to needles of the same length, we complemented the *Y. enterocolitica* *yscP* $_{\Delta 97-465}$  mutation with the *yscP* $_{\text{pestitisKIM5}}$  gene (15). The shorter *Y. pestis* gene restored length control but programmed shorter needles ( $41 \pm 8$  nm) (Fig. 2).

To investigate whether the needle length reduction was a result of the shortening of YscP and not subtle residue changes, we complemented the *yscP* $_{\Delta 97-465}$  mutation with

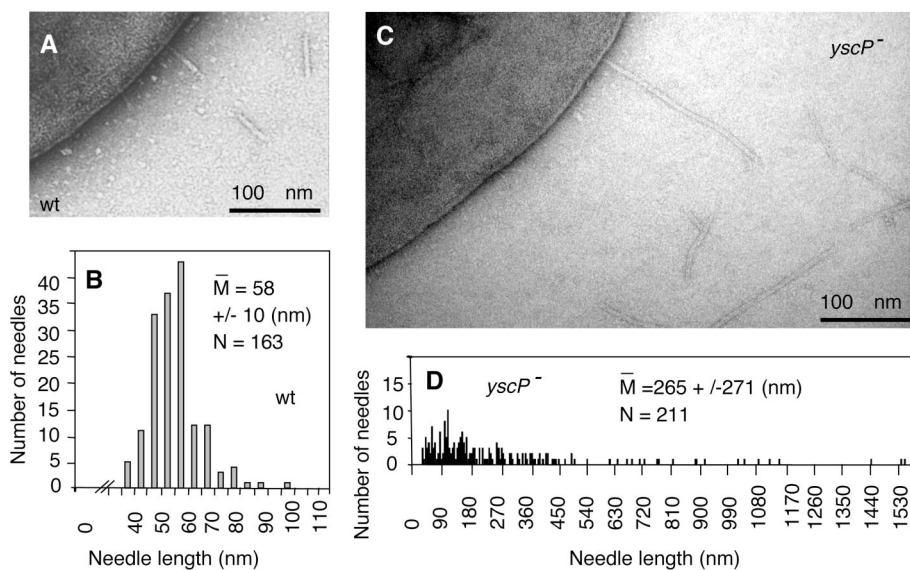


**Fig. 1.** YscP is required for needle-length control. Electron micrographs of *Y. enterocolitica* wild type (wt) (A) and *yscP* $_{\Delta 97-465}$  mutant (C) showing the needles of the injectisomes. Detached needles were measured at the vicinity of at least 10 to 15 different bacteria. Histograms of lengths are given in (B) (for wild type) and (D) (for *yscP* $_{\Delta 97-465}$  mutant). Note the altered distribution of lengths in the mutant.  $\bar{M}$ , mean of the lengths;  $N$ , number of needles measured.

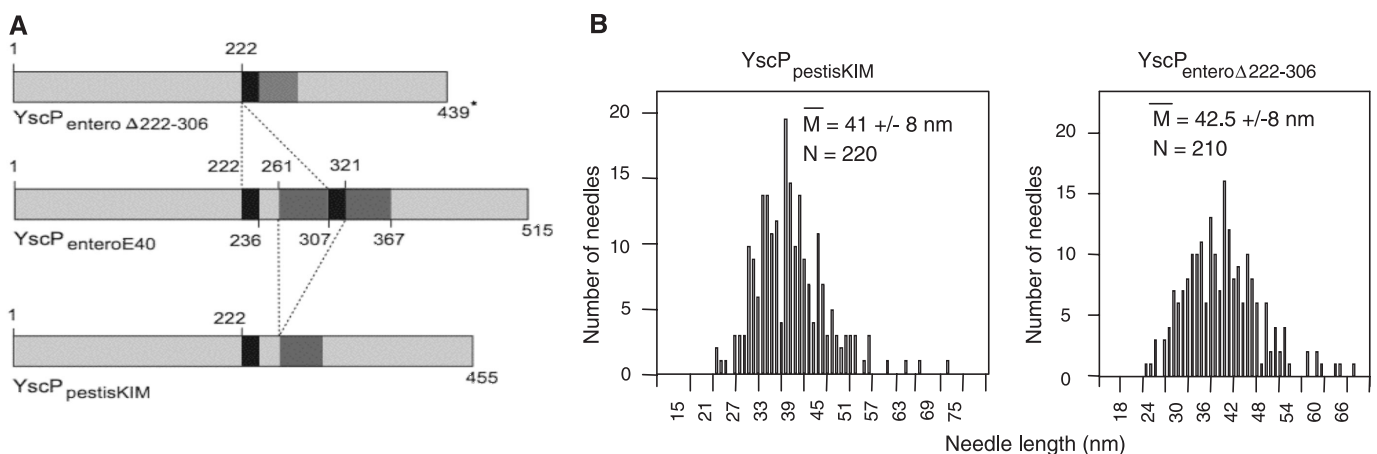
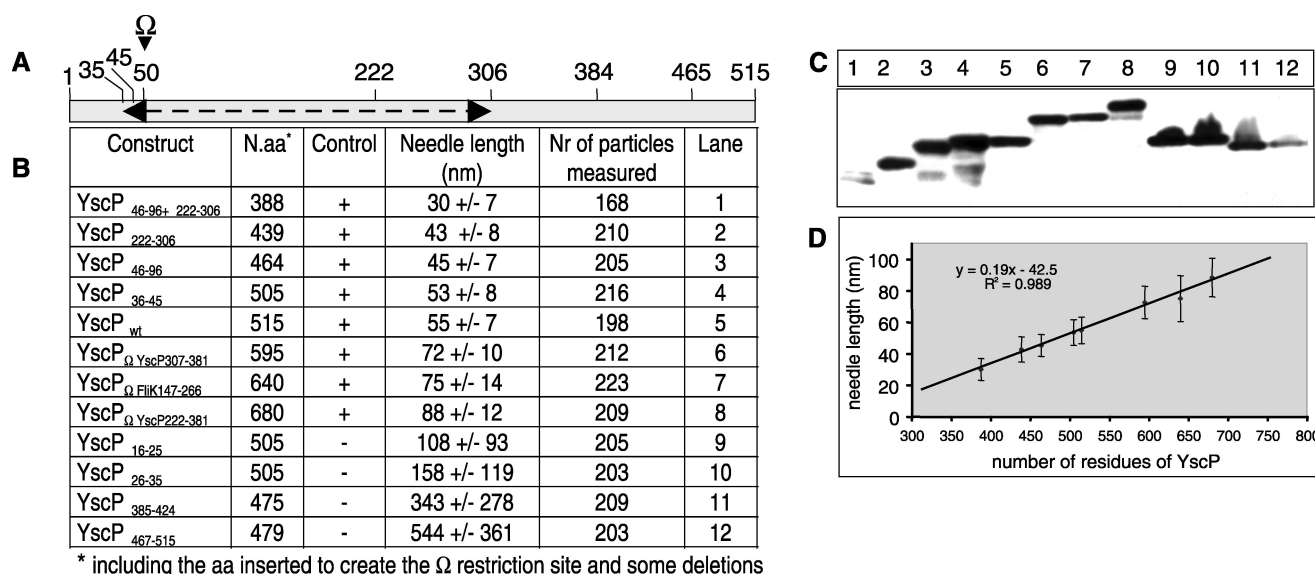


**Fig. 2.** YscP is shorter in *Y. pestis* than in *Y. enterocolitica* and determines shorter needles. (A) Residues 222 to 236 and 261 to 306 from YscP are duplicated in *Y. enterocolitica* E40 and W22703 but not in *Y. pestis* KIM. The *yscP* gene from *Y. pestis* KIM and the *yscP* gene from *Y. enterocolitica* deprived of these repeats were cloned down-

stream from an arabinose-inducible promoter and expressed in the *Y. enterocolitica* *yscP* $_{\Delta 97-465}$  mutant. The figure marked with an asterisk includes a few amino acids inserted to generate the deletion. (B) Histograms of the needle lengths from recombinant *Y. enterocolitica* bacteria.



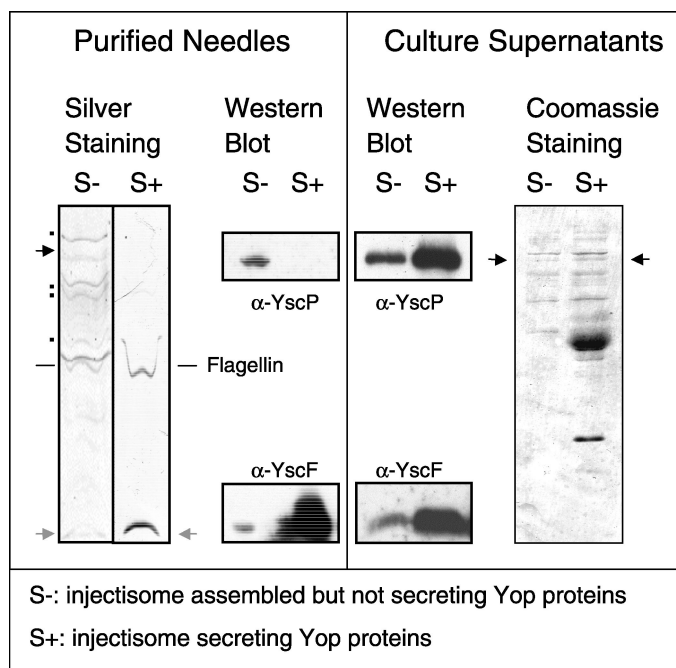
\* including the aa inserted to create the Ω restriction site and some deletions

**Fig. 3.** The needle length is proportional to the number of residues in YscP. (A) Various deletions and insertions were introduced in *yscP<sub>enteroE40</sub>* cloned downstream from the arabinose promoter. Insertions occurred in a restriction site inserted after residue 49 (Ω). The dotted arrow spans the region

where deletions and insertions modify the needle length. (B) Needle length measurements. N. aa, number of amino acids; Nr, number. (C) Expression of the various constructs in *Y. enterocolitica yscP<sub>Δ97-465</sub>* monitored by Western blotting. (D) Plot of the lengths versus the number of residues in YscP.

the allele *yscP<sub>enteroΔ222-306</sub>*<sup>+</sup> encoding YscP<sub>entero</sub> without its repeat. The truncated YscP<sub>enteroΔ222-306</sub> programmed short needles (42.5 ± 8 nm) (Fig. 2), suggesting that the needle length indeed correlated with the size of YscP. To further investigate this hypothesis, we engineered a set of deletions within the cloned *yscP<sub>entero</sub>* gene and used them to complement the *yscP<sub>Δ97-465</sub>* mutation (Fig. 3). Proteins truncated within the first 35 or the last 130 residues were unable to control the length, even though their expression levels were comparable to that of the wild type (Fig. 3). In contrast, YscP with deletions up to 126 amino acids between residues 36 and 306 retained length control but programmed shorter needles. Moreover, the length of the needles was proportional to the size of the YscP protein (Fig. 3). We then inserted a second copy of residues 307 to 381 or 222 to 381 after residue 49, thus generating YscP proteins containing the same 60-residue sequence three or four times (Fig. 3). These mutants programmed longer needles with lengths of 72 ± 10 nm and 88 ± 12 nm, respectively. Insertion of residues 147 to 265 from FliK at the same position also resulted in a functional protein but longer needles (75 ± 14.5 nm). Thus, a strict linear relationship existed between needle length and the number of amino acids in YscP, with 1.9 Å per YscP residue (Fig. 3). To rule out bias as a result of an inadequate gene dosage or gene expression of the complementation plasmids, we replaced the wild-type *yscP* allele on the virulence plasmid by two truncated alleles (*yscP<sub>Δ46-96</sub>* and *yscP<sub>Δ222-306</sub>*). In this native genetic environment, the two alleles again programmed shorter needles than those of the

**Fig. 4.** Association of YscP with the needles. *Y. enterocolitica* E40 deprived of the effectors (ΔHOPEMT) was grown in conditions that are (S+) or are not (S-) permissive for Yop secretion (11). Detached needles purified from 2 × 10<sup>9</sup> (S+) or 10<sup>10</sup> (S-) bacteria were analyzed by silver stained SDS-polyacrylamide gel electrophoresis (SDS-PAGE) and Western blotting (WB) (left). Needle samples prepared from S+ bacteria contain YscF (bottom arrows) and flagellin (middle) as a contaminant but no YscP (top). In contrast, needle samples prepared from S- bacteria contain YscP (top arrow), flagellin, and unidentified contaminants (dots). Proteins from the supernatant from 10<sup>8</sup> bacteria from the same cultures were analyzed by Coomassie-stained SDS-PAGE and WB (right). YscP is visible as a faint band in both the S+ and the S- supernatants (arrows). The darkest band stained in the S+ supernatant is YopB+D. YscF is not visible by Coomassie staining. The prominent bands in the supernatant of S- are cellular contaminants.



wild type (47.5 ± 10 nm and 44 ± 8.5 nm, respectively). Thus, YscP appeared to serve as a ruler determining the length of the needle. This is unprecedented in bacteria but it evokes the molecular rulers controlling the length of bacteriophage tails (16–18), which are structures resembling the needle in morphology, size, and even function. A differ-

ence between the two systems is that tails do not assemble in the absence of the ruler whereas needles are of undetermined length in the absence of YscP. The length per residue is also slightly different for tail rulers (1.5 Å per ruler residue).

If YscP acts as a ruler measuring the growing needle, one might expect it to be associated



## REPORTS

with the needle, at least during the needle elongation stage. To test this, we purified needles from *Y. enterocolitica* incubated in conditions that are either nonpermissive or permissive for secretion (11). Under nonpermissive conditions, some YscP was found in the needle fraction as well as in the culture supernatant, whereas under secretion-permissive conditions YscP was found only in the culture supernatant and not in the needle fraction any more (Fig. 4). These data, fitting with previous reports on the localization of YscP (13, 14), show that YscP is associated with newly synthesized needles that are not secreting Yops but not with needles that are secreting Yops.

We propose that YscP controls the length of the needle by acting as a molecular ruler during the stepwise assembly of the injectisome. Because deletions affecting both N- and C-termini of YscP lead to a loss of length control, we hypothesize that the two ends of YscP act as anchors. One end would be attached to the basal body, whereas the other would be connected to the growing tip of the needle. Whatever the anchor mechanism may be, when the needle reaches its mature length, YscP would be fully stretched and signal, via its internal anchor, to the secretion apparatus, which would stop exporting YscF and switch to other substrates. This model (fig. S1) does not contradict the switch function of YscP (8, 19, 20) but rather includes it in a more complex dual function, which may also exist in some phage tail rulers (21). Taking into account the length of 1.9 Å per residue, the ruler domain of YscP would consist of about 300 to 350 residues, leaving more than 150 residues for anchoring and signaling. The fact that YscP is secreted also fits the model, because an internal ruler would be expected to obstruct the 2- to 3-nm-wide secretion channel (22). This evokes again the phage tail rulers, which are thought to exit the tail before the tail exerts its function (21, 23). Given the similarity between all the type-III secretion systems (5) and the fact that Spa32 (9, 10) InvJ (24), and FliK (25) are also secreted proteins, it is likely that the mechanism demonstrated here for YscP may apply to the control of the needle length in the other bacteria as well as the length of the flagellar hook. The proposed organization of FliK in three regions—export, hinge<sub>(147–265)</sub>, and switch (25)—is also compatible with this view. Finally, the fact that YscP, InvJ, Spa32, and FliK diverged more during evolution suggests that rulers are subjected to fewer constraints. They nevertheless have to share intrinsic properties still to be discovered.

### References and Notes

- G. R. Cornelis, *Nature Rev. Mol. Cell Biol.* **3**, 742 (2002).
- T. Kubori, A. Sukhan, S. I. Aizawa, J. E. Galan, *Proc. Natl. Acad. Sci. U.S.A.* **97**, 10225 (2000).
- T. G. Kimbrough, S. I. Miller, *Proc. Natl. Acad. Sci. U.S.A.* **97**, 11008 (2000).
- A. Blocker et al., *Mol. Microbiol.* **39**, 652 (2001).
- S. I. Aizawa, *FEMS Microbiol. Lett.* **202**, 157 (2001).
- R. M. Macnab, *Annu. Rev. Microbiol.* **57**, 77 (2003).
- T. Hirano, S. Yamaguchi, K. Oosawa, S. Aizawa, *J. Bacteriol.* **176**, 5439 (1994).
- S. Makishima, K. Komoriya, S. Yamaguchi, S. I. Aizawa, *Science* **291**, 2411 (2001).
- K. Tamano, E. Katayama, T. Toyotome, C. Sasakawa, *J. Bacteriol.* **184**, 1244 (2002).
- J. Magdalena et al., *J. Bacteriol.* **184**, 3433 (2002).
- Yersinia* builds injectisomes when temperature reaches 37°C, the host temperature. However, Yop secretion is only triggered upon contact with a target cell or artificially by chelating Ca<sup>2+</sup> ions. The usual procedure consists of growing bacteria at 28°C in oxalated rich medium and then switching the culture to 37°C. In these secretion-permissive conditions, the production of injectisomes is also stimulated. When bacteria are grown at 37°C in the presence of 5 mM Ca<sup>2+</sup>, they make injectisomes but they do not secrete Yops (nonpermissive conditions). Materials and methods are available as supporting material on Science Online.
- E. Hoicyzk, G. Blobel, *Proc. Natl. Acad. Sci. U.S.A.* **98**, 4669 (2001).
- I. Stainier et al., *Mol. Microbiol.* **37**, 1005 (2000).
- P. L. Payne, S. C. Straley, *J. Bacteriol.* **181**, 2852 (1999).
- For complementation, *yscP* DNA was amplified by polymerase chain reaction and cloned in the pBAD expression vector. Expression was induced with arabinose.
- I. Katsura, *Nature* **327**, 73 (1987).
- I. Katsura, R. W. Hendrix, *Cell* **39**, 691 (1984).
- N. K. Abuladze, M. Gingery, J. Tsai, F. A. Eisinger, *Virology* **199**, 301 (1994).
- T. Minamino, R. M. Macnab, *J. Bacteriol.* **182**, 4906 (2000).
- P. J. Edqvist et al., *J. Bacteriol.* **185**, 2259 (2003).
- M. L. Pedulla et al., *Cell* **113**, 171 (2003).
- F. S. Cordes et al., *J. Biol. Chem.* **278**, 17103 (2003).
- R. L. Duda, M. Gingery, F. A. Eisinger, *Virology* **151**, 296 (1986).
- C. M. Collazo, M. K. Zierler, J. E. Galan, *Mol. Microbiol.* **15**, 25 (1995).
- T. Minamino, B. Gonzalez-Pedrajo, K. Yamaguchi, S. I. Aizawa, R. M. Macnab, *Mol. Microbiol.* **34**, 295 (1999).
- We thank M. Duerrenberger for the electron microscopy facility; V. Huschauer for contributing to the needle purification protocol; S. I. Aizawa for advice; M. Kuhn for technical assistance; S. Straley and K. Hughes for supplying *yscP<sub>pestisK1M</sub>* and *Salmonella* LT2; and C. Thompson, U. Jenal, H. Shin, and J. Mota for suggestions. This work was supported by the Swiss National Science Foundation (grant 32-65393.01) and the Swiss Office Fédéral de l'Éducation et de la Science (European Union Human Potential—Research Training Network CT-2000-00075).

### Supporting Online Material

www.sciencemag.org/cgi/content/full/302/5651/1757/DC1

Materials and Methods

Fig. S1

References

11 September 2003; accepted 16 October 2003

# Inflammatory Blockade Restores Adult Hippocampal Neurogenesis

Michelle L. Monje, Hiroki Toda, Theo D. Palmer\*

Cranial radiation therapy causes a progressive decline in cognitive function that is linked to impaired neurogenesis. Chronic inflammation accompanies radiation injury, suggesting that inflammatory processes may contribute to neural stem cell dysfunction. Here, we show that neuroinflammation alone inhibits neurogenesis and that inflammatory blockade with indomethacin, a common nonsteroidal anti-inflammatory drug, restores neurogenesis after endotoxin-induced inflammation and augments neurogenesis after cranial irradiation.

The birth of new neurons within the hippocampal region of the central nervous system continues throughout life, and the amount of neurogenesis correlates closely with the hippocampal functions of learning and memory (1, 2). The generation of new neurons within the hippocampus is mediated by proliferating neural stem or progenitor cells (NPC) (3–5) that are widespread within the adult brain but is instructed by local signaling to produce neurons only in discrete areas (6, 7). Alterations in the microenvironment of the stem cell may allow ectopic neurogenesis to occur (8, 9) or even block essential neurogenesis, leading to deficits in learning and memory (10–12) such as that observed in

patients who receive therapeutic cranial radiation therapy (13). In animal models, cranial irradiation ablates hippocampal neurogenesis, in part by damaging the neurogenic microenvironment, leading to a blockade of endogenous neurogenesis (12, 13). Injury induces pro-inflammatory cytokine expression both peripherally and within the central nervous system and induces stress hormones, such as glucocorticoids, that inhibit hippocampal neurogenesis (10). The extensive microglial inflammation and release of pro-inflammatory cytokines that accompanies this irradiation-induced failure suggests that inflammatory processes may influence neural progenitor cell activity (12, 14, 15).

To determine the effects of inflammation on adult hippocampal neurogenesis, we injected bacterial lipopolysaccharide (LPS) into adult female rats to induce systemic inflammation (16–19). The intraperitoneal (i.p.) administration of LPS causes a peripheral in-

Stanford University, Department of Neurosurgery, MSLS P309, Mail Code 5487, 1201 Welch Road, Stanford, CA 94305–5487, USA.

\*To whom correspondence should be addressed. E-mail: tpalmer@stanford.edu

## Supporting Online Material

### Materials and Methods

*Yersinia enterocolitica* MRS40(pYV40) (S1), an ampicillin-sensitive derivative of E40(pYV40)(S2) was used for genetics and electron microscopy. An effector multimitant, called ΔHOPEMT, MRS40(pIML421)(S3) was used to prepare needles. The various pYV plasmid mutants and the expression plasmids are listed in Table S1. The oligonucleotides used for genetic constructions are given in table S2.

Bacteria were routinely grown on Luria-Bertani agar plates and in liquid Luria-Bertani medium. For the induction of the *yop* regulon, *Y. enterocolitica* bacteria were inoculated to an OD<sub>600</sub> of 0.1 and cultivated in brain-heart infusion (BHI; Remel) supplemented with 4 mg/ml glycerol, 20 mM MgCl<sub>2</sub> and 20 mM sodium oxalate (BHI-Ox) for 2 h at 28 °C, then shifted to 37 °C and incubated for 4 h(S4). Expression of the different *yscP* genes cloned downstream from the pBAD promoter was induced by adding 0.2 % arabinose to the culture just before the shift at 37 °C, and again two hours later. Ampicillin was used at a concentration of 200 g/ml to select for the expression plasmids.

Alleles to be inserted in the pYV plasmids were subcloned into the pKNG101 suicide vector and the allelic exchange was selected by plating diploid bacteria on sucrose(S5).

Proteins from the supernatant were precipitated overnight at 4°C with trichloroacetic acid 10% (w/v) final. Electrophoresis was carried out in 12 % or 15 % (w/v) polyacrylamide gels in the presence of SDS (SDS-PAGE). Proteins secreted by 3x10<sup>8</sup> bacteria were loaded by lane. For the total bacterial cells, the proteins from 10<sup>7</sup> bacteria were loaded by lane. After electrophoresis, proteins were stained with Coomassie brilliant blue (Pierce) or transferred by electroblotting to a nitrocellulose

membrane. Immunoblotting was carried out using rabbit polyclonal antibodies (anti-YscP(S6)), polyclonal anti-YscF antibodies raised against the synthetic YscF peptide (NMSGFTKGNDIADLDAVAQTLK) (Centre d'Economie Rurale, Marloie, Belgium). Detection of immunoblots was performed with secondary antibodies conjugated to horse-radish peroxidase (1:2000; Dako) before development with supersignal chemiluminescent substrate (Pierce).

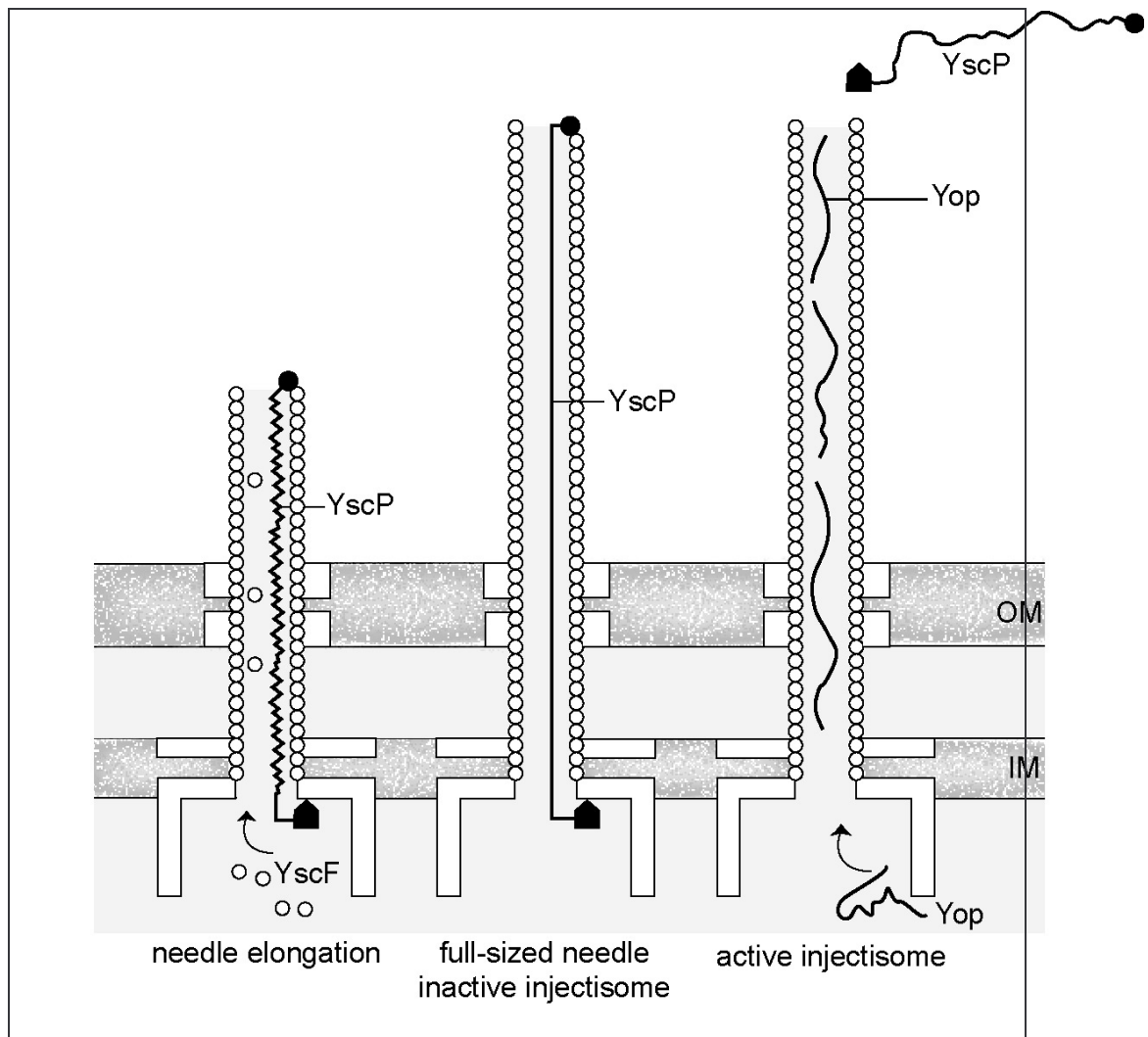
Visualization of the needle-like structures at the cell surface of the bacteria was done by electron microscopy as described by Hoiczky and Blobel(S7). After 4 hours of induction at 37 °C, bacteria were harvested at 2,000  $\times$  g and resuspended gently in Tris-HCl, pH 7.5. Droplets were applied for 1 min to freshly glow-discharged, formvar-carbon coated grids, and negatively stained with 1% (wt/vol) uranylacetate. Bacteria were visualized in a Philips Morgagni 268D electron microscope at a nominal magnification of  $\times$  44,000 and an acceleration voltage of 80 kV. Sizes were measured with the "Soft Imaging System" software (Hamburg, Germany). The corresponding cells were analysed in parallel for the presence of YscF by immunoblot.

In order to purify needles, bacteria were cultivated for 2h at 28 °C in BHI-Ox or BHI-Ca<sup>2+</sup>, then shifted to 37 °C and incubated for 4h(S4). Bacteria were harvested by centrifugation (10 min at 5'700  $\times$  g) and washed once in 1/30 of the culture volume with 20 mM TrisHCl (pH 7.5). The washing supernatant was passed through a 0.45  $\mu$ m mesh filter and centrifugated for 30 min at 17'500  $\times$  g. The pellet was resuspended in 1/60 of the initial culture volume of TrisHCl 20 mM (pH 7.5), CHAPS 0.1% (w/v) and centrifuged again for 30 min at 17'500  $\times$  g. The supernatant was collected and the needles were precipitated for one hour one ice with polyethylene glycol 6000 (10% w/v) and NaCl (100 mM). The needles were then collected by 30-



min centrifugation at  $17'500 \times g$  and resuspended in 1/300 of initial culture volume of 20 mM TrisHCl (pH 7.5).

**Figure S1**



**Legend to fig S1**

Proposed model for the control of the YscF-needle length by the YscP ruler.

**Table S2: Oligonucleotides used in this study**

Oligo code	Oligonucleotide sequence	Underlined
3072	gatcc <u>catgg</u> ccaataaaatcaccactcgt	<i>NcoI</i>
3073	gatcga <u>attctt</u> attcttcagcctcccactc	<i>EcoRI</i>
3066	ttcatactcaggttctaattgg	
3067	gcacgtgccgattttgagcaa	
3068	ttgcaaatcatgatgcagctt	
3069	cataataataaggtaatcgt	
3070	caacagcgcttgctcaaaatc	
3071	gaagagcccgcgtagacctgta	
3078	gtcag <u>cgccgctt</u> gtctagacgaagaaccgttaccttt	<i>NorI, XbaI</i>
3079	gtcag <u>cgccgc</u> catacatctccagcaaggt	<i>NorI</i>
3124	ttgggatgacgattacc	
3126	catgattaaacttatct	
3187	gatc <u>cgccgc</u> caatctctagacgcgctcttct	<i>NorI, XbaI</i>
3188	gatc <u>cgccgc</u> ctagacctgtacgtccgatgac	<i>NorI</i>
3239	gtcatggcggacgtacaggtc	
3240	gaagaaccgttaccttca	
3242	agacaaggaatacatctc	
3243	ctgcgcccggctcatcc	
3244	ttctagtctaccgctag	
3245	gaagctttaagaattta	
3083	gtcag <u>cgccgctt</u> gtctagagctgccggacaacctgac	<i>NorI, XbaI</i>
3084	gtcag <u>cgccgc</u> ctaacggcgcgctgagtac	<i>NorI</i>

### Supplementary references

- S1. M. R. Sarker, M. P. Sory, A. P. Boyd, M. Iriarte, G. R. Cornelis, *Infect. Immun.* **66**, 2976 (1998).
- S2. M. P. Sory, G. R. Cornelis, *Mol. Microbiol.* **14**, 583 (1994).
- S3. M. Iriarte, G. R. Cornelis, *Mol. Microbiol.* **29**, 915 (1998).
- S4. G. Cornelis, J. C. Vanootegem, C. Sluifers, *Microb. Pathog.* **2**, 367 (1987).
- S5. K. Kaniga, I. Delor, G. R. Cornelis, *Gene* **109**, 137 (1991).
- S6. I. Stainier *et al.*, *Mol. Microbiol.* **37**, 1005 (2000).
- S7. E. Hoiczky, G. Blobel, *Proc. Natl. Acad. Sci. U. S. A.* **98**, 4669 (2001).
- S8. P. L. Payne, S. C. Straley, *J. Bacteriol.* **181**, 2852 (1999).

## 3 Results

### **3.2 Protective Anti-V Antibodies Inhibit Pseudomonas and Yersinia Translocon Assembly within Host Membranes**

Gouré J. \*, Broz P. \*, Attree O., Cornelis G.R., and Attree I.

**Journal of Infectious Diseases** 192:218-25 (2005)

*\*These authors contributed equally to the work*

## Summary

Pathogenic *Yersinia* species and *P. aeruginosa* share a similar type III secretion system. The translocon consists of the proteins YopB/PopB, YopD/PopD and LcrV/PcrV; the latter is known to be a protective antigen. The translocators cause hemolysis of erythrocytes infected with wildtype *P. aeruginosa*. Wildtype *Y. enterocolitica* is only slightly hemolytic, but a multiknockout mutant deprived of all the effectors and of YopN ( $\Delta$ HOPEMN) is hemolytic. We showed that anti-PcrV and also antibodies directed against LcrV from *Y. pestis* protect erythrocytes from *P. aeruginosa* caused lysis, while anti-PopB and anti-PopD antibodies have no effect. Similarly the anti-LcrV antibodies inhibited the hemolytic activity of  $\Delta$ HOPEMN *Y. enterocolitica*.

Wildtype *Yersinia* inserted the translocators YopB and YopD into erythrocyte membranes but no LcrV could be detected. A mutant in *lcrV* ( $\Delta$ HOPEMNV) inserted reduced amounts of YopB and YopD into erythrocyte membranes but could not assemble a functional pore. The assembly of the translocation pore, composed of the translocators YopB/YopD and PopB/PopD was disturbed in immunoprotected membranes mimicking the phenotypes of V knockout mutants. Thus, protective antibodies against the V antigens of *Yersinia* and *P. aeruginosa* act at the level of the formation of the translocation pore in membranes of infected host cells by blocking the function of the V antigen. The V antigen could act as an extrabacterial chaperone or assembly scaffold for the translocation pore.

## Statement of my work

I contributed to this publication by performing all the experiments done with *Y. enterocolitica* i.e. the figures 3 and 4. I was involved in writing the manuscript.

# Protective Anti-V Antibodies Inhibit *Pseudomonas* and *Yersinia* Translocon Assembly within Host Membranes

Julien Goure,<sup>1,a</sup> Petr Broz,<sup>3,a</sup> Olivier Attree,<sup>2</sup> Guy R. Cornelis,<sup>3</sup> and Ina Attree<sup>1</sup>

<sup>1</sup>Biochimie et Biophysique des Systèmes Intégrés, CEA-Grenoble, UMR5092 CNRS, Grenoble, and <sup>2</sup>Centre de Recherches du Service de Santé des Armées, La Tronche, France; <sup>3</sup>Biozentrum der Universität Basel, Switzerland

Pathogenic *Yersinia* species and *Pseudomonas aeruginosa* share a similar type III secretion/translocation system. The translocation system consists of 3 secreted proteins, YopB/PopB, YopD/PopD, and LcrV/PcrV; the latter is known to be a protective antigen. In an in vitro assay, the translocation system causes the lysis of erythrocytes infected with wild-type (*wt*) *P. aeruginosa*. *wt* *Y. enterocolitica* is not hemolytic, but a multiknockout mutant deprived of all the effectors and of YopN ( $\Delta$ HOPEMN) is hemolytic. In the presence of antibodies against PcrV and *Y. pestis* LcrV, the hemolytic activity of *P. aeruginosa* was inhibited. Similarly, the hemolytic activity of  $\Delta$ HOPEMN was inhibited in the presence of anti-LcrV antibodies. The assembly of the translocon, composed of PopB/D and YopB/D proteins, was disturbed in immunoprotected erythrocyte membranes, mimicking the phenotypes of V knockout mutants. Thus, protective antibodies against the V antigens of *Yersinia* species and *P. aeruginosa* act at the level of the formation of the translocon pore in membranes of infected host cells by blocking the function of LcrV/PcrV. The hemolysis assay could be adapted for high-throughput screening of anti-infectious compounds that specifically target the type III translocon.

Injectisomes are complex nanomachines that allow pathogenic or symbiotic bacteria to inject proteins across the membrane of eukaryotic host cells. They consist of a basal body that contains a type III secretion (T3S) apparatus and a stiff needle that can be extended by a flexible pilus or filament [1, 2]. Upon contact with a eukaryotic cell membrane, the injectosome secretes, presumably in a sequential manner, a set of proteins called “translocators” and “intracellular effectors” [3, 4]. The translocators are a group of, generally, 3 proteins that are absolutely required for the proper delivery of the effectors across the host cell membrane [3–12].

Pathogenic members of the genus *Yersinia*—for ex-

ample, *Y. pestis* (the causative agent of plague) and the enteric pathogens *Y. enterocolitica* and *Y. pseudotuberculosis*—share a common injectosome called “Ysc” and a common set of translocators and effectors called “Yops.” The translocators are called “YopB,” “YopD,” and “LcrV.” The latter is a bona fide Yop; it has a different name because it was discovered as a soluble protective antigen linked to virulence (hence, it is named “V antigen”) >40 years ago [13, 14], long before the concept of T3S had been shaped [15]. Interestingly, the opportunistic pathogen *Pseudomonas aeruginosa*, which is evolutionarily remote from enterobacteriaceae, has a very similar injectosome called “Psc” and a set of similar translocators called “PopB,” “PopD,” and “PcrV” [16–18]. Both sets of translocators have been shown to form pores in erythrocytes (red blood cells [RBCs]) [5, 9], in eukaryotic cell membranes [19, 20], and in liposomes [21]. Formation of pores is readily detectable with wild-type (*wt*) *P. aeruginosa* but not with *wt* *Y. enterocolitica*. Only *Y. enterocolitica* mutants that are devoid of the effectors or of the control protein YopN form readily detectable pores [5, 11, 20]. An interpretation of this observation is that translocated Yop effectors obstruct the translocation chan-

Received 15 December 2004; accepted 11 February 2005; electronically published 7 June 2005.

Financial support: French Cystic Fibrosis Association “Vaincre la Mucoviscidose” (grant I10327 to I.A.); “Emergence 2003” program from the Rhône-Alpes region (support to I.A.); Swiss National Science Foundation (grant 32-65393.01).

<sup>a</sup> J.G. and P.B. contributed equally to the work.

Reprints or correspondence: Dr. Ina Attree, DRDC/BBSI, CEA Grenoble, 17 rue des Martyrs, 38054 Grenoble cedex 09, France (iattreedelic@cea.fr).

The Journal of Infectious Diseases 2005;192:218–25

© 2005 by the Infectious Diseases Society of America. All rights reserved. 0022-1899/2005/19202-0005\$15.00

**Table 1. Bacterial strains.**

Strains	Relevant genotype or phenotype	Reference
<i>P. aeruginosa</i> , CHA	Mucoid, cytotoxic cystic fibrosis isolate	[32]
<i>Y. enterocolitica</i> E40	Wild-type strain with the plasmid pYV40	[39]
ΔHOPEMN	pYV40 <i>yopE</i> <sub>21</sub> <i>yopH</i> Δ <sub>41–352</sub> <i>yopO</i> Δ <sub>65–558</sub> <i>yopP</i> <sub>23</sub> <i>yopM</i> <sub>23</sub> <i>yopN</i> <sub>45</sub>	[11]
ΔHOPEMNV	pYV40 <i>yopE</i> <sub>21</sub> <i>yopH</i> Δ <sub>41–352</sub> <i>yopO</i> Δ <sub>65–558</sub> <i>yopP</i> <sub>23</sub> <i>yopM</i> <sub>23</sub> <i>yopN</i> <sub>45</sub> <i>lcrV</i> Δ <sub>6–319</sub>	[11]
ΔHOPEMNVQ	pYV40 <i>yopE</i> <sub>21</sub> <i>yopH</i> Δ <sub>41–352</sub> <i>yopO</i> Δ <sub>65–558</sub> <i>yopP</i> <sub>23</sub> <i>yopM</i> <sub>23</sub> <i>yopN</i> <sub>45</sub> <i>lcrV</i> Δ <sub>6–319</sub> <i>yopQ</i> <sub>17</sub>	[20]
ΔHOPEMNB	pYV40 <i>yopE</i> <sub>21</sub> <i>yopH</i> Δ <sub>41–352</sub> <i>yopO</i> Δ <sub>65–558</sub> <i>yopP</i> <sub>23</sub> <i>yopM</i> <sub>23</sub> <i>yopN</i> <sub>45</sub> <i>yopB</i> Δ <sub>89–217</sub>	[20]
ΔHOPEMND	pYV40 <i>yopE</i> <sub>21</sub> <i>yopH</i> Δ <sub>41–352</sub> <i>yopO</i> Δ <sub>65–558</sub> <i>yopP</i> <sub>23</sub> <i>yopM</i> <sub>23</sub> <i>yopN</i> <sub>45</sub> <i>yopD</i> Δ <sub>121–165</sub>	[20]
ΔN	pYV40 <i>yopN</i> <sub>45</sub>	[6]

**NOTE.** *P. aeruginosa*, *Pseudomonas aeruginosa*; *Y. enterocolitica*, *Yersinia enterocolitica*.

nel [5, 20]. However, it has also been shown that the Rho-GAP activity of YopE prevents membrane damage in cells infected with *wt* bacteria [22]. When YopN is missing, secretion is contact independent and effectors are not efficiently translocated [11]. The structure of the translocation pore, the stage during which the translocation pore is inserted, and how it is connected to the needle of the injectisome are not clear yet. It is tempting to consider the translocation pore as an integral part of the injectisome, but, unlike the needle, it could be assembled only after contact with a target cell. It has been shown that PopB and PopD are able to oligomerize *in vitro* and that their interaction with lipids promotes the formation of ringlike structures with external and internal diameters of 80 and 40 Å, respectively [23]. Although PcrV is unable to interact with lipids either *in vitro* or *in vivo* [9, 23], it is required for proper assembly of the PopB/D translocon in membranes of infected erythrocytes [9].

*Y. pestis* LcrV possesses a highly protective antigenic character, and antibody therapy against bubonic and pneumonic plague has been shown to be effective when tested in animal models of disease [24–26]. Similarly, in animal models, active immunization with PcrV or passive immunization with anti-V antibodies provides a high level of protection against lethal *P. aeruginosa* infections [7, 27]. Furthermore, administration of anti-PcrV F(ab')<sub>2</sub> in a *P. aeruginosa*–provoked sepsis model reduced the inflammatory response and bacteremia levels [28]. Although the mechanism of action is not known, even *in vitro*, anti-V antibodies prevent the cytotoxicity of bacteria toward cultured cells [7, 29, 30].

In the present study, we examined the action of anti-V antibodies on formation of the translocation pore in *P. aeruginosa* and *Y. enterocolitica* hemolysis assays. It has already been shown with *P. aeruginosa* that a high level of hemolysis can be obtained at a low MOI (MOI, 1) within 1 h of coinubation. Another advantage of this model is that RBCs are not a limiting factor, and their membranes can be isolated after infection and analyzed for translocon proteins without being contaminated with infecting bacteria [9, 31]. In the present study, we applied the

RBC assay to *Yersinia* species by using poly-Yop effector mutants of *Y. enterocolitica* [20]. We demonstrate that the antibodies against the V antigens, through their direct interaction with V proteins, inhibit bacteria-induced hemolysis by acting at the level of type III translocon assembly in host cell membranes, for both pathogenic species.

## MATERIALS AND METHODS

**Bacterial strains and growth conditions.** The bacterial strains used in the present study are listed in table 1. The *P. aeruginosa* strain used was the cytotoxic cystic fibrosis isolate CHA [19, 32]. *P. aeruginosa* were grown either on *Pseudomonas* isolation agar (Difco) plates or in liquid Luria broth (LB) medium at 37°C with agitation. All the mutants of *Y. enterocolitica* used were derived from the strain E40, a strain from serotype O:9 [4, 11]. *Y. enterocolitica* strains were inoculated to an OD<sub>600</sub> of 0.1 and cultivated in brain-heart infusion broth (ICN) for 3 h at 37°C. *In vitro*, secretion of *Y. enterocolitica* was triggered by sodium oxalate [11].

**Production and purification of antibodies.** The production and purification of the rabbit-derived anti-PcrV, anti-PopB, and anti-PopD polyclonal antibodies (PABs) have been described elsewhere [9, 23]. MAb166 [27] was provided by D. W. Frank (Medical College of Wisconsin). The LcrV coding sequence was obtained from genomic DNA of the *Y. pestis* strain EV76 (gift from E. Carniel, Pasteur Institute, Paris) by polymerase chain reaction (PCR) using the primers 5'-GATAAGAA-TTCGAGCCTACGAACAAAACCCA-3' and 5'-AAGGATCGT-CGACTTACATAATTACCTCGTGTCA-3'. The PCR product was digested with *EcoRI* and *Sall* and cloned into the expression plasmid pGEX-6P-2 (Amersham Biosciences). A soluble glutathione-S-transferase (GST)–LcrV fusion was produced in *Escherichia coli* and purified on GSTrap (Amersham Biosciences). The GST-LcrV protein fusion bound on the column was cleaved with PreScission Protease (Amersham), resulting in the elution of purified LcrV. Three CD1 mice were immunized with 100-μL intramuscular injections of 10 μg of purified LcrV in PBS con-

taining 2% alhydrogel (Superfos Biosector) and 10  $\mu\text{g}$  of CpG oligonucleotide [33] as adjuvant. In each mouse, after 2 immunizations separated by a 2-week interval, the ELISA titer (the highest dilution giving twice the optical density obtained with naive CD1 serum) of anti-LcrV serum antibodies was  $>1:50,000$ . For production of anti-LcrV PABs, the best-responding mouse was given an intraperitoneal (ip) booster injection of the same respective amounts of LcrV, alhydrogel, and CpG, followed 5 days later by a final ip injection containing LcrV, CpG, and  $5 \times 10^5$  TG180 sarcoma cells. The ascitis fluid was collected 1 week later, and IgG was purified on protein A (Mab Trap; Amersham). The BCA protein assay kit (Pierce) was used to determine the concentration of purified antibodies.

**Hemolysis assays and immunoprotection experiments.** Hemolysis assays were performed as described elsewhere [9]. Briefly, sheep RBCs (Eurobio) were washed 3 times in PBS (pH 7.4) (150 mmol/L NaCl) and resuspended in RPMI 1640 medium (Sigma) at  $5 \times 10^8$  RBCs/mL at 4°C. Bacteria were grown in LB to an  $\text{OD}_{600}$  of 1.0, centrifuged, and resuspended in RPMI 1640 at  $5 \times 10^8$  bacteria/mL. Hemolysis assays were initiated by mixing 100  $\mu\text{L}$  of RBCs and 100  $\mu\text{L}$  of bacteria in round-bottom 96-well plates, which were then centrifuged at 2000 g for 10 min and incubated for 1 h at 37°C. The release of hemoglobin was measured, and the percentage of hemolysis was calculated as described elsewhere [31]. Immunoprotection experiments were performed by incubating bacteria for 45 min

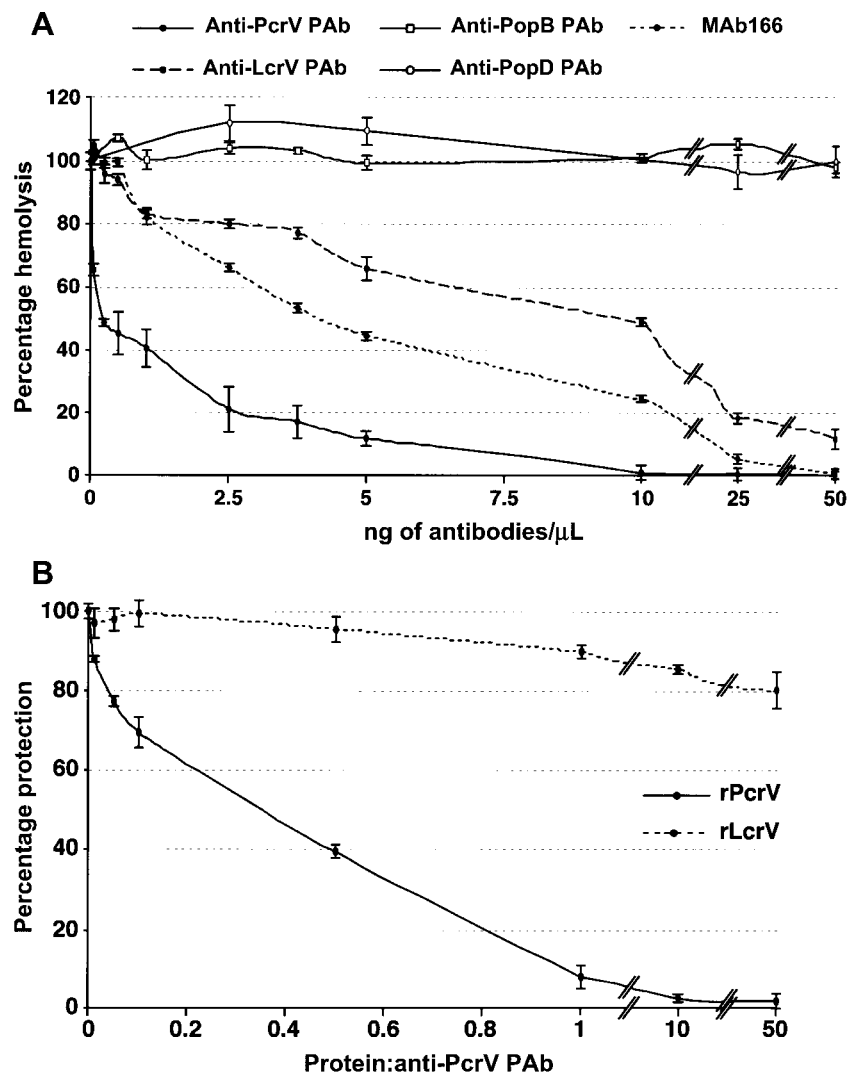


**Figure 1.** Immunoprotection of red blood cells (RBCs) against *Pseudomonas aeruginosa*-induced hemolysis. *A*, Lysis of RBCs by type III secretion of *P. aeruginosa* (MOI, 1) at 37°C, after 1 h in the presence of different antibodies added to the bacteria before coinoculation. Anti-PcrV and anti-PopB polyclonal antibodies (PABs) were affinity purified from rabbit serum, anti-LcrV PABs were purified on protein A from mouse serum, and anti-PopD was total rabbit serum. MAb166 is a protective monoclonal antibody against PcrV [27]. *B*, Titration of protective antibodies by recombinant LcrV (rLcrV) or PcrV (rPcrV). The hemolysis assay was performed in the presence of immunoprotective anti-PcrV PABs added in quantities necessary to achieve 90%–100% protection. Purified rPcrV and rLcrV proteins were added to the assay, and hemolysis was measured after 1 h of incubation.



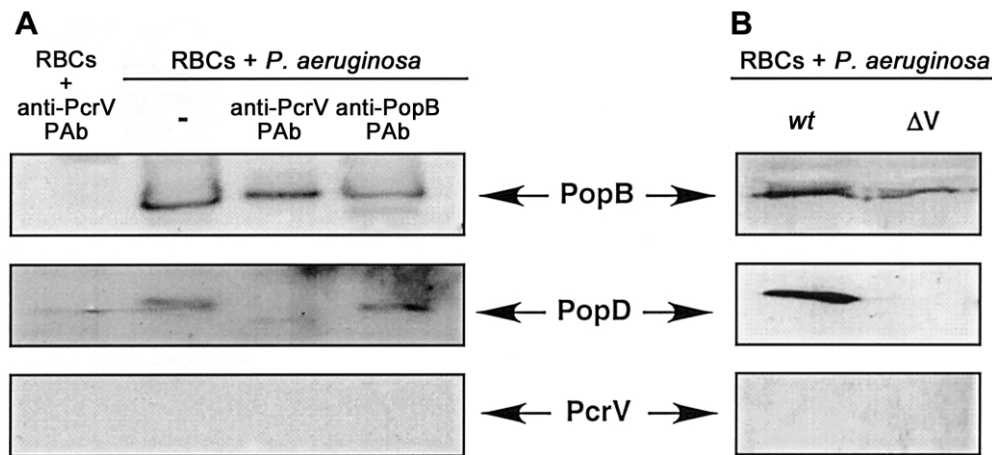


**Figure 2.** Assembly of the *Pseudomonas aeruginosa* PopB/D translocon in immunoprotected red blood cell (RBC) membranes. *A*, RBC membranes isolated on sucrose density gradients after performance of hemolysis assays in the presence of either protective anti-PcrV polyclonal antibodies (PABs) or anti-PopB PABs. *B*, RBC membranes isolated after hemolysis assay with the wild-type (*wt*) and the *pcrV* mutant ( $\Delta V$ ) [9]. The translocon content of PopB, PopD, and PcrV within membranes was analyzed by Western blotting.

with different concentrations of antibodies at room temperature, before the standard hemolytic assay. Negative controls included corresponding preimmune rabbit serum. In titration experiments, a constant concentration of 5 ng/ $\mu$ L PABs was added to bacteria, then increasing amounts of the recombinant PcrV or LcrV were incubated with the bacteria-PAB mixture for 45 min at room temperature.

**RBC membrane isolation.** RBCs were resuspended in Tris-saline (30 mmol/L Tris and 150 mmol/L NaCl [pH 7.5]) at  $1 \times 10^{10}$  cells/mL. Before the infection,  $3 \times 10^9$  bacteria were incubated with 180  $\mu$ g of PABs in 700  $\mu$ L of Tris-saline buffer for 45 min at room temperature. Then, hemolytic reactions were prepared in 50-mL conical tubes. The mixture of bacteria and antibodies was mixed with 300  $\mu$ L of RBCs at  $1 \times 10^{10}$  cells/mL and 1 mL of a  $2 \times$  protease inhibitor cocktail (Complete; Roche). Samples were centrifuged at 2000 *g* for 10 min at room temperature and incubated for 1 h at 37°C. Hemolysis was assessed spectrophotometrically, as described above. Then, 3 mL of distilled water at 4°C was added to each sample to lyse all RBCs, and these were vortexed and centrifuged again to remove bacteria. The RBC membranes were isolated by flotation on a sucrose density gradient, as described elsewhere [9]. The material at the 44%/25% sucrose interface was collected, diluted in Tris-saline, and concentrated by centrifugation in a TLA-100.3 rotor (Beckman) at 450,000 *g* for 20 min at 4°C. The pellets were resuspended in Laemmli sample buffer and analyzed by Western blotting.

**Immunoblotting analysis.** Immunoblotting analysis was performed with primary PABs against YopB (gift from Å. Forsberg, Umeå University), PopB, PopD, and PcrV [9]; monoclonal antibodies (MAbs) against YopD [20] and LcrV [11]; and a secondary antibody conjugated to horseradish peroxidase (Sig-

ma). Membranes were developed by use of an enhanced chemiluminescence kit (Amersham Biosciences).

## RESULTS AND DISCUSSION

Since PcrV has been found to be necessary for assembly of PopB/D pores in RBC membranes [9], we asked whether antibodies against PcrV would interfere with the PopB/D-dependent hemolysis induced by cytotoxic *P. aeruginosa* strain CHA. Affinity-purified PABs against translocator proteins PopB and PopD did not inhibit hemolysis. Concentrations of both antibodies up to 50 ng/ $\mu$ L had no protective effect. In contrast, affinity-purified anti-PcrV PABs [9] mixed with either bacteria or RBCs before infection inhibited hemolysis in a dose-dependent manner (figure 1A). Concentrations of antibodies as low as 0.25 ng/ $\mu$ L were able to reduce *P. aeruginosa*-induced lysis by 50%. Increasing the concentration of antibodies up to 10 ng/ $\mu$ L in the infection assay resulted in complete protection of RBCs from lysis. MAb166 is an anti-PcrV MAb that has been shown to protect mice from lethal *P. aeruginosa* infection [27]. In the hemolysis assay, MAb166 prevented hemolysis, but an 18-fold greater concentration of MAb166 than of PABs was required to obtain 50% inhibition. The higher neutralization activity of the PABs could be due to the binding of several PcrV epitopes or to a higher affinity of some antibody component, compared with MAb166. The former hypothesis is favored because, in a competition ELISA, a 100-fold excess of PAB did not hinder the binding of MAb166 to recombinant PcrV (rPcrV) (data not shown). This could have practical importance, because efficient neutralization of PcrV by MAbs would then require a combination of several MAbs, as seems to be the case for botulinum toxin type A [34].

LcrV from *Yersinia* species and PcrV from *P. aeruginosa* share 41% amino acid identity [16], and they most likely share the same function in the assembly of the translocon. We raised mouse PABs against recombinant LcrV (rLcrV) from *Y. pestis*. Similar to anti-PcrV PABs and MAb166, anti-LcrV PABs inhibited *P. aeruginosa*-induced hemolysis (i.e., 50% inhibition was obtained with 10 ng/ $\mu$ L anti-LcrV PABs). In summary, these data show that the PABs against PcrV and LcrV, as well as the protective MAb166, hinder cytotoxic *P. aeruginosa* from lysing RBCs.

LcrV and PcrV are surface-exposed antigens ([29, 35] and I.A., unpublished data) and, therefore, are probably accessible to antibodies. To further confirm that the protection against hemolysis was due to the direct interaction between antibodies and the antigen during the infection process, we set up competition experiments in which the antibodies necessary to achieve 90%–100% protection were kept constant and increasing amounts of the recombinant antigen were added to the infection mixture. With rPcrV, as few as 3–4 molecules/10 molecules of antibodies were sufficient to restore 50% hemolysis, showing that the protection is due to direct PcrV/antibody interaction (figure 1B).

RBC lysis occurs by osmotic shock following the formation of PopB/D pores within erythrocyte membranes. Since PcrV is required for formation of functional Pop pores, we addressed the question of whether PopB/D inserts into membranes in the presence of anti-V antibodies. The hemolysis assay was scaled up, and antibodies were added at levels necessary to achieve 90%–100% protection. After 1 h of incubation, the RBCs were lysed by the addition of water, and the membranes were purified by sucrose density gradient, as described elsewhere [9]. The purified membranes were examined for the presence of Pop translocators by Western blotting. *P. aeruginosa*-infected RBC membranes contained both translocators, PopB and PopD, as reported elsewhere (figure 2) [9]. Notably, in the presence of anti-PcrV PABs, PopD protein was absent from infected RBC membranes (figure 2), corroborating the phenotype of the PcrV knockout bacteria that were unable to assemble the functional translocon (figure 2) [9]. It should be noted that systematically less PopB could be detected in membranes purified from these immunoprotection experiments. Antibodies against PopB were not able to disturb PopB/D pores inserted into host membranes (figure 2), which is in agreement with the incapacity of these antibodies to immunoprotect infected RBCs. These results show that anti-PcrV antibodies either block the proper insertion of pore-forming proteins or destabilize them within membranes. That PopB was still found in immunoprotected membranes, although it was unable to form functional pores, suggests that protective antibodies do not prevent contact between the host cell and the bacterial injectisome.

Since the serum raised against the *Y. pestis* rLcrV prevented, to some degree, *P. aeruginosa* T3S-induced hemolysis, we applied the hemolysis test to several *Y. enterocolitica* strains. As

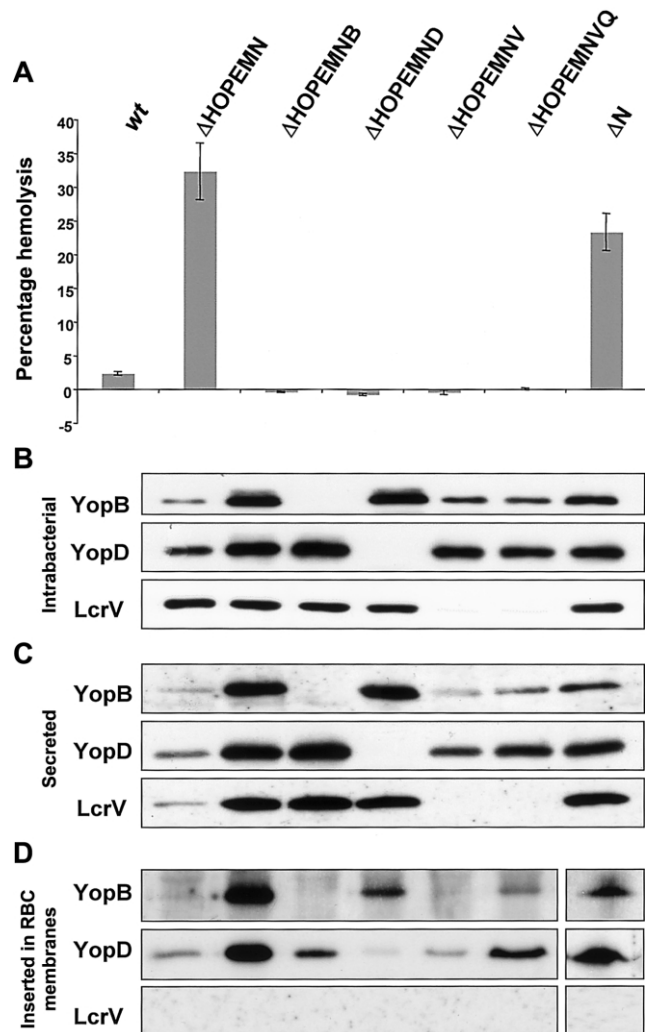


**Figure 3.** Lysis of red blood cells (RBCs) by the Ysc-Yop type III secretion system from *Yersinia enterocolitica*. The removal of YopQ minimizes the negative effect of the *lcrV* deletion on synthesis of YopB and YopD [11]. *A*, Percentage hemolysis after 1 h of contact (MOI, 1). *B*, *C*, and *D*, Western blot analysis of YopB, YopD, and LcrV performed on intrabacterial proteins (*B*), the total amount of proteins secreted by the bacteria during the infection (*C*), and proteins inserted into the membranes of erythrocytes (*D*). *wt*, wild-type bacteria;  $\Delta$ HOPEMN, a multi-effector  $Ca^{2+}$ -blind knockout [20];  $\Delta$ HOPEMNB,  $\Delta$ HOPEMN lacking translocator YopB [20];  $\Delta$ HOPEMND,  $\Delta$ HOPEMN lacking translocator YopD [20];  $\Delta$ HOPEMNV,  $\Delta$ HOPEMN lacking translocator LcrV [11];  $\Delta$ HOPEMNVQ,  $\Delta$ HOPEMNV lacking YopQ;  $\Delta$ N, *wt* lacking regulator YopN [6].

was already reported by several authors [5, 20], the *wt Yersinia* strains had very low hemolytic activity, even when the bacteria–host cell contact was forced with centrifugation. Indeed, no detectable hemolysis could be observed at 1 h after infection (figure 3A). Neyt et al. [20] and Marenne et al. [11] reported that, in contrast to the *wt* strain, the mutant strain  $\Delta$ HOPEMN, which lacks T3S effectors (YopH, -O, -P, -E, and -M) as well as the control protein YopN [36], provokes macrophage cell lysis through the formation of pores presumably constituted

by the translocators YopB and YopD. Notably, in the standard RBC assay,  $\Delta$ HOPEMN bacteria lysed ~30% of the erythrocytes within 1 h of coincubation (MOI, 1), a value lower than that observed with cytotoxic *P. aeruginosa* but still very significant (figure 3A).  $\Delta$ HOPEMN-induced hemolysis was dependent on the presence of LcrV, since the mutant  $\Delta$ HOPEMNV showed only a basal level of hemolysis. In addition, LcrV was not directly hemolytic to RBCs, since the mutants  $\Delta$ HOPEMNB and  $\Delta$ HOPEMND, which secrete the same amounts of LcrV as *wt* bacteria, were not hemolytic. This result is in agreement with data showing that *P. aeruginosa* strains that secrete PcrV are nonhemolytic [9]. *lcrV* mutants are known to produce less YopB and YopD, compared with *wt* bacteria [37–39], and this effect can be attenuated by also mutating *yopQ* (figure 3C) [11]. We thus also tested a  $\Delta$ HOPEMNVQ mutant in the hemolysis assay, and it was also found to be nonhemolytic (figure 3A), showing that the lack of hemolysis observed with  $\Delta$ HOPEMNV was not due to insufficient secretion of YopB and YopD but was directly due to the absence of LcrV (figure 3C).

Since PcrV is required for correct formation of PopB/D pores, we addressed the function of LcrV in *Y. enterocolitica*. RBC membrane fractions were examined for the presence of the translocators after infection with the same strains of *Y. enterocolitica* (figure 3D). Only YopD was readily detectable in membranes of RBCs infected with *wt* bacteria. In contrast, YopB and YopD were readily detectable in membranes of RBCs infected with  $\Delta$ HOPEMNVQ, but the amount of both translocators, especially YopB, was reduced, compared with that in  $\Delta$ HOPEMN or  $\Delta$ N bacteria. This may simply reflect the fact that  $\Delta$ HOPEMNVQ bacteria secrete less YopB/D than do  $\Delta$ HOPEMN bacteria, but it should be noted that they secrete at least as much YopB as do *wt* bacteria (figure 3C). Nevertheless, although both YopB and YopD were detected in the membrane, no pore was formed. This suggests that, although LcrV is necessary for the proper assembly of the YopB/D pore in the host cell membrane, it is not necessary for the insertion of the translocators within host membranes.

Anti-LcrV antibodies and anti-PcrV antibodies were then tested for their capacity to protect erythrocytes from hemolysis by  $\Delta$ HOPEMN. As can be seen in figure 4A, anti-LcrV PABs were capable of protecting RBCs. The specific anti-LcrV serum was as immunoprotective as were the PcrV PABs in the *P. aeruginosa*/RBC assay. However anti-PcrV PABs had no protective effect on  $\Delta$ HOPEMN-induced hemolysis, suggesting that, al-

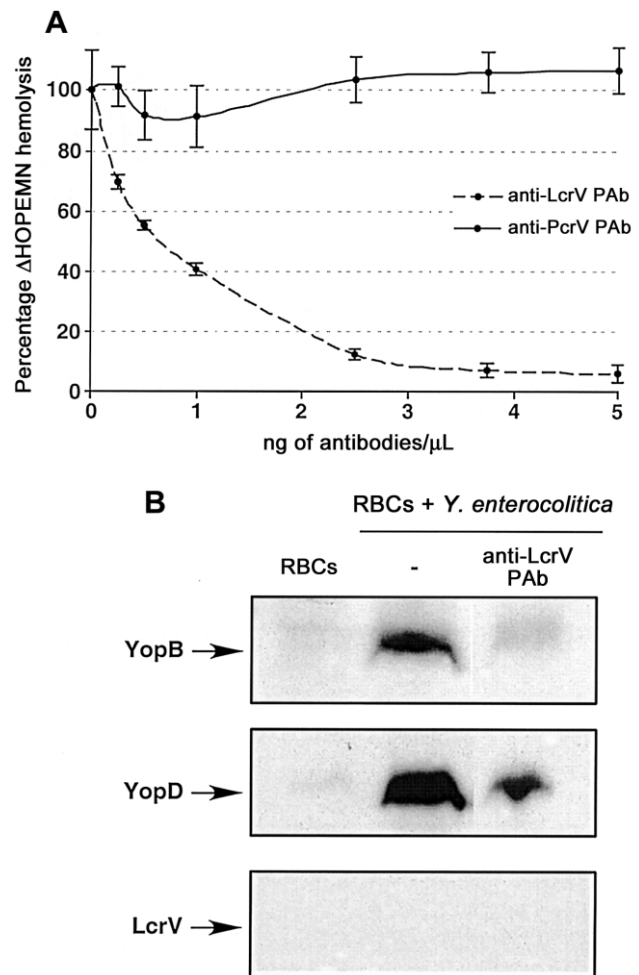


**Figure 4.** Immunoprotection of red blood cells (RBCs) from  $\Delta$ HOPEMN-induced hemolysis, by use of anti-LcrV or anti-PcrV antibodies. *A*, Percentage hemolysis in the presence of various amounts of affinity-purified anti-PcrV polyclonal antibodies (PABs) and protein A-purified anti-LcrV PABs. *B*, Western blot analysis of YopB, YopD, and LcrV performed on the membranes of erythrocytes either not protected or protected by anti-LcrV antibodies.  $\Delta$ HOPEMN, a multi-effector  $Ca^{2+}$ -blind knockout [20].

though some epitopes are shared by LcrV and PcrV, other neutralization epitopes are unique to LcrV.

Next, we addressed the question of whether YopB/D pores are formed in the presence of anti-LcrV antibodies.  $\Delta$ HOPEMN bacteria were preincubated for 30 min with antibodies at levels necessary to achieve 90%–100% protection. Immunoprotected membranes were purified and examined for the presence of the translocators by Western blotting. The amount of YopB was severely reduced in the presence of protective antibodies. It should be noted that less YopD could be detected in immunoprotected membranes (figure 4B). This suggests that anti-LcrV antibodies, similar to anti-PcrV antibodies, prevent the assembly of the functional translocation pore.

PcrV/LcrV protective antigens would thus act as extracellular chaperones or scaffolds in the sense that they would bind

unfolded PopB/YopB and PopD/YopD emerging from the bacterium and ensure their correct folding and assembly into a functional pore. This hypothesis, which is supported by the fact that the T3S apparatus exports unfolded proteins [40], is compatible with the known localization of LcrV at the bacterial surface [29, 35]. It implies that the V antigen interacts, at least transiently, with the B and D antigens, which is in agreement with the observation of Sarker et al. [39]. However, it does not imply that the V antigen remains bound to the assembled pore and, thus, is not contradictory to results showing the absence of direct interactions between PcrV and Pop proteins folded in vitro [9, 23]. Finally, although it is inconsistent with the idea that the purified LcrV forms channels on its own, the chaperone or scaffold hypothesis is compatible with the observation that LcrV determines the size of the pore [10, 18].

In conclusion, we have demonstrated that the protective antibodies against the V antigens (PcrV and LcrV) of *P. aeruginosa* and *Yersinia* species act by preventing the assembly of a functional type III translocon in host cell membranes. In addition, our work has shown that the hemolysis assay is well suited for study of the function of the type III translocon and could be adapted for screening of anti-infectious molecules that specifically target bacterial toxin translocons.

## Acknowledgments

We thank Prof. Dara W. Frank for providing MAb166, Dr. Åke Forsberg for providing anti-YopB antibody, Dr. Elisabeth Carniel for providing *Yersinia pestis* EV76 genomic DNA, Sylvie Elsen for helpful discussions, and Valerie Gros for excellent technical assistance.

## References

- Galan JE, Collmer A. Type III secretion machines: bacterial devices for protein delivery into host cells. *Science* **1999**; 284:1322–8.
- Cornelis GR, Van Gijsegem F. Assembly and function of type III secretory systems. *Annu Rev Microbiol* **2000**; 54:735–74.
- Rosqvist R, Magnusson KE, Wolf-Watz H. Target cell contact triggers expression and polarized transfer of *Yersinia* YopE cytotoxin into mammalian cells. *EMBO J* **1994**; 13:964–72.
- Sory MP, Cornelis GR. Translocation of a hybrid YopE-adenylate cyclase from *Yersinia enterocolitica* into HeLa cells. *Mol Microbiol* **1994**; 14: 583–94.
- Hakansson S, Schesser K, Persson C, et al. The YopB protein of *Yersinia pseudotuberculosis* is essential for the translocation of Yop effector proteins across the target cell plasma membrane and displays a contact-dependent membrane disrupting activity. *EMBO J* **1996**; 15:5812–23.
- Boland A, Sory MP, Iriarte M, Kerbouch C, Wattiau P, Cornelis GR. Status of YopM and YopN in the *Yersinia* Yop virulon: YopM of *Y. enterocolitica* is internalized inside the cytosol of PU5-1.8 macrophages by the YopB, D, N delivery apparatus. *EMBO J* **1996**; 15:5191–201.
- Sawa T, Yahr TL, Ohara M, et al. Active and passive immunization with the *Pseudomonas* V antigen protects against type III intoxication and lung injury. *Nat Med* **1999**; 5:392–8.
- Lee VT, Tam C, Schneewind O. LcrV, a substrate for *Yersinia enterocolitica* type III secretion, is required for toxin targeting into the cytosol of HeLa cells. *J Biol Chem* **2000**; 275:36869–75.
- Goure J, Pastor A, Faudry E, Chabert J, Dessen A, Attree I. The V antigen

of *Pseudomonas aeruginosa* is required for assembly of the functional PopB/PopD translocation pore in host cell membranes. *Infect Immun* **2004**; 72:4741–50.

- Holmström A, Olsson J, Cherepanov P, et al. LcrV is a channel size-determining component of the Yop effector translocon of *Yersinia*. *Mol Microbiol* **2001**; 39:620–32.
- Marenne MN, Journet L, Mota LJ, Cornelis GR. Genetic analysis of the formation of the Ysc-Yop translocation pore in macrophages by *Yersinia enterocolitica*: role of LcrV, YscF and YopN. *Microb Pathog* **2003**; 35:243–58.
- Sundin C, Wolfgang MC, Lory S, Forsberg A, Frithz-Lindsten E. Type IV pili are not specifically required for contact dependent translocation of exoenzymes by *Pseudomonas aeruginosa*. *Microb Pathog* **2002**; 33: 265–77.
- Burrows TW, Bacon GA. The effects of loss of different virulence determinants on the virulence and immunogenicity of strains of *Pasteurella pestis*. *Br J Exp Pathol* **1958**; 39:278–91.
- Lawton WD, Erdman RL, Surgalla MJ. Biosynthesis and purification of V and W antigen in *Pasteurella pestis*. *J Immunol* **1963**; 91:179–84.
- Cornelis GR, Wolf-Watz H. The *Yersinia* Yop virulon: a bacterial system for subverting eukaryotic cells. *Mol Microbiol* **1997**; 23:861–7.
- Yahr TL, Mende-Mueller LM, Friese MB, Frank DW. Identification of type III secreted products of the *Pseudomonas aeruginosa* exoenzyme S regulon. *J Bacteriol* **1997**; 179:7165–8.
- Frithz-Lindsten E, Holmstrom A, Jacobsson L, et al. Functional conservation of the effector protein translocators PopB/YopB and PopD/YopD of *Pseudomonas aeruginosa* and *Yersinia pseudotuberculosis*. *Mol Microbiol* **1998**; 29:1155–65.
- Bröms JE, Sundin C, Francis MS, Forsberg A. Comparative analysis of type III effector translocation by *Yersinia pseudotuberculosis* expressing native LcrV or PcrV from *Pseudomonas aeruginosa*. *J Infect Dis* **2003**; 188:239–49.
- Dacheux D, Attree I, Schneider C, Toussaint B. Cell death of human polymorphonuclear neutrophils induced by a *Pseudomonas aeruginosa* cystic fibrosis isolate requires a functional type III secretion system. *Infect Immun* **1999**; 67:6164–7.
- Neyt C, Cornelis GR. Insertion of a Yop translocation pore into the macrophage plasma membrane by *Yersinia enterocolitica*: requirement for translocators YopB and YopD, but not LcrG. *Mol Microbiol* **1999**; 33: 971–81.
- Tardy F, Homble F, Neyt C, et al. *Yersinia enterocolitica* type III secretion-translocation system: channel formation by secreted Yops. *EMBO J* **1999**; 18:6793–9.
- Viboud GI, Bliska JB. A bacterial type III secretion system inhibits actin polymerization to prevent pore formation in host cell membranes. *EMBO J* **2001**; 20:5373–82.
- Schoehn G, Di Guilmi AM, Lemaire D, Attree I, Weissenhorn W, Dessen A. Oligomerization of type III secretion proteins PopB and PopD precedes pore formation in *Pseudomonas*. *EMBO J* **2003**; 22:4957–67.
- Une T, Brubaker RR. Roles of V antigen in promoting virulence and immunity in yersiniae. *J Immunol* **1984**; 133:2226–30.
- Roggenkamp A, Geiger AM, Leitritz L, Kessler A, Heesemann J. Passive immunity to infection with *Yersinia* spp. mediated by anti-recombinant V antigen is dependent on polymorphism of V antigen. *Infect Immun* **1997**; 65:446–51.
- Motin VL, Nakajima R, Smirnov GB, Brubaker RR. Passive immunity to yersiniae mediated by anti-recombinant V antigen and protein A-V antigen fusion peptide. *Infect Immun* **1994**; 62:4192–201.
- Frank DW, Vallis A, Wiener-Kronish JP, et al. Generation and characterization of a protective monoclonal antibody to *Pseudomonas aeruginosa* PcrV. *J Infect Dis* **2002**; 186:64–73.
- Shime N, Sawa T, Fujimoto J, et al. Therapeutic administration of anti-PcrV F(ab)<sub>2</sub> in sepsis associated with *Pseudomonas aeruginosa*. *J Immunol* **2001**; 167:5880–6.
- Pettersson J, Holmstrom A, Hill J, et al. The V-antigen of *Yersinia* is surface exposed before target cell contact and involved in virulence protein translocation. *Mol Microbiol* **1999**; 32:961–76.

30. Weeks S, Hill J, Friedlander A, Welkos S. Anti-V antigen antibody protects macrophages from *Yersinia pestis*-induced cell death and promotes phagocytosis. *Microb Pathog* **2002**; 32:227–37.
31. Blocker A, Gounon P, Larquet E, et al. The tripartite type III secretion of *Shigella flexneri* inserts IpaB and IpaC into host membranes. *J Cell Biol* **1999**; 147:683–93.
32. Toussaint B, Delic-Attree I, Vignais PM. *Pseudomonas aeruginosa* contains an IHF-like protein that binds to the *algD* promoter. *Biochem Biophys Res Commun* **1993**; 196:416–21.
33. Davis HL, Weeratna R, Waldschmidt TJ, et al. CpG DNA is a potent enhancer of specific immunity in mice immunized with recombinant hepatitis B surface antigen. *J Immunol* **1998**; 160:870–6.
34. Nowakowski A, Wang C, Powers DB, et al. Potent neutralization of botulinum neurotoxin by recombinant oligoclonal antibody. *Proc Natl Acad Sci USA* **2002**; 99:11346–50.
35. Fields KA, Nilles ML, Cowan C, Straley SC. Virulence role of V antigen of *Yersinia pestis* at the bacterial surface. *Infect Immun* **1999**; 67:5395–408.
36. Forsberg A, Viitanen AM, Skurnik M, Wolf-Watz H. The surface-located YopN protein is involved in calcium signal transduction in *Yersinia pseudotuberculosis*. *Mol Microbiol* **1991**; 5:977–86.
37. Bergman T, Hakansson S, Forsberg A, et al. Analysis of the V antigen *lcrGVH-yopBD* operon of *Yersinia pseudotuberculosis*: evidence for a regulatory role of LcrH and LcrV. *J Bacteriol* **1991**; 173:1607–16.
38. Skrzypek E, Straley SC. Differential effects of deletions in *lcrV* on secretion of V antigen, regulation of the low-Ca<sup>2+</sup> response, and virulence of *Yersinia pestis*. *J Bacteriol* **1995**; 177:2530–42.
39. Sarker MR, Neyt C, Stainier I, Cornelis GR. The *Yersinia* Yop virulon: LcrV is required for extrusion of the translocators YopB and YopD. *J Bacteriol* **1998**; 180:1207–14.
40. Feldman MF, Muller S, Wuest E, Cornelis GR. SycE allows secretion of YopE-DHFR hybrids by the *Yersinia enterocolitica* type III Ysc system. *Mol Microbiol* **2002**; 46:1183–97.

## 3 Results

### 3.3 The V-antigen of Yersinia Forms a Distinct Structure at the Tip of Injectisome Needles

Mueller C.A.\*, Broz P.\*, Müller S.A., Ringler P., Erne-Brand F., Sorg I., Kuhn M., Engel A., and  
Cornelis G.R.

**Science** 310: 674-676 (2005)

*\*These authors contributed equally to the work*

## Summary

The V-antigen of *Yersinia* and *P. aeruginosa* are required for the correct assembly of a functional TTS translocation pore in the target cell membrane. Further, antibodies against the V-antigen prevented the formation of the translocation pore and inhibited effector translocation. Thus the V-antigens were proposed to act as an extrabacterial chaperone or assembly platform for the formation of the translocation pore. The obvious location for such a protein would be at the tip of the injectisome needle, where the secreted proteins are supposed to emerge.

Transmission electron micrographs of wildtype *Y. enterocolitica* indicated that the needles protruding from the bacterial surface end with a well-defined structure. STEM analysis of purified needles revealed that this so-called “tip complex” comprises a head, a neck and a base. The tip complex is the same in secreting as well as in non-secreting conditions. To determine the components of the needle fraction we analyzed purified needles. The two translocators LcrV and YopD, as well as YscF the needle subunit were found. Crosslinking of purified needles suggested that YscF and LcrV interact, thus LcrV might be a structural component of the needle.

The tip complex was absent on needles from bacteria deprived of LcrV ( $\Delta$ HOPEMNVQ) and could be brought back by complementing the mutation in *trans*. Control needles (mutants in *yopN*, *yopQ* or *yopBD*) exhibited a wildtype tip complex. Thus the formation of the tip involved LcrV, but not YopQ, YopN or YopBD.

Immunogold labeling of wildtype needles with anti-LcrV antibodies demonstrated a strong binding to the tip complex. Antibodies against YopB and YopD did not label the tip complex and anti-YscF antibodies bound to the needle itself. Together these results clearly proved that LcrV forms the observed tip complex.

*P. aeruginosa* and *A. salmonicida* possess an injectisome closely related to that of *Yersinia*. Their respective LcrV orthologs, PcrV (32.3 kDa) and AcrV (40.2 kDa) are different in size to LcrV (37.6 kDa). We demonstrated that PcrV as well as AcrV could functionally complement an *lcrV* deletion in *Y. enterocolitica*. The needles exhibited distinct tip complexes similar to wildtype needles that were smaller in the case of PcrV and larger with AcrV.

Altogether these results shown that the injectisome needle is topped with a distinct structure called the “tip complex” that is formed by the major protective antigen of *Yersinia*, LcrV.

### Statement of my work

I contributed to this work by providing TEM images of attached needles (Fig. S1), by generating the anti-LcrV antibodies, by affinity-purifying all the antibodies used in this study and by performing the hemolysis experiments necessary for this study. I also did the crosslinking of purified needles to show interaction between LcrV and YscF. I cloned the LcrV orthologs, PcrV and AcrV and checked their functional complementation. I also contributed in the writing the manuscript.



simple orogastric administration. Thus, identification of inhibitors of virulence represents a path to anti-infective discovery that is quite different from conventional approaches that target only bacterial processes that are essential both in vivo and in vitro. We further predict that drugs such as virstatin may act synergistically with conventional antibiotics, because they act through independent mechanisms to block in vivo bacterial replication or survival.

References and Notes

1. K. Andries *et al.*, *Science* **307**, 223 (2005).
2. M. K. Waldor, J. J. Mekalanos, in *Enteric Infections and Immunity*, L. J. Paradise, Ed. (Plenum, New York, 1996), pp. 37–55.
3. Materials and methods are available as supporting material on Science Online.
4. M. K. Waldor, J. J. Mekalanos, *Science* **272**, 1910 (1996).
5. V. J. DiRita, *Mol. Microbiol.* **6**, 451 (1992).
6. D. E. Higgins, E. Nazareno, V. J. DiRita, *J. Bacteriol.* **174**, 6974 (1992).
7. R. C. Brown, R. K. Taylor, *Mol. Microbiol.* **16**, 425 (1995).
8. J. Bina *et al.*, *Proc. Natl. Acad. Sci. U.S.A.* **100**, 2801 (2003).
9. E. S. Krukonis, R. R. Yu, V. J. DiRita, *Mol. Microbiol.* **38**, 67 (2000).

10. DTH3060 is derived from *E. coli* strain VJ787 (*put::ctx-lacZ*) by deletion of *tolC*, an outer membrane porin, to confer greater sensitivity to virstatin.
11. J. M. Blatny, T. Brautaset, H. C. Winther-Larsen, P. Karunakaran, S. Valla, *Plasmid* **38**, 35 (1997).
12. G. A. Champion, M. N. Neely, M. A. Brennan, V. J. DiRita, *Mol. Microbiol.* **23**, 323 (1997).
13. Strain S533 was obtained from the Mekalanos lab collection of *V. cholerae* strain, originally isolated in 1981 from Soongnern Hospital in Thailand.
14. CI represents the ratio of test strain to wild type recovered from the intestine (or after overnight in vitro growth) divided by the ratio of input test strain to wild type. C6706 was marked with a *lacZ* mutation that does not affect colonization but allows it to be distinguished from S533 colonies by blue/white detection on LB-agar plates with Xgal. When the number of bacteria recovered were below the detection limit, 1 was chosen as the denominator to calculate the CI.
15. M. J. Angelichio, J. Spector, M. K. Waldor, A. Camilli, *Infect. Immun.* **67**, 3733 (1999).
16. R. K. Taylor, V. L. Miller, D. B. Furlong, J. J. Mekalanos, *Proc. Natl. Acad. Sci. U.S.A.* **84**, 2833 (1987).
17. G. H. Rabbani, M. R. Islam, T. Butler, M. Shahrier, K. Alam, *Antimicrob. Agents Chemother.* **33**, 1447 (1989).
18. S. H. Lee, D. L. Hava, M. K. Waldor, A. Camilli, *Cell* **99**, 625 (1999).
19. S. Roychoudhury *et al.*, *Proc. Natl. Acad. Sci. U.S.A.* **90**, 965 (1993).

20. J. S. Wright III, R. Jin, R. P. Novick, *Proc. Natl. Acad. Sci. U.S.A.* **102**, 1691 (2005).
21. M. Hentzer *et al.*, *EMBO J.* **22**, 3803 (2003).
22. A. M. Kauppi, R. Nordfelth, H. Uvell, H. Wolf-Watz, M. Elofsson, *Chem. Biol.* **10**, 241 (2003).
23. B. E. Turk *et al.*, *Nat. Struct. Mol. Biol.* **11**, 60 (2004).
24. We thank the National Cancer Institute's Initiative for Chemical Genetics (S. L. Schreiber, P.I.) and the Harvard Institute of Chemistry and Cell Biology for their support of and assistance with the high-throughput small molecule screen; the New England Regional Center of Excellence in Biodefense and Infectious Disease Research for its continued support of research activities involving the identification of small molecule inhibitors of bacterial virulence; and S. Chiang, J. Mougous, and J. Zhu for review of the manuscript. Supported by NIH grant nos. K08 AI06708-01 (D.T.H.) and AI26289 (J.J.M.) and by an NSF predoctoral fellowship (E.A.S.).

Supporting Online Material

www.sciencemag.org/cgi/content/full/1116739/DC1  
Materials and Methods

SOM Text

Tables S1 to S3

References and Notes

29 June 2005; accepted 22 September 2005

Published online 13 October 2005;

10.1126/science.1116739

Include this information when citing this paper.

# The V-Antigen of *Yersinia* Forms a Distinct Structure at the Tip of Injectisome Needles

Catherine A. Mueller,<sup>1\*</sup> Petr Broz,<sup>1\*</sup> Shirley A. Müller,<sup>1,2</sup>  
Philippe Ringler,<sup>1,2</sup> Françoise Erne-Brand,<sup>1,2</sup> Isabel Sorg,<sup>1</sup>  
Marina Kuhn,<sup>1</sup> Andreas Engel,<sup>1,2</sup> Guy R. Cornelis<sup>1†</sup>

Many pathogenic bacteria use injectisomes to deliver effector proteins into host cells through type III secretion. Injectisomes consist of a basal body embedded in the bacterial membranes and a needle. In *Yersinia*, translocation of effectors requires the YopB and YopD proteins, which form a pore in the target cell membrane, and the LcrV protein, which assists the assembly of the pore. Here we report that LcrV forms a distinct structure at the tip of the needle, the tip complex. This unique localization of LcrV may explain its crucial role in the translocation process and its efficacy as the main protective antigen against plague.

Type III secretion (T3S) is commonly used by Gram-negative pathogenic bacteria to introduce effector proteins into target host cells (1). *Yersinia pestis* and *Y. enterocolitica*, causing bubonic plague and gastroenteritis respectively, share the same T3S system consisting of the Ysc (Yop secretion) injectisome, or “needle complex,” and the secreted Yop (*Yersinia* outer protein) effector proteins. Three translocator proteins, YopB, YopD, and LcrV, are necessary to deliver the effectors across the target cell membrane (2–5). LcrV is required for the correct assembly of the

translocation pore formed by YopB and YopD in the membrane of the target cell (2, 6). LcrV (also known as V antigen) is a soluble protein important for virulence (7) and is a protective antigen against plague (8). Antibodies against LcrV prevent the formation of the translocation pore (6) and block the delivery of the effector Yops (9). The injectisome is composed of a basal body resembling that of the flagellum and a needle (10). The needle has a helical structure (11) and in *Yersinia* is formed by the 9.5-kD protein YscF (12, 13).

Transmission electron micrographs of the surface of *Y. enterocolitica* E40 bacteria suggested that the injectisome needle ends with a well-defined structure (fig. S1). To characterize this structure, we purified needles from multi-effector knockout bacteria (strain ΔHOPEMT) that had been incubated under either secretion-

permissive or -nonpermissive conditions (14), then analyzed them by scanning transmission electron microscopy (STEM). A distinct “tip complex” was observed for the wild-type needles, comprising a head, a neck, and a base (Fig. 1A, arrow, and fig. S2A). The tip structure was the same in both cases, but more needles were produced under secretion-permissive conditions (15). The purified needle fraction from secreting bacteria was analyzed to determine the components of the tip complex (fig. S3A). LcrV, YopD, and the needle subunit YscF were found. Other proteins included flagellins, which are usual contaminants of needle preparations (13). Upon cross-linking of purified needles, products formed between YscF and LcrV, suggesting that the latter is a structural component of the needle (fig. S3B).

The tip complex observed for wild-type needles was absent from needles prepared from bacteria deprived of LcrV (ΔHOPEMNQ) (table S1) (16). Instead, this end of the needle was distinctly pointed (Fig. 1B, asterisk, and fig. S2B). The tip complex was restored after the mutation was complemented in trans with *lcrV*<sup>+</sup> (Fig. 1B, right, and fig. S2B). Needles from single *yopN* or *yopQ* knockout bacteria were analyzed as controls and displayed the same tip complex as the wild-type needles (fig. S4). Thus, the formation of the tip complex involved LcrV but not YopN or YopQ.

Needles from a *yopBD* double mutant (15) were analyzed to exclude the possibility that YopD and, although not detected on the gels, the third translocator protein YopB were tip complex components. The appearance of the tip complex was unchanged (fig. S4).

When wild-type needles were incubated with affinity-purified polyclonal antibodies to LcrV, the latter specifically bound to the tip

<sup>1</sup>Biozentrum der Universität Basel and <sup>2</sup>Maurice E. Müller Institute, Klingelbergstrasse 50-70, CH-4056, Basel, Switzerland.

\*These authors contributed equally to this work.

†To whom correspondence should be addressed. E-mail: guy.cornelis@unibas.ch

**Fig. 1.** STEM images of negatively stained wild-type needles. (A) Characteristic tip complexes (arrow), comprising a head, a neck, and a base, of wild-type needles isolated from  $\Delta$ HOPENMVQ bacteria grown in secretion-permissive (left) and -nonpermissive (right) conditions. (B) Needles formed by *lcrV* mutant bacteria ( $\Delta$ HOPENMVQ, left) and by the complemented mutant ( $\Delta$ HOPENMVQ+*lcrV*, right). The needles of *lcrV* mutant bacteria are distinctly pointed at one end (asterisk). The tip complex was restored by complementation of the *lcrV* mutation in trans. Scale bar, 20 nm.

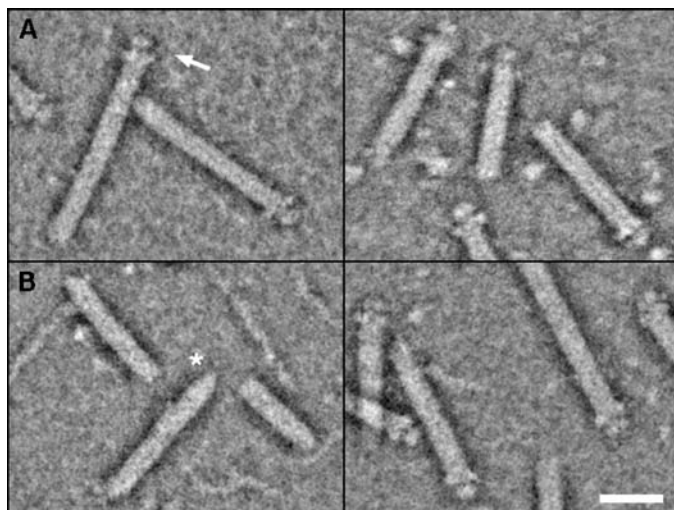


**Fig. 2.** STEM images of wild-type needles incubated with antibodies to LcrV and negatively stained. The antibodies generally attached to the head domain of the tip complex. The small central panels show individual antibodies. Scale bar, 20 nm.

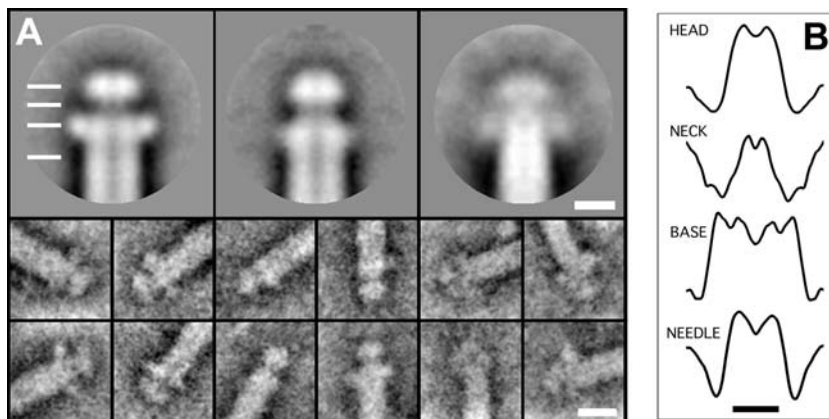
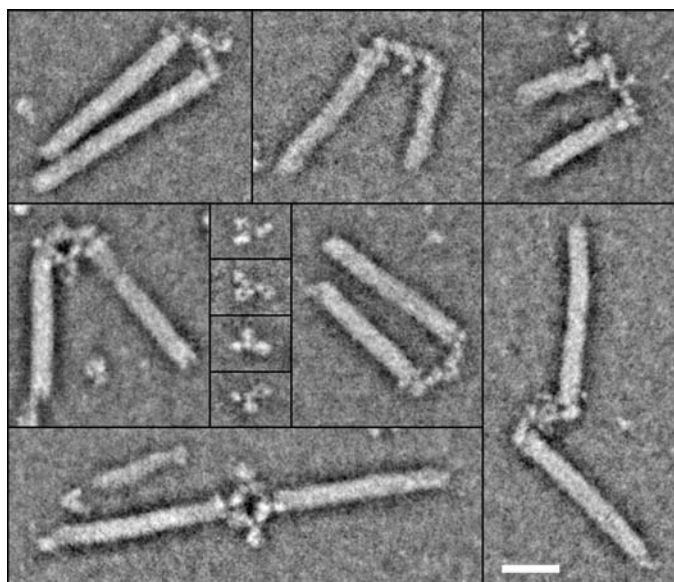


**Fig. 3.** The tip structures of  $\Delta$ HOPENMVQ bacteria complemented with LcrV or its orthologs PcrV and AcrV, imaged by STEM. (A) Projection averages (top) and typical single images (bottom) of the tip complexes formed by LcrV (left; resolution 1.5 nm), PcrV (center; resolution 1.5 nm), and AcrV (right; resolution 2.5 nm). A central channel seems to permeate both the needle and the tip complex. The PcrV tip complex is similar to the LcrV tip complex but has a smaller base. Tip structures formed by AcrV (right) were more variable and larger than those made of LcrV. (B) Profiles from the LcrV tip complex average at the locations indicated by white lines in (A), suggesting a central channel. Scale bars, 5 nm in (A) and (B), 10 nm in galleries.

complex, and we observed many examples of two needles joined tip to tip by a single antibody (Fig. 2). No antibodies to LcrV attached to needles purified from the *lcrV* mutant strain ( $\Delta$ HOPENMVQ). Furthermore, antibodies directed against YopB or YopD did not bind to wild-type needles (17). In contrast, affinity-purified polyclonal antibodies against YscF bound to the needle end opposite the tip complex (fig. S5). Together, these results clearly indicate that LcrV forms the observed tip complex.

*Pseudomonas aeruginosa* and *Aeromonas salmonicida* possess an injectisome closely related to that of *Yersinia*. Their respective LcrV orthologs, PcrV (32.3 kD) and AcrV (40.2 kD), are different in size to LcrV (37.2 kD). The *pcrV*<sup>+</sup> and *acrV*<sup>+</sup> genes were used to complement the *lcrV* deletion in *Y. enterocolitica* E40 ( $\Delta$ HOPENMVQ). The recombinant bacteria could assemble translocation pores. Their needles contained proteins with the size of PcrV and AcrV (fig. S6) and exhibited distinct tip complexes (Fig. 3). The head and neck domains of the tip complex formed by PcrV (Fig. 3A, center) were similar to those formed by LcrV, but the base was narrower (fig. S7). The tip complex formed by AcrV was larger (Fig. 3A, right, and fig. S7), more variable in shape, and more fragile, being absent or altered for many needles. This is reflected by the lower resolution of the AcrV average. In all three cases, a central channel seemed to permeate both the needle and the tip complex (Fig. 3B and fig. S7).

That the needle has a defined tip structure at its distal end, comprising LcrV, is in agreement with previous reports showing that LcrV is surface-exposed (3, 4) and essential for the assembly of a functional translocation pore (6). LcrV may act as an assembly platform for this pore (fig. S8) (6). The IpaD protein from *Shigella* may function in an analogous fashion (18), although it has no clear sequence homology to LcrV. LcrV can also be compared to the EspA filament of enteropathogenic *Escherichia coli*, which forms a physical bridge between the needle and the host cell (19). The EspA homolog, SseB of *Salmonella* SPI-2, forms an undefined sheathlike structure on the distal end of the T3S needle (20).

The localization of LcrV at the tip of the needle and its role in the assembly of the pore may explain the protective action of antibodies to LcrV. Possibly, the antibodies interfere with the function of the tip complex, impairing the translocation process.

#### References and Notes

1. J. E. Galan, A. Collmer, *Science* **284**, 1322 (1999).
2. G. R. Cornelis, H. Wolf-Watz, *Mol. Microbiol.* **23**, 861 (1997).
3. J. Petterson *et al.*, *Mol. Microbiol.* **32**, 961 (1999).
4. K. A. Fields, M. L. Nilles, C. Cowan, S. C. Straley, *Infect. Immun.* **67**, 5395 (1999).
5. M. N. Marenne, L. Journet, L. J. Mota, G. R. Cornelis, *Microb. Pathog.* **35**, 243 (2003).
6. J. Goure, P. Broz, O. Attree, G. R. Cornelis, I. Attree, *J. Infect. Dis.* **192**, 218 (2005).
7. T. W. Burrows, *Nature* **177**, 426 (1956).



8. W. D. Lawton, M. J. Surgalla, *J. Infect. Dis.* **113**, 39 (1963).
9. A. V. Philipovskiy *et al.*, *Infect. Immun.* **73**, 1532 (2005).
10. T. Kubori *et al.*, *Science* **280**, 602 (1998).
11. F. S. Cordes *et al.*, *J. Biol. Chem.* **278**, 17103 (2003).
12. E. Hoiczky, G. Blobel, *Proc. Natl. Acad. Sci. U.S.A.* **98**, 4669 (2001).
13. L. Journet, C. Agrain, P. Broz, G. R. Cornelis, *Science* **302**, 1757 (2003).
14. *Yersinia* builds injectisomes when the temperature reaches 37°C, the host's body temperature. Yop secretion is triggered by contact with a target cell or artificially by chelation of Ca<sup>2+</sup> ions (15).
15. Materials and methods are available as supporting material on Science Online.
16. Removal of *lcrV* leads to reduced synthesis of YopB and YopD because of a regulatory effect of *lcrV* on their expression. This undesired effect can be compensated by deleting *yopQ* (5).
17. C. A. Mueller *et al.*, unpublished data.
18. W. L. Picking *et al.*, *Infect. Immun.* **73**, 1432 (2005).
19. S. J. Daniell *et al.*, *Cell. Microbiol.* **3**, 865 (2001).
20. D. Chakravorty, M. Rohde, L. Jager, J. Deiwick, M. Hensel, *EMBO J.* **24**, 2043 (2005).
21. We thank P. Jenö for mass spectrometry analyses, M. Duerrenberger for use of the TEM facility, and J. M. Meyer and J. Frey for supplying *P. aeruginosa* PAO1 and *A. salmonicida* JF2267. Supported by the Swiss National Science Foundation (grant nos. 32-

65393.01 to G.C. and 3100-059415 to A.E.) and by the Maurice E. Müller Foundation of Switzerland.

**Supporting Online Material**

[www.sciencemag.org/cgi/content/full/310/5748/674/DC1](http://www.sciencemag.org/cgi/content/full/310/5748/674/DC1)

Materials and Methods

Figs. S1 to S8

Tables S1 and S2

References and Notes

5 August 2005; accepted 4 October 2005  
10.1126/science.1118476

## Bats Are Natural Reservoirs of SARS-Like Coronaviruses

Wendong Li,<sup>1,2</sup> Zhengli Shi,<sup>2\*</sup> Meng Yu,<sup>3</sup> Wuze Ren,<sup>2</sup> Craig Smith,<sup>4</sup> Jonathan H. Epstein,<sup>5</sup> Hanzhong Wang,<sup>2</sup> Gary Crameri,<sup>3</sup> Zhihong Hu,<sup>2</sup> Huajun Zhang,<sup>2</sup> Jianhong Zhang,<sup>2</sup> Jennifer McEachern,<sup>3</sup> Hume Field,<sup>4</sup> Peter Daszak,<sup>5</sup> Bryan T. Eaton,<sup>3</sup> Shuyi Zhang,<sup>1,6\*</sup> Lin-Fa Wang<sup>3\*</sup>

Severe acute respiratory syndrome (SARS) emerged in 2002 to 2003 in southern China. The origin of its etiological agent, the SARS coronavirus (SARS-CoV), remains elusive. Here we report that species of bats are a natural host of coronaviruses closely related to those responsible for the SARS outbreak. These viruses, termed SARS-like coronaviruses (SL-CoVs), display greater genetic variation than SARS-CoV isolated from humans or from civets. The human and civet isolates of SARS-CoV nestle phylogenetically within the spectrum of SL-CoVs, indicating that the virus responsible for the SARS outbreak was a member of this coronavirus group.

Severe acute respiratory syndrome (SARS) was caused by a newly emerged coronavirus, now known as SARS coronavirus (SARS-CoV) (1, 2). In spite of the early success of etiological studies and molecular characterization of this virus (3, 4), efforts to identify the origin of SARS-CoV have been less successful. Without knowledge of the reservoir host distribution and transmission routes of SARS-CoV, it will be difficult to prevent and control future outbreaks of SARS.

Studies conducted previously on animals sampled from live animal markets in Guangdong, China, indicated that masked palm civets (*Paguma larvata*) and two other species had been infected by SARS-CoV (5). This led to a large-scale culling of civets to prevent further SARS outbreaks. However, subsequent

studies have revealed no widespread infection in wild or farmed civets (6, 7). Experimental infection of civets with two different human isolates of SARS-CoV resulted in overt clinical symptoms, rendering them unlikely to be the natural reservoir hosts (8). These data suggest that although *P. larvata* may have been the source of the human infection that precipitated the SARS outbreak, infection in this and other common species in animal markets was more likely a reflection of an “artificial” market cycle in naïve species than an indication of the natural reservoir of the virus.

Bats are reservoir hosts of several zoonotic viruses, including the Hendra and Nipah viruses, which have recently emerged in Australia and East Asia, respectively (9–11). Bats may be persistently infected with many viruses but rarely display clinical symptoms (12). These characteristics and the increasing presence of bats and bat products in food and traditional medicine markets in southern China and elsewhere in Asia (13) led us to survey bats in the search for the natural reservoir of SARS-CoV.

In this study, conducted from March to December of 2004, we sampled 408 bats representing nine species, six genera, and three families from four locations in China (Guangdong, Guangxi, Hubei, and Tianjin) after trapping them in their native habitat (Table 1). Blood, fecal, and throat swabs were col-

lected; serum samples and cDNA from fecal or throat samples were independently analyzed, double-blind, with different methods in our laboratories in Wuhan and Geelong (14).

Among six genera of bat species surveyed (*Rousettus*, *Cynopterus*, *Myotis*, *Rhinolophus*, *Nyctalus*, and *Miniopterus*), three communal, cave-dwelling species from the genus *Rhinolophus* (horseshoe bats) in the family *Rhinolophidae* demonstrated a high SARS-CoV antibody prevalence: 13 out of 46 bats (28%) in *R. pearsoni* from Guangxi, 2 out of 6 bats (33%) in *R. pussilus* from Guangxi, and 5 out of 7 bats (71%) in *R. macrotis* from Hubei. The high seroprevalence and wide distribution of seropositive bats is expected for a wildlife reservoir host for a pathogen (15).

The serological findings were corroborated by polymerase chain reaction (PCR) analyses with primer pairs derived from the nucleocapsid (N) and polymerase (P) genes (table S1). Five fecal samples tested positive, all of them from the genus *Rhinolophus*: three in *R. pearsoni* from Guangxi and one each in *R. macrotis* and *R. ferrumequinum*, respectively, from Hubei. No virus was isolated from an inoculation of Vero E6 cells with fecal swabs of PCR-positive samples.

A complete genome sequence was determined directly from PCR products from one of the fecal samples (sample Rp3) that contained relatively high levels of genetic material. The genome organization of this virus (Fig. 1), tentatively named SARS-like coronavirus isolate Rp3 (SL-CoV Rp3), was essentially identical to that of SARS-CoV, with the exception of three regions (Fig. 1, shaded boxes). The overall nucleotide sequence identity between SL-CoV Rp3 and SARS-CoV Tor2 was 92% and increased to ~94% when the three variable regions were excluded. The variable regions are located at the 5' end of the S gene (equivalent to the S1 coding region of coronavirus S protein) and the region immediately upstream of the N gene. These regions have been identified as “high mutation” regions among different SARS-CoVs (5, 16, 17). The region upstream of the N gene is known to be prone to deletions of various sizes (5, 16, 18).

Predicted protein products from each gene or putative open reading frame (ORF) of SL-CoV Rp3 and SARS-CoV Tor2 were com-

<sup>1</sup>Institute of Zoology, Chinese Academy of Sciences (CAS), Beijing, China. <sup>2</sup>State Key Laboratory of Virology, Wuhan Institute of Virology, CAS, Wuhan, China. <sup>3</sup>Commonwealth Scientific and Industrial Research Organization (CSIRO) Livestock Industries, Australian Animal Health Laboratory, Geelong, Australia. <sup>4</sup>Department of Primary Industries and Fisheries, Queensland, Australia. <sup>5</sup>The Consortium for Conservation Medicine, New York, USA. <sup>6</sup>Guangzhou Institute of Biomedicine and Health, Guangzhou, China.

\*To whom correspondence should be addressed. E-mail: zshi@wh.iiov.cn (Z.S.); zhangsy@ioz.ac.cn (S.Z.); linfa.wang@csiro.au (L.-F.W.)



Supporting Online Material for  
**The V-Antigen of *Yersinia* Forms a Distinct Structure at the Tip of  
Injectisome Needles**

Catherine A. Mueller, Petr Broz, Shirley A. Müller, Philippe Ringler,  
Françoise Erne-Brand, Isabel Sorg, Marina Kuhn, Andreas Engel,  
Guy R. Cornelis†

†To whom correspondence should be addressed. E-mail: [guy.cornelis@unibas.ch](mailto:guy.cornelis@unibas.ch)

Published 28 October 2005, *Science* **310**, 674 (2005)  
DOI: 10.1126/science.1118476

**This PDF file includes:**

Materials and Methods

Figs. S1 to S8

Tables S1 and S2

References and Notes

## Supporting Online Material

### Materials and Methods

This study was carried out with *Y. enterocolitica* E40 (1) carrying several mutations on the virulence pYV plasmid, listed in Table S1.

The oligonucleotides used for the genetic constructions are listed in Table S2.

To delete the complete *yopB* and *yopD* genes, flanking regions of the *yopB* (pYVe227 (accession NC\_002120) bp 17702-17196, primers 3854/3862) and the *yopD* (pYVe227 bp 15076-14861, primers 3863/3861) genes (2) were cloned by overlapping PCR into pBluescript KS+II with *Sall* and *XbaI* restriction sites. The resulting plasmid was called pISO82 (Table S1). The *Sall-XbaI* fragment of pISO82 containing the flanking regions of the *yopB* and *yopD* genes was cloned into the same sites of the suicide vector pKNG101 (Table S1), resulting in the mutator plasmid pISO83 (Table S1). The *yopB* and *yopD* genes on the *Y. enterocolitica* MRS40 pYV plasmid were deleted by allelic exchange with pISO83 as described previously (3). The resulting *Y. enterocolitica* mutant pYV plasmid was called pISO4005 (Table S1).

The *lcrV* mutation was complemented by plasmid pMN12 containing *lcrV*<sup>+</sup> downstream of the *yopE* promoter (3).

The *pcrV* and *acrV* (4) sequences were amplified by PCR on genomic DNA from *Pseudomonas aeruginosa* PAO1 (accession NC\_002516, primers 3808/3809) and *Aeromonas salmonicida* JF2267 (accession AJ516009, primers 3810/3811). The PCR products were digested with *NcoI/EcoRI* and *AflIII/EcoRI* and cloned into the *NcoI/EcoRI* sites of the expression vector pBAD/MycHisA giving plasmids pPB24 and pPB25 (Table S1).

Bacteria were routinely grown on Luria-Bertani agar plates and in liquid Luria-Bertani medium. Ampicillin was used at a concentration of 200 µg/ml to select for the expression plasmids. For the induction of the *yop* regulon (secretion permissive conditions) *Y. enterocolitica* bacteria were inoculated to an OD<sub>600</sub> of 0.1 and cultivated in brain-heart infusion (BHI; Remel) supplemented with a carbon source, 20 mM MgCl<sub>2</sub> and 20 mM sodium oxalate (BHI-Ox) for 2 hours at room temperature, then shifted to 37 °C and incubated for 4 hours (5). To keep the *yop* regulon in a non-induced state (secretion non-permissive conditions) bacteria were inoculated to an OD<sub>600</sub> of 0.1 and cultivated in BHI supplemented with a carbon source, 20 mM MgCl<sub>2</sub> and 5 mM CaCl<sub>2</sub> (BHI-Ca<sup>2+</sup>) for 2 hours at room temperature, then shifted to 37 °C and incubated for 4 hours.

Expression of the different genes cloned downstream of the pBAD promoter was induced by adding 0.2 % arabinose to the culture just before the shift to 37 °C, and again 2 hours later. The carbon source was glycerol (4 mg/ml) when expressing genes from the pBAD promoter, and glucose (4 mg/ml) in the other cases. The supernatant of every culture used for needle purification was analysed for secreted Yop proteins.

Secreted proteins of all the strains were analyzed by Coomassie stained SDS-PAGE, to verify that YopB and YopD were well secreted (data not shown). Secreted proteins were precipitated for 1 hour at 4 °C with trichloroacetic acid 10 % (w/v) final

and separated by SDS-PAGE. In each case, proteins secreted by  $3 \times 10^8$  bacteria were loaded per lane. After electrophoresis, proteins were stained with Coomassie brilliant blue (Pierce) or transferred to nitrocellulose membranes. Immunoblotting was carried out using rabbit polyclonal antibodies directed against YscF (MIPA 80) and LcrV (MIPA 220). Detection was performed with secondary antibodies conjugated to horseradish peroxidase (1:2000; Dako) before development with supersignal chemiluminescent substrate (Pierce).

To prepare the anti-LcrV antibodies (MIPA 220), *lcrV* DNA was amplified from pYV40 DNA (primers 3283/3290). The PCR product was digested with *NdeI* and *BamHI*, and cloned into the expression vector pET28a (Novagen) giving plasmid pPB10 (Table S1). A soluble His-LcrV protein was produced in *E. coli* BL21 (DE3) pLysS and purified on chelating sepharose beads (Amersham Biosciences). A rabbit was immunized by 4 injections with a total of 1 mg of His-LcrV in 20 mM phosphate buffer (CER, Marloie, Belgium). The serum was affinity-purified on His-LcrV immobilized on nitrocellulose membranes. The serum was then concentrated on a ProteinG-column (MabTrap Amersham Biosciences). The Bradford assay (BioRad) was used to determine the concentration of purified antibodies.

To produce polyclonal anti-YscF antibodies (MIPA 223), *yscF* DNA was amplified from pYV40 DNA (primers 3759/3760). The PCR product was digested with *BamHI* and *XhoI*, and cloned into the expression vector pGEX4T3 (Amersham Biosciences) giving plasmid pISO66 (table S1). YscF was produced as a glutathione S-transferase fusion protein encoded by plasmid pISO66. Expression of the protein was induced in *E. coli* TOP10 by addition of isopropyl- $\beta$ -D-thiogalactopyranoside (0.2 mM final concentration), as soon as the culture reached an OD<sub>600</sub> of 0.6. Four hours after induction, bacteria were collected, lysed by sonication in lysis buffer (PBS, 1 % Triton-X100, 5mM dithiotreitol, 1 mM phenylmethylsulfonylfluoride and protease inhibitor cocktail complete Mini (Roche)), and purified by affinity chromatography with glutathione-Sepharose beads (Amersham Biosciences). The beads were washed five times with PBS at 4 °C. YscF was eluted from the beads by thrombin cleavage (thrombin protease 50 units/ml in PBS) for 1 hour at room temperature. The thrombin was then removed by incubation with benzamidine-Sepharose beads. A rabbit was immunized by 4 injections with a total of 1 mg of YscF (CER, Marloie, Belgium). The serum was purified on a Protein G-column (MabTrap Amersham Biosciences). The Bradford assay (BioRad) was used to determine the concentration of purified antibodies.

Hemolytic assays were carried out as described by Goure *et al.* (6).

To purify needles, *Yersinia* bacteria were cultivated in non-permissive or permissive conditions for secretion (3, 5) using the following protocols: Non-permissive conditions (BHI-Ca<sup>2+</sup>): Less injectisomes are built under non-permissive conditions, due to a known feedback regulatory effect (5, 7). Bacteria from 3 litres of culture were harvested by centrifugation (20 min at 4000 x g) and resuspended in 20 mM TrisHCl, pH 7.5 (1/30 of the initial culture volume). The bacteria were sheared by passing the suspension through an 18G needle using a syringe. They were then pelleted by centrifugation (10 min at 8300 x g). The supernatant was collected and passed through a 0.45  $\mu$ m mesh filter (cellulose acetate membrane). The filtrate was concentrated 10 fold

using an Amicon Stirred Ultraconcentration Cell # 8200 (YM30 membrane (Ultracel YM = Regenerated Cellulose Acetate, 30K), 5 bar pressure). The supernatant was further concentrated using a Millipore Ultrafree-15 Centrifugal filter device Biomax-10K and centrifuged for 30 min at 20000 x g. The pellet, containing needles, was resuspended in 20 mM TrisHCl, pH 7.5 (1/48000 of the initial culture volume) and analyzed by SDS-PAGE, immunoblotting and electron microscopy.

Permissive conditions (BHI-Ox): Bacteria from 300 ml of culture were harvested by centrifugation (10 min at 5700 x g) and washed once with 20 mM TrisHCl, pH 7.5 (1/30 of the initial culture volume). The washing supernatant was passed through a 0.45  $\mu$ m mesh filter (cellulose acetate membrane) and centrifuged for 30 min at 20000 x g. The resulting pellet was resuspended in 20 mM TrisHCl, pH 7.5 (1/3000 of the initial culture volume) and analyzed by SDS-PAGE, immunoblotting and electron microscopy.

For the cross-linking experiments, purified needles were diluted 25 x in 20 mM TrisHCl, pH 7.5 and put on ice. Glutaraldehyde (Sigma) was added to a final concentration of 0.4 % (v/v). The cross-linking reaction was allowed to proceed for 15 minutes and was then quenched by the addition of 1 M TrisHCl, pH 8 (1/10 of the reaction volume). The cross-linked products were analyzed by SDS-PAGE and Western blotting.

Visualization of the needle-like structures on the cell surface of bacteria was done by electron microscopy as described by Hoiczky and Blobel (8). After 4 hours of induction at 37 °C, bacteria were harvested at 2000 x g and carefully resuspended in 20 mM TrisHCl, pH 7.5. Droplets were adsorbed to freshly glow-discharged, formvar-carbon coated grids, and negatively stained with 2 % (w/v) uranyl acetate. Bacteria were visualized in a Philips Morgagni 268D electron microscope at an acceleration voltage of 80 kV.

For scanning transmission electron microscopy (STEM), the purified needles were diluted with buffer (20 mM TrisHCl, pH 7.5) as required, adsorbed to thin carbon film, washed on 4 droplets of quartz double-distilled water and stained with 2 % (w/v) sodium phosphotungstate. Digital dark-field images were recorded using a Vacuum Generators STEM HB5 interfaced to a modular computer system (Tietz Video and Image Processing Systems GmbH, D-8035 Gauting). The microscope was operated at 100 kV and a nominal magnification of 500000 x, using doses that ranged between 9000 and 13000 electrons/nm<sup>2</sup>. The contrast was reversed to show protein in bright shades in the figures.

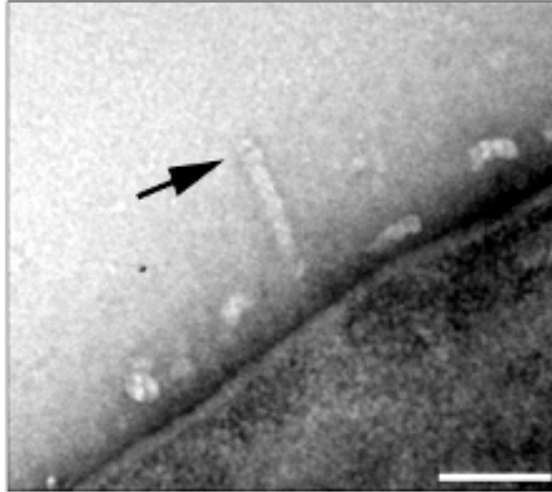
To calculate the averages of the tip complexes, subframes were manually selected from the STEM dark-field images recorded at a nominal magnification of 500000 x and angularly and translationally aligned to an arbitrary reference using the SEMPER program package (9). A first average calculated from 52-95 aligned subframes was two-fold symmetrized along the cylinder axis and used to calculate a refined average. Those subframes that had a cross-correlation value > 0.65 were included in the final average; 65 of the 95 initially selected for the wt, 36 of 52 for the PcrV ortholog, and 35 of 58 for the AcrV ortholog. A two-fold symmetry was then applied. The resolution was determined from the Fourier ring correlation function of the independent averages calculated from the odd and even numbered subframes applying the 0.5 criterion.

For the immuno-electron microscopy experiments, 5  $\mu$ l aliquots of the purified needles suspended in 20 mM TrisHCl, pH 7.5 were incubated for 45 min with 2.5  $\mu$ l of antibody solution at room temperature, and diluted up to 20 x with buffer immediately before grid preparation. In each case, both the initial antibody concentration employed and the dilution made before adsorption were adjusted to obtain optimum imaging conditions (sufficient needles and a low background of free antibodies) even though a large excess of antibodies was used for the reaction. The following, affinity purified, rabbit polyclonal antibodies were used: anti-LcrV (0.268 mg/ml, MIPA 220), anti-YopD (0.04 mg/ml, MIPA 24), anti-YopB (0.7 mg/ml, MIPA 38) and anti-YscF (1.4 mg/ml, MIPA 223).



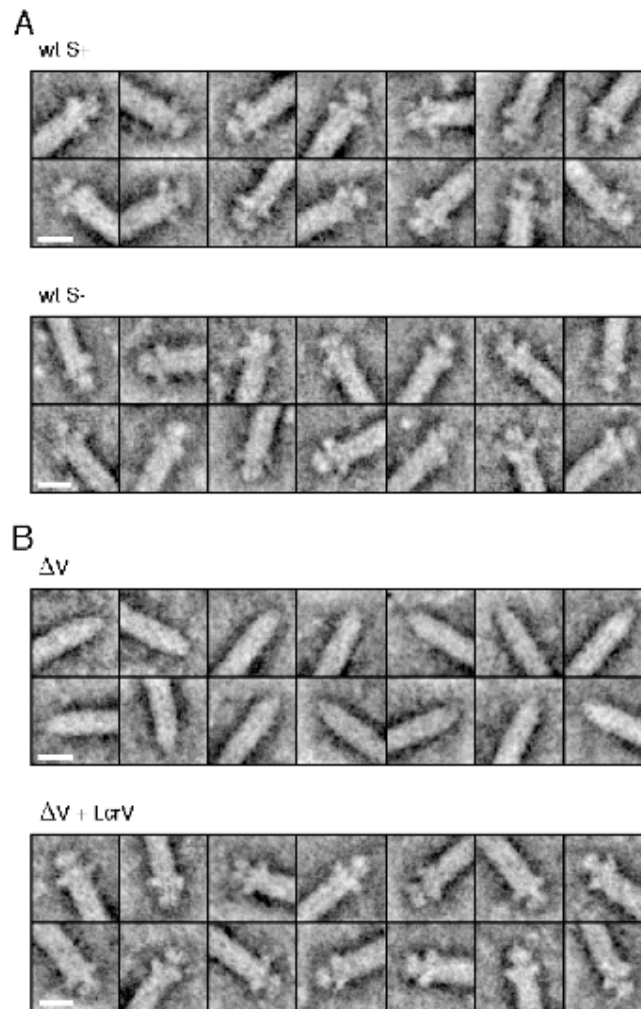
Figures

Figure S1



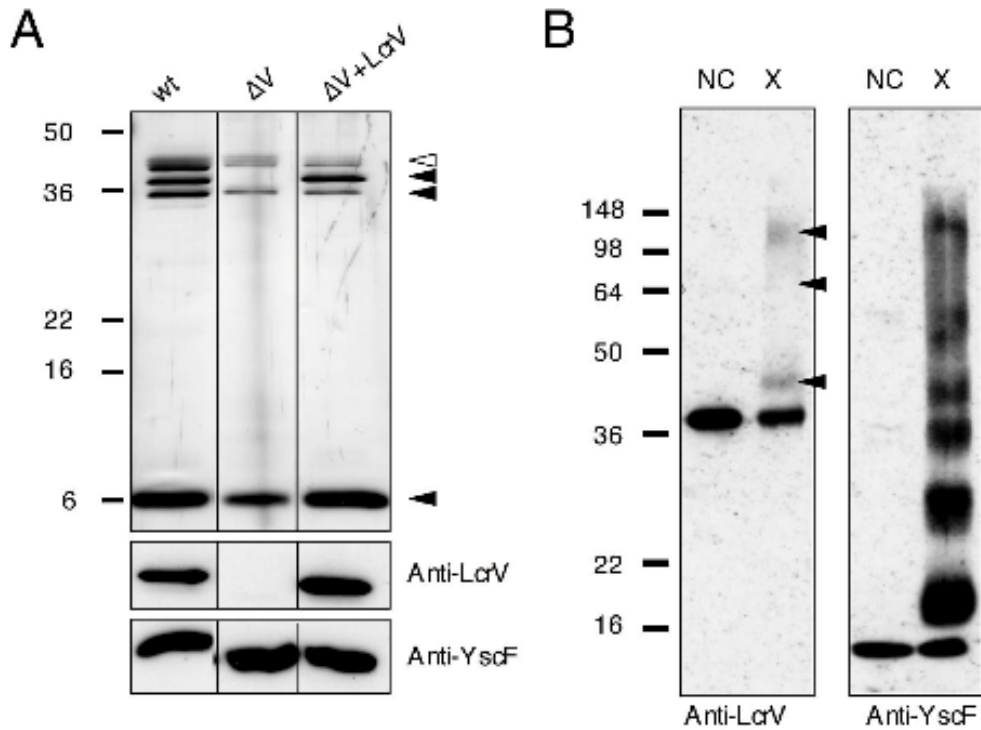
**Fig. S1** Transmission electron micrograph of *Y. enterocolitica* E40 strain  $\Delta$ HOPEMT negatively stained with 2 % uranyl acetate. Needles protrude from the cell surface and have a distinct structure at their tip (arrow). Scale bar: 40 nm.

Figure S2



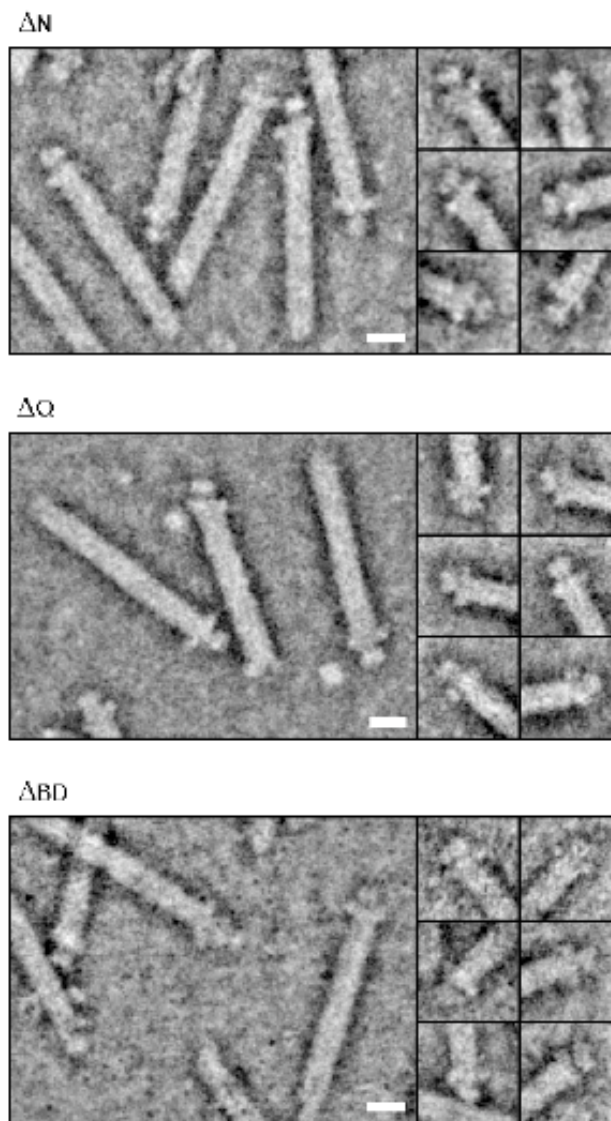
**Fig. S2** Galleries showing the tip complexes of needles detailed in Fig. 1. Scale bars: 10 nm. (A) Tip complex of wt needles formed under secretion-permissive (S<sup>+</sup>) and non-permissive (S<sup>-</sup>) conditions. (B) Tip complex of needles formed by the *lcrV* mutant ( $\Delta V$  needles) and the *lcrV* mutant complemented with *lcrV*<sup>+</sup> ( $\Delta V + LcrV$  needles).

Figure S3



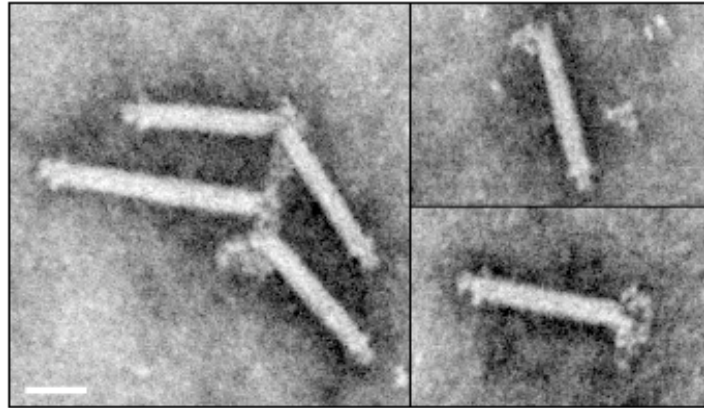
**Fig. S3** (A) Silver stained SDS-PAGE (top) and Western blots (bottom) of the needles purified from different *Y. enterocolitica* strains. The black arrowheads indicate the bands corresponding to LcrV (37.2 kDa), YopD (33.2 kDa) and YscF (9.5 kDa). The flagellin contamination is marked by a white arrowhead. (B) Cross-linking with glutaraldehyde. Purified needles were incubated with 0.4 % (v/v) glutaraldehyde for 15 minutes and analyzed by SDS-PAGE and Western blotting with anti-LcrV and anti-YscF antibodies: NC, not cross-linked; X, cross-linked. The arrowheads indicate cross-linked products of LcrV. The lowest of these bands corresponds to a complex of about 45 kDa i.e., one LcrV and one YscF. Cross-linking of the needle subunit YscF lead to a ladder-like pattern as expected.

Figure S4



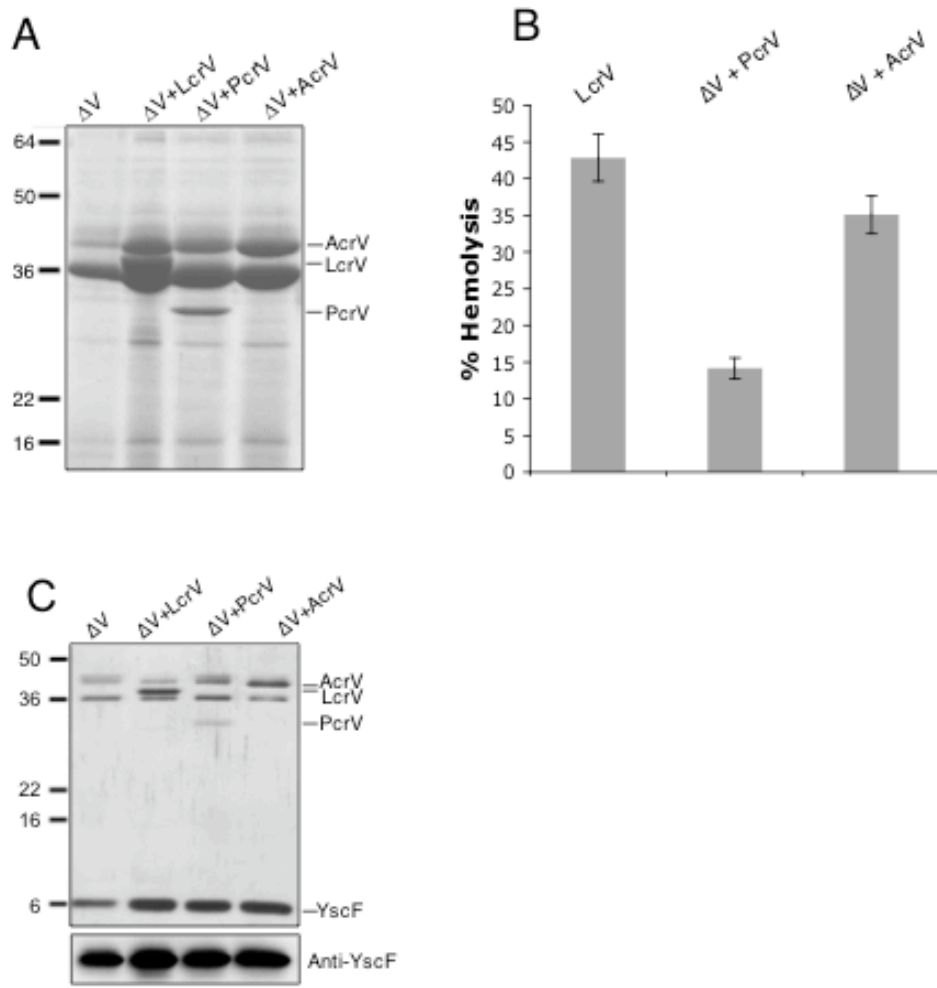
**Fig. S4** Images and compiled galleries showing the tip complexes of needles isolated from *yopN* ( $\Delta N$ ), *yopQ* ( $\Delta Q$ ), *yopBD* ( $\Delta BD$ ) mutants. Scale bars: 10 nm.

Figure S5



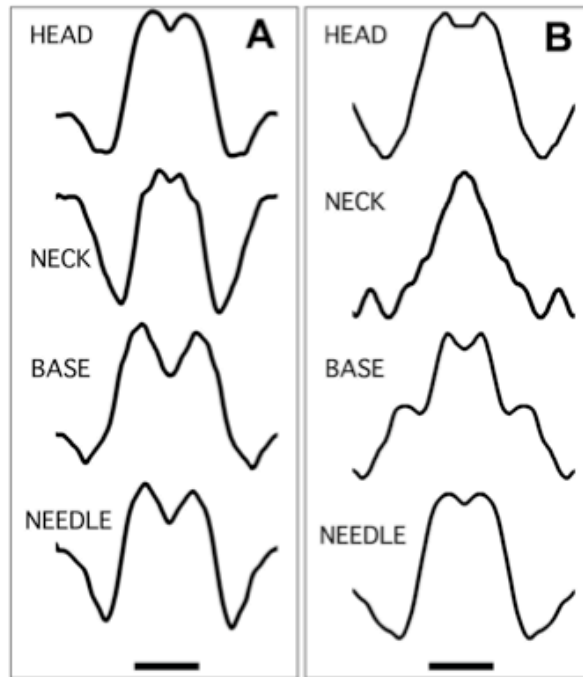
**Fig. S5** Anti-YscF antibody labeling of wt needles imaged by dark-field STEM. Clusters of antibodies bind to the needle ends that do not have a tip complex, sometimes also linking two needles together. The sides of the needles were not labelled. Presumably the helical packing of YscF in the needle effectively buries all reactive epitopes. Scale bar: 20 nm.

Figure S6



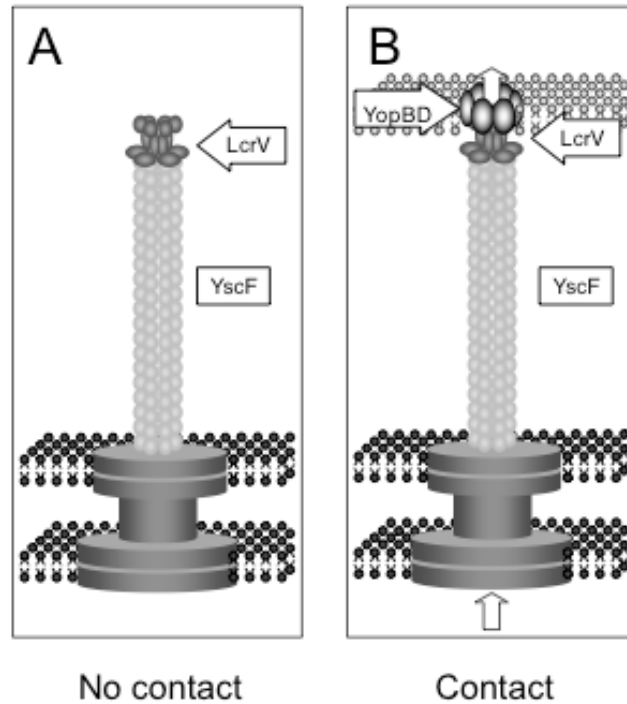
**Fig. S6** LcrV-orthologs from *P. aeruginosa* and *A. salmonicida* transcomplement the *lcrV* mutant of *Y. enterocolitica* (A) Coomassie stained SDS-PAGE of proteins secreted by *Y. enterocolitica*  $\Delta$ HOPEMNVQ ( $\Delta$ V),  $\Delta$ HOPEMNVQ complemented with LcrV ( $\Delta$ V+LcrV),  $\Delta$ HOPEMNVQ complemented with PcrV from *P. aeruginosa* ( $\Delta$ V+PcrV) and  $\Delta$ HOPEMNVQ complemented with AcrV from *A. salmonicida* ( $\Delta$ V+AcrV). (B) Lytic activity on red blood cells after 2 hours of contact with *Y. enterocolitica*  $\Delta$ HOPEMNVQ (LcrV),  $\Delta$ HOPEMNVQ+PcrV ( $\Delta$ V+PcrV) and  $\Delta$ HOPEMNVQ+AcrV ( $\Delta$ V+AcrV). (C) Silver stained SDS-PAGE (top) and Western blotting (bottom) of the purified needles from *Y. enterocolitica*  $\Delta$ HOPEMNVQ transcomplemented with the LcrV-orthologs from *P. aeruginosa* (PcrV; 32.2 kDa) and *A. salmonicida* (AcrV; 40.2 kDa). AcrV and flagellin are of similar molecular weight.

Figure S7



**Fig. S7** Profiles perpendicular to the needle axis calculated from the averages of PcrV (A) and AcrV (B) tip structures. The locations of the profiles are the same as for the wt tip structure shown in Fig. 3. A central channel is indicated by the dip in the profile evident in all except the neck profile from the AcrV complex. The magnitude of the central dip is related to the resolution of the average and to the ratio of inner to outer radius of the cylindrical structure (16). Scale bar: 5nm in (A) and (B).

Figure S8



**Fig. S8** Hypothetical model of the function of the LcrV tip complex. (A) No contact to host cell: LcrV forms the complex at the tip of the needle. This implies that LcrV is exported before contact with a target cell (or before secretion is triggered by  $\text{Ca}^{2+}$ -chelation) and hence that LcrV has a special status in the export hierarchy. However, it is not yet known whether LcrV is present at the tip while the needle grows or whether it is installed at the tip when the needle has reached its final length. Although localized at the tip of the needle, LcrV does not act as a polymerizing cap, like the hook- and filament-caps of the flagellum (17), because the needle subunits assemble normally in its absence (Fig 1B). YopN is not present at the tip of the needle as shown in Fig S4 and by work of others (18) (B) Contact with host cell membrane: The tip complex assists the assembly of the translocation pore, serving as an assembly platform.



## Tables

Plasmid	Current designation	Relevant characteristics	References
<i>pYV plasmids</i>			
pYV40	wt	pYV plasmid of <i>Y. enterocolitica</i> E40	(10)
pIML421	$\Delta$ HOPEMT	pYV40 <i>yopE</i> <sub>21</sub> <i>yopH</i> <sub><math>\Delta</math>1-352</sub> <i>yopO</i> <sub><math>\Delta</math>65-558</sub> <i>yopP</i> <sub>23</sub> <i>yopM</i> <sub>23</sub> <i>yopT</i> <sub>135</sub>	(11)
pMN4003	$\Delta$ HOPEMNVQ	pYV40 <i>yopE</i> <sub>21</sub> <i>yopH</i> <sub><math>\Delta</math>1-352</sub> <i>yopO</i> <sub><math>\Delta</math>65-558</sub> <i>yopP</i> <sub>23</sub> <i>yopM</i> <sub>23</sub> <i>yopN</i> <sub>45</sub> <i>lcrV</i> <sub><math>\Delta</math>6-319</sub> <i>yopQ</i> <sub>17</sub>	(3)
pIM417	$\Delta$ HOPEMN	pYV40 <i>yopE</i> <sub>21</sub> <i>yopH</i> <sub><math>\Delta</math>1-352</sub> <i>yopO</i> <sub><math>\Delta</math>65-558</sub> <i>yopP</i> <sub>23</sub> <i>yopM</i> <sub>23</sub> <i>yopN</i> <sub>45</sub>	(12)
pIM41	$\Delta$ N	pYV40 <i>yopN</i> <sub>45</sub>	(13)
pABL402	$\Delta$ Q	pYV40 <i>yopQ</i> <sub>17</sub>	(14)
pISO4005	$\Delta$ BD	pYV40 <i>yopB</i> <i>yopD</i>	This work
<i>Clones and vectors</i>			
pBAD/ <i>Myc</i> -HisA			Invitrogen
pET28a			Novagen
pGEX4T3			Amersham
pISO66		pGEX4T3 <i>yscF</i> <sup>+</sup>	This work
pISO82		pBluescriptKS+IIpYVe227bp17702- 17196/bp15076-14861	This work
pISO83		pKNG101pYVe227bp17702- 17196/bp15076-14861	This work
pKNG101		Suicide vector <i>ori</i> <sub>R6K</sub> <sup>+</sup> <i>secBR</i> <sup>+</sup> <i>oriT</i> <sub>R2K</sub> <sup>+</sup> <i>strAB</i>	(15)
pMN12		pBBR1MCS-2 <i>P</i> <sub>yopE</sub> <i>lcrV</i> <sup>+</sup>	(3)
pPB10		pET28a- <i>lcrV</i> <sup>+</sup>	This work
pPB24		pBAD/ <i>Myc</i> -HisA- <i>pcrV</i> <sup>+</sup>	This work
pPB25		pBAD/ <i>Myc</i> -HisA- <i>acrV</i> <sup>+</sup>	This work

**Table S1** Plasmids used in this study.

Codes	Oligonucleotides	Underlined sites
3808	ATCATGCCATGGCAGAAAGTCAGAAACCTTAATGCC	<i>NcoI</i>
3809	CCGGGCGAATTCCTAGATCGCGCTGAGAATGTC	<i>EcoRI</i>
3810	TGCCACATGTCAAGCACAAATCCCTGACTACAAC	<i>AflIII</i>
3811	CCGGGCGAATTCCTCAAATTGCGCCAAGAATGTC	<i>EcoRI</i>
3283	GATCGGATCCCTACCTCGTGTCATCTAG	<i>BamHI</i>
3290	GGGAATTCCATATGATTAGAGCCTACGAA	<i>NdeI</i>
3759	GATCGGATCCATGAGTAATTTCTCTGGGTTTAC	<i>BamHI</i>
3760	GATCCTCGAGTTATGGGAACTTCTGTAGGATG	<i>XhoI</i>
3854	ATCATGGTTCGACATGCAACAAGAGACGACAGAC	<i>Sall</i>
3861	ATCATGTCTAGACAGGTCTTGAGCTACTACATG	<i>XbaI</i>
3862	TTAACTAACCAAGGTCATAAATGGTCATGGGTTATC AACGCACTCATG	
3863	CATGAGTGCGTTGATAACCCATGACCATTTATGACCT TGGTTAGTTAA	

**Table S2** Oligonucleotides used in this study.

## References

1. M. P. Sory, G. R. Cornelis, *Mol. Microbiol.* **14**, 583 (1994).
2. M. Iriarte, G. R. Cornelis, in *Pathogenicity islands and other mobile virulence elements* J. B. Kaper, J. Hacker, Eds. (American Society for Microbiology, Washington DC, 1999) pp. 91.
3. M. N. Marenne, L. Journet, L. J. Mota, G. R. Cornelis, *Microb. Pathogen.* **35**, 243 (2003).
4. S. E. Burr, K. Stuber, J. Frey, *J. Bacteriol.* **185**, 6583 (2003).
5. G. Cornelis, J. C. Vanootegem, C. Sluifers, *Microb. Pathogen.* **2**, 367 (1987).
6. J. Goure, P. Broz, O. Attree, G. R. Cornelis, I. Attree, *J. Infect. Dis.* **192**, 218 (2005).
7. J. Pettersson *et al.*, *Science* **273**, 1231 (1996).
8. E. Hoiczyk, G. Blobel, *Proc. Natl. Acad. Sci. U.S.A.* **98**, 4669 (2001).
9. S. A. Müller, K. N. Goldie, R. Bürki, R. Häring, A. Engel, *Ultramicroscopy* **46**, 317 (1992).
10. M. P. Sory, A. Boland, I. Lambermont, G. R. Cornelis, *Proc. Natl. Acad. Sci. U. S. A.* **92**, 11998 (1995).
11. M. Iriarte, G. R. Cornelis, *Mol. Microbiol.* **29**, 915 (1998).
12. C. Neyt, G. R. Cornelis, *Mol. Microbiol.* **33**, 971 (1999).
13. A. Boland *et al.*, *EMBO J.* **15**, 5191 (1996).
14. A. Boland, G. R. Cornelis, *Infect. Immun.* **66**, 1878 (1998).
15. K. Kaniga, I. Delor, G. R. Cornelis, *Gene* **109**, 137 (1991).
16. A. C. Steven, B. L. Trus, P. M. Steinert, J. S. Wall, *Proc. Natl. Acad. Sci. U. S. A.* **81**, 6363 (1984).
17. R. M. Macnab, *Annu. Rev. Microbiol.* **57**, 77 (2003).
18. F. Ferracci, Schubot F. D., Waugh D. S., Plano, G. V., *Mol. Microbiol.* **57**, 970 (2005).

## 3 Results

### 3.4 Unpublished results

### 3.4.1 The orientation of the LcrV molecule in the tip complex

(STEM analysis was done in collaboration with Philippe Ringler, Françoise Erne-Brand, Shirley A. Müller and Andreas Engel)

(The modeling of the LcrV tip complex was done by Ansgar Philippsen)

#### Introduction

The crystal structure of the V-antigen from *Y. pestis* shows that this protein is dumbbell shaped (Fig. 17, Derewenda *et al.*, 2004). It consists of two globular domains connected by two long alpha helices. Modeling of the LcrV molecule into the structure of the tip complex, suggested that the globular domains would form the head and the base of the tip complex (A. Philippsen, unpublished data). However, the molecule can be orientated in two ways, either with the N-terminal domain forming the base or the other way round forming the head of the tip complex. To determine which model was true, we decided to investigate the orientation of LcrV in the tip complex. We started two different approaches to answer this question.

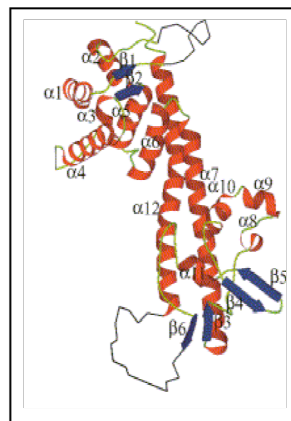


**Fig. 17.** Structure of LcrV from *Y. pestis* (Derewenda *et al.*, 2004).

The first approach was to find a permissive site in LcrV to insert a tag. This would allow to immunolabel tip complexes with antibodies binding to one specific epitope. So far only polyclonal anti-LcrV antibodies that bound to different epitopes in LcrV were used. As the crystal structure of the molecule is known, the immunolabelling would allow to determine how the molecule is oriented.

The second approach takes advantage of the size differences between LcrV (37.6 kDa) and its orthologs, PcrV (32.3 kDa) from *Pseudomonas aeruginosa* and AcrV (40.2 kDa) from *Aeromonas salmonicida*. These two bacteria are endowed with a T3S system closely related to the T3S system of *Yersinia* spp. The PcrV and AcrV proteins are able to complement a mutation in the *lcrV* gene of *Yersinia* and form smaller and larger tip complexes respectively. Alignment of the three proteins reveals that the size differences are restricted to the two

globular domains of the proteins (residues 1-145 and 183-278), while the two long helices,  $\alpha 7$  and  $\alpha 12$ , that connect them are conserved (Fig. 18A, B). For example, AcrV differs from LcrV only by two big insertions in the second globular domain that make the whole protein over 3 kDa larger. In order to determine the orientation of the LcrV molecule in the tip complex we decided to take advantage of the visible size differences between tip complexes formed by LcrV, PcrV and AcrV, by engineering hybrids between these three proteins. The hybrids would be considerably smaller or larger than wildtype LcrV in one of the globular domains. Therefore they should form tip complexes with slight changes in the head or the base parts, which can then be observed by STEM. This would tell us which domains of the molecule form which parts of the tip complex.

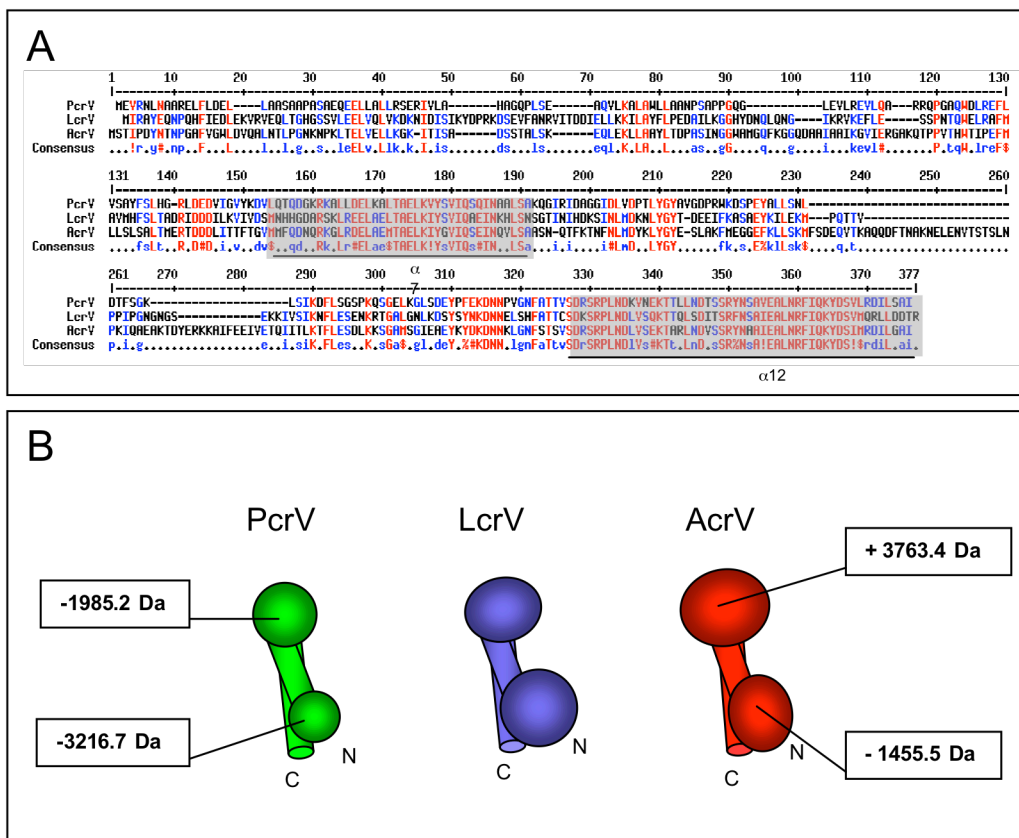


**Fig. 18.** (A) Alignment of PcrV from *P. aeruginosa*, LcrV from *Y. enterocolitica* and AcrV from *A. salmonicida* using Multalin ([www.expasy.ch](http://www.expasy.ch)). The two helices,  $\alpha 7$  and  $\alpha 12$ , connecting the globular domains are marked in gray. (B) Schematic representations of the structures of the three proteins PcrV (green), LcrV (blue) and AcrV (red). The size differences in the globular domains in comparison to LcrV are indicated.

## Results and Discussion

### Insertion of a 6xHis tag into LcrV

We generated the vector pPB22 (**Appendix A**) carrying *lcrV* with a *his*-tag in the aminotermus. To test whether the N-terminally His-tagged LcrV complements a mutation in the *lcrV* gene, plasmid pPB22 was transformed into *Y. enterocolitica*  $\Delta$ HOPEMNV bacteria. Secretion was induced *in vitro* and the culture supernatant was analyzed. His-LcrV was secreted suggesting that the His-tag in the N-terminus of the protein did not interfere with its secretion (data not shown). This result was surprising because it is known for the effector proteins that already small changes in the N-terminus lead to a loss of secretion.

To verify functional complementation, *Y. enterocolitica*  $\Delta$ HOPEMNV complemented with pPB22 was tested in a red blood cell hemolysis assay. The His-tagged protein was capable of complementing the mutation (data not shown), indicating that the His-tag does not interfere with the formation of the tip complex and its function.

An important prerequisite for the immunolabelling is to determine if the tag is accessible to antibodies. This was tested in an antibody protection assay with antibodies directed against the His-tag. The antibodies protected the erythrocytes only slightly from lysis by *Y. enterocolitica*  $\Delta$ HOPEMNV + pPB22 (**Fig. 19**). This result suggested that the His-tag is probably partially buried in the structure and not accessible to antibodies.

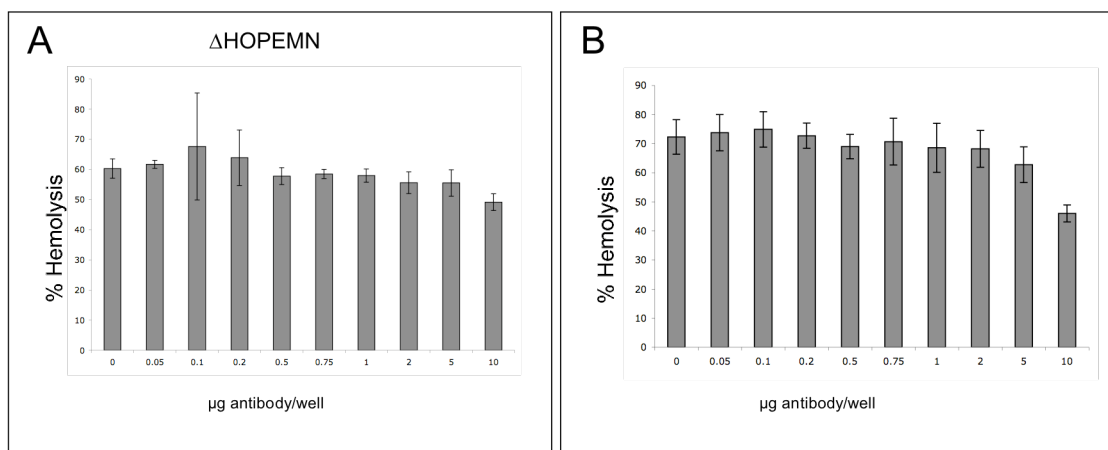


**Fig. 19.** Hemolysis caused by *Y. enterocolitica*  $\Delta$ HOPEMN (**A**) and  $\Delta$ HOPEMNV complemented with pPB22 (**B**) in the presence of anti-His antibodies. The bacteria were pre-incubated with the antibodies for 20 minutes at 37°C and the red blood cells were infected for 1 h at 37°C.

### Insertion of a FLAG-tag into LcrV

We constructed two plasmids, pPB46 and pPB47, capable of expressing FLAG-tagged LcrV. The FLAG tag was inserted in a loop between strands  $\beta$ 4 and  $\beta$ 5 (**Fig. 20**). This loop varies between different species and strains of *Yersinia* and is exposed at the surface, according to the crystal structure. The difference between the two constructs is that in pPB46

the tag is inserted between aa 227 and 228 and in pPB47 the tag replaces aa 226 to 233 of LcrV. Both constructs were transformed into *Y. enterocolitica* ΔHOPEMNV and secretion was checked *in vitro*. Both constructs were secreted, suggesting that the FLAG-tag did not interfere with secretion (data not shown). To verify functional complementation, we tested *Y. enterocolitica* ΔHOPEMNV harboring plasmids pPB46 or pPB47 in a hemolysis assay. Both constructs were able to complement the mutation in the *lcrV* gene, even though not to the same level as the wildtype protein (Fig. 21).

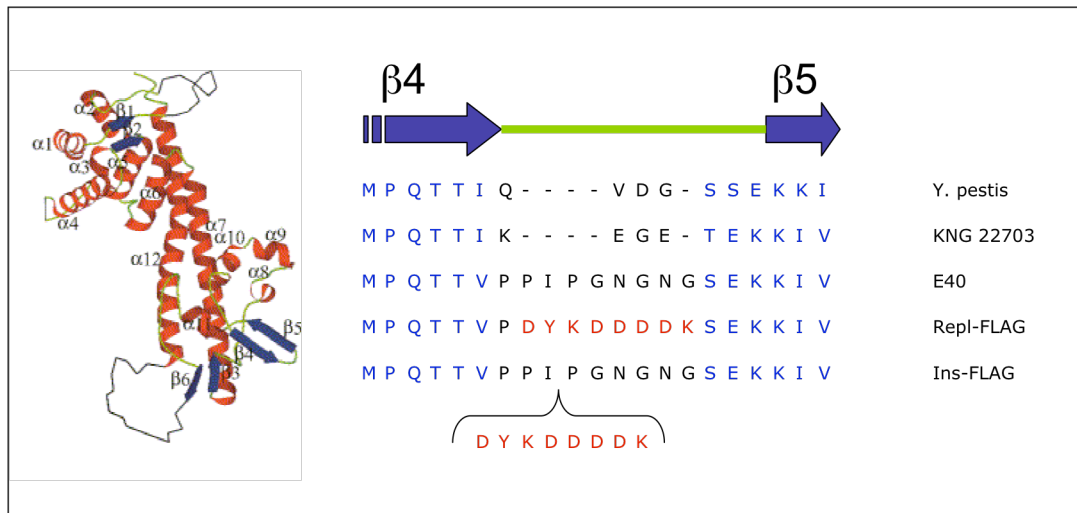


**Fig. 20.** Structure of LcrV of *Y. pestis* as published by Derewenda et al. 2004 and graphical representation of the loop between strands  $\beta 4$  and  $\beta 5$ . The length and amino acid composition of this loop varies between *Y. pestis*, and the two *Y. enterocolitica* strains KNG22703 and E40. The FLAG tag was either inserted in this loop (pPB46) or replaces a part of the loop (pPB47).

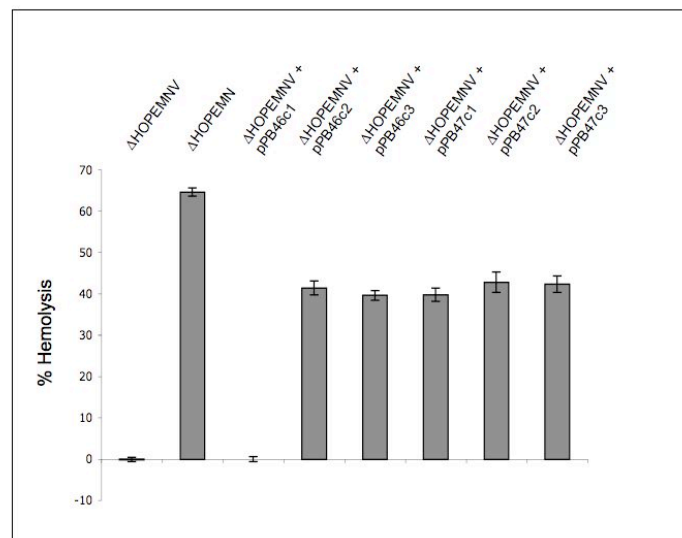


**Fig. 21.** Hemolysis caused by *Y. enterocolitica* ΔHOPEMNV complemented with plasmids pPB46 and pPB47. Three clones were analyzed for each plasmid.



To determine the accessibility of the FLAG tag, we checked if anti-FLAG antibodies were able to protect red blood cells from hemolysis by  $\Delta$ HOPEMNV bacteria expressing the FLAG-tagged LcrV proteins (**Fig. 22**). Strong inhibition of hemolysis was observed for the  $\Delta$ HOPEMNV bacteria carrying pPB46 (**Fig. 22C**). Already 0.1  $\mu$ g of antibodies per well was enough to reduce hemolysis by 80%, but only high concentrations lead to complete protection. The FLAG antibodies were therefore more efficient in blocking hemolysis than anti-LcrV antibodies at low concentrations (**Fig. 22D**). In contrast the  $\Delta$ HOPEMNV bacteria carrying plasmid pPB47 or pPB42 (wt LcrV as a control, **Fig. 22A, B**), were still able to cause more than 70% of hemolysis even at highest antibody concentrations. These results demonstrated that the FLAG tag inserted between aa 227 and 228, in the case of pPB46, is exposed at the surface of the protein and accessible to antibodies. In contrast to this a FLAG tag that replaces the aa 226 to 233 (pPB47), seems to be buried in the structure and not accessible. The very efficient inhibition of hemolysis observed for pPB46 makes it an ideal candidate for immunolabelling. Instead of using whole anti-FLAG antibodies, anti-FLAG Fabs could be used. Fabs are smaller and would allow a much more accurate localization of the tag.

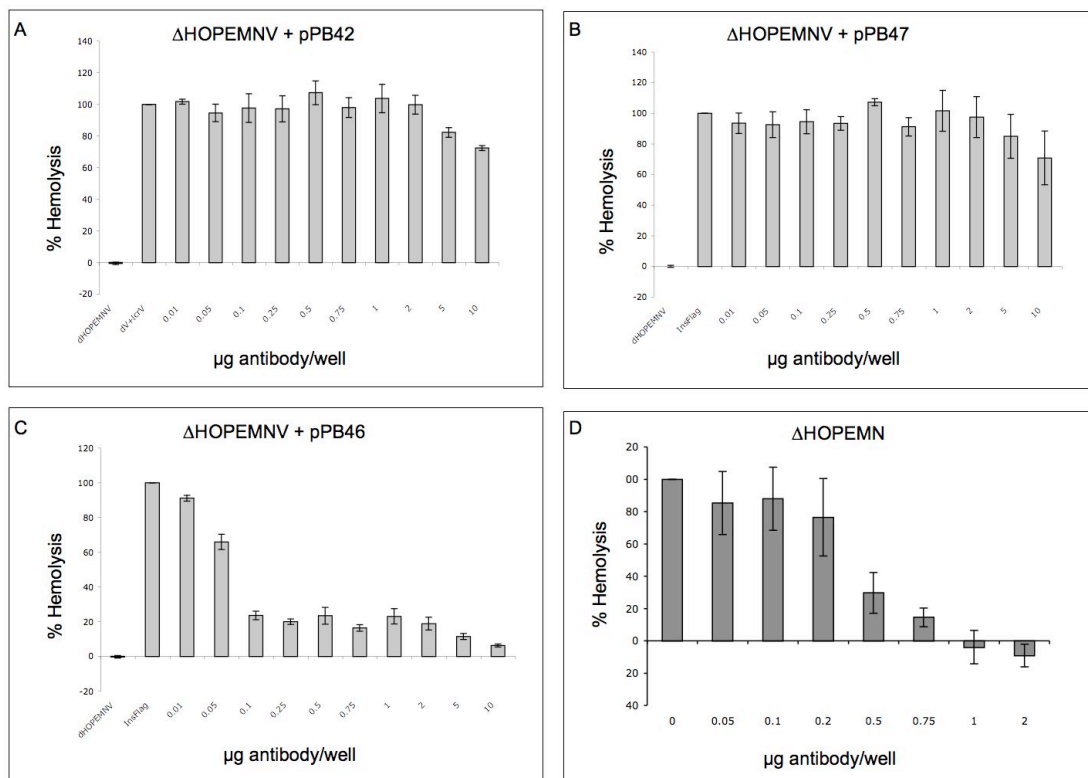


**Fig. 22.** Hemolysis caused by *Y. enterocolitica*  $\Delta$ HOPEMNV complemented with pPB42 (wt LcrV, **A**), pPB47 (**B**) or pPB46 (**C**) in the presence of anti-FLAG antibodies. (**D**) Hemolysis caused by *Y. enterocolitica*  $\Delta$ HOPEMNV in the presence of anti-LcrV antibodies. The bacteria were pre-incubated with the antibodies for 20 minutes at 37° C and the red blood cells were infected for 1 h at 37°C.

### Generation of Hybrids between LcrV, PcrV and AcrV

In total we generated 16 different hybrids (**Appendix A**) between LcrV, PcrV and AcrV but we restricted the analysis to four constructs: pPB30, 31, 34 and 35. These plasmids would allow expression of different hybrid proteins (H5, H6, H8 and H10, **Fig. 23**), which would have large size differences in certain domains, in comparison to wildtype LcrV. The expression of the hybrid proteins was first tested in *E. coli*. All four hybrids were expressed and had the expected size (data not shown). To check if the hybrid proteins were expressed and secreted by *Yersinia*, the plasmids were transformed into *Y. enterocolitica* ΔHOPEMNV bacteria. Secretion was triggered by Ca<sup>2+</sup> chelation and the culture supernatant was analyzed. All hybrid proteins were secreted into the culture supernatant in comparable amounts (**Fig. 24A**).

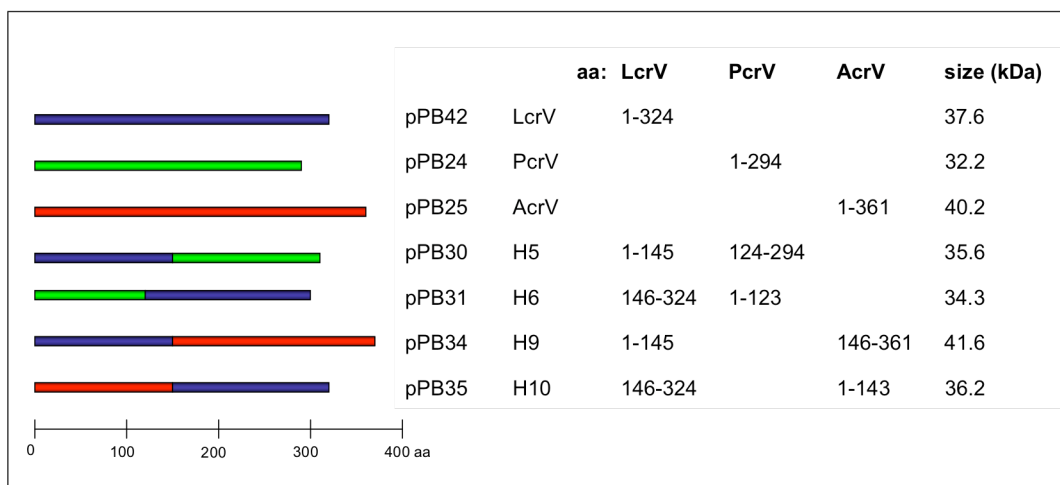


**Fig. 23.** Schematic representation of the four Hybrid proteins (H5, H6, H9 and H10) and the corresponding wildtype proteins. Expression plasmids, hybrid compositions and sizes are indicated.

The ability of the hybrid proteins to form functional tip complexes was tested by measuring pore formation in a hemolysis assay (**Fig. 24B**). In parallel we tested ΔHOPEMNV bacteria complemented with wildtype LcrV, PcrV or LcrV proteins to compare the levels of hemolysis. The results indicated that even though all hybrid proteins were secreted, not all could complement the *lcrV* mutation with the same efficacy. We observed that whenever the N-terminus was from LcrV, the hybrids caused approximately the same level of hemolysis as wildtype LcrV. On the other hand when the N-terminus was from PcrV the hemolysis was reduced to low levels as observed for wildtype PcrV. Similar results were obtained with hybrids composed of AcrV and LcrV. We concluded that the N-terminus of the hybrid proteins determined the efficacy of the hemolysis. This effect could be direct, i.e. the N-terminal domain itself interacts with the pore components YopB and YopD or it could be indirect, i.e. the N-terminus is required for the stability of the whole tip complex and thus is affecting its pore forming ability. To answer this question the interaction sites between the LcrV-tip complex and the translocators need to be defined.

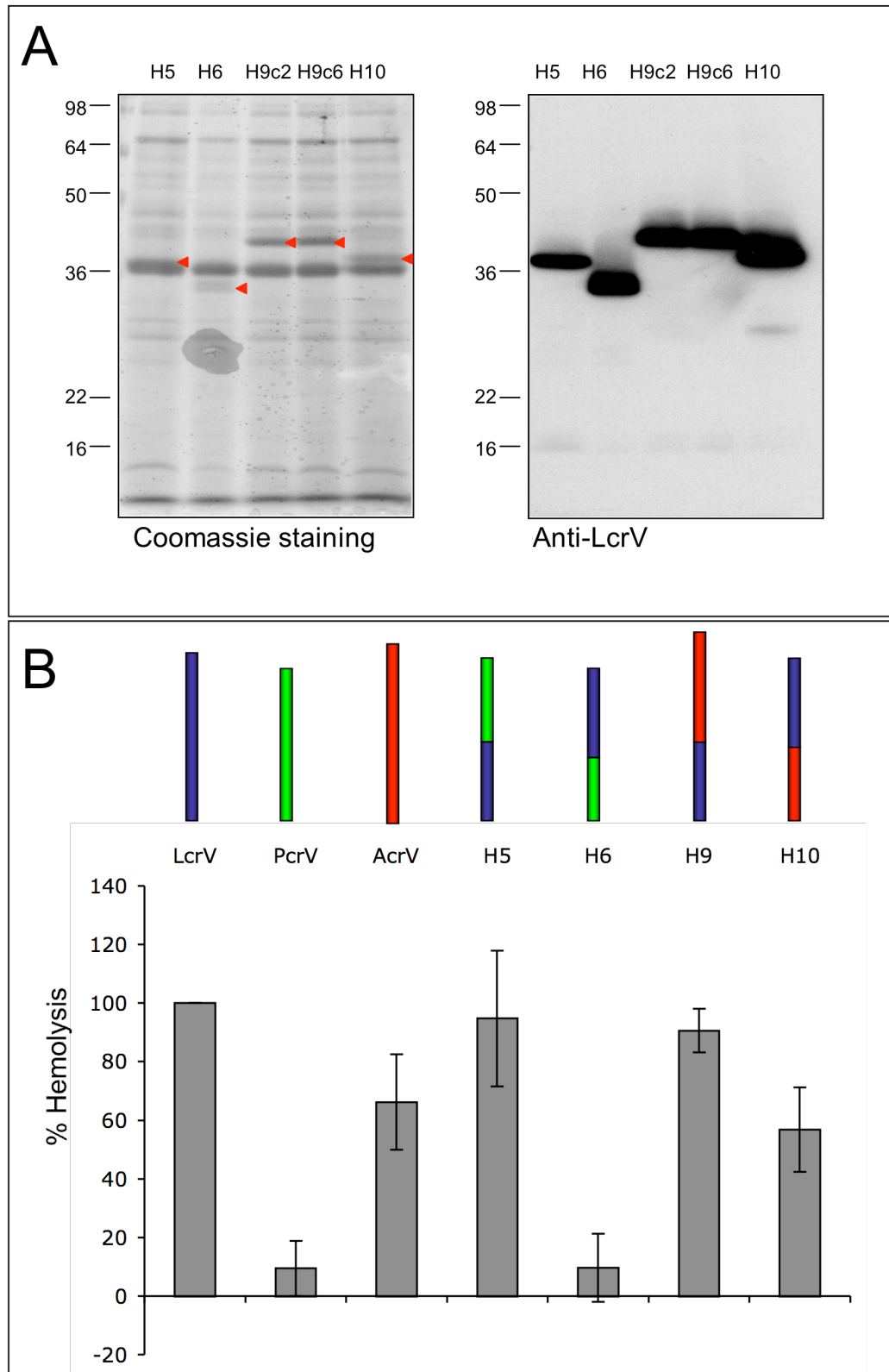


**Fig. 24. (A)** Coomassie stained SDS-PAGE and western blot analysis of proteins secreted by *Y. enterocolitica*  $\Delta$ HOPEMNV complemented with hybrids H5, H6, H9 and H10. The secreted hybrid proteins are indicated by red arrowheads. Two clones were analyzed for hybrid H9. **(B)** Lytic activity on red blood cells after 2 h of contact with *Y. enterocolitica*  $\Delta$ HOPEMNV complemented with wildtype LcrV, PcrV, AcrV or the hybrid proteins H5, H6, H9 and H10.

In order to determine the orientation of the LcrV molecules forming the tip complex, we compared the size of hybrid tip complexes to the size of tip complexes formed by the LcrV, PcrV and AcrV wildtype proteins. Needles were prepared and purified as described before and subjected to analysis by STEM. Averages of all hybrid tip complexes could be produced (**Fig. 25**). As published before, tip complexes formed by LcrV consist of three distinct parts: the head, the neck and the base. Tip complexes formed by PcrV have a smaller base, while both the neck and the head are still comparable to the LcrV tip complex. Tip complexes formed by the LcrV-PcrV hybrid protein had the characteristic shape, consisting of a head, a neck and a base similar to wildtype LcrV tip complexes. However, in this hybrid protein the first globular domain of PcrV was replaced by the corresponding domain of LcrV, which is over 3.2 kDa bigger. This replacement led to a significant increase of the base part in comparison to PcrV tip complexes, whilst the rest of the tip complex seemed unchanged. This suggested that the N-terminal globular domain forms the base. According to this the second globular domain forms the head of the tip complex. The results obtained with the PcrV-LcrV hybrid protein confirmed this hypothesis. Here the N-terminal globular domain of LcrV was exchanged by the smaller domain of PcrV (-3.2 kDa). As expected we observed that tip complexes made by this hybrid had a smaller base, resembling tip complexes formed by PcrV.

Tip complexes formed by AcrV were larger and more diverse in shape. The base had a different shape, the neck was less pronounced and the head appeared broader than in the LcrV tip complex. In the LcrV-AcrV hybrid the second globular domain, which, according to our hypothesis, would form the head of the tip complex is almost 4 kDa larger than in LcrV. Consistent with this, the tip complexes formed by this protein had a “normal” base, but the head was larger and different in shape. The last hybrid, AcrV-LcrV, had the smallest size difference to the LcrV wildtype protein. The N-terminal globular domain of LcrV was replaced by the corresponding domain of AcrV, leading to a reduction in size of 1.5 kDa. Thus we expected to see a change in the base part of the tip complex. No reduction of the base could be observed, but the base had indeed a different shape resembling the base of the AcrV tip complex.

The results presented above allow us to present a simple model of the tip complex formed by LcrV (**Fig. 26**). In this model the molecule would be oriented with the N- and C terminus to the needle, the first globular domain forming the base of the tip complex, the second globular domain forming the head of the tip complex. The two long alpha helices ( $\alpha 7$  and  $\alpha 12$ ) connect the two globular domains and face inward.

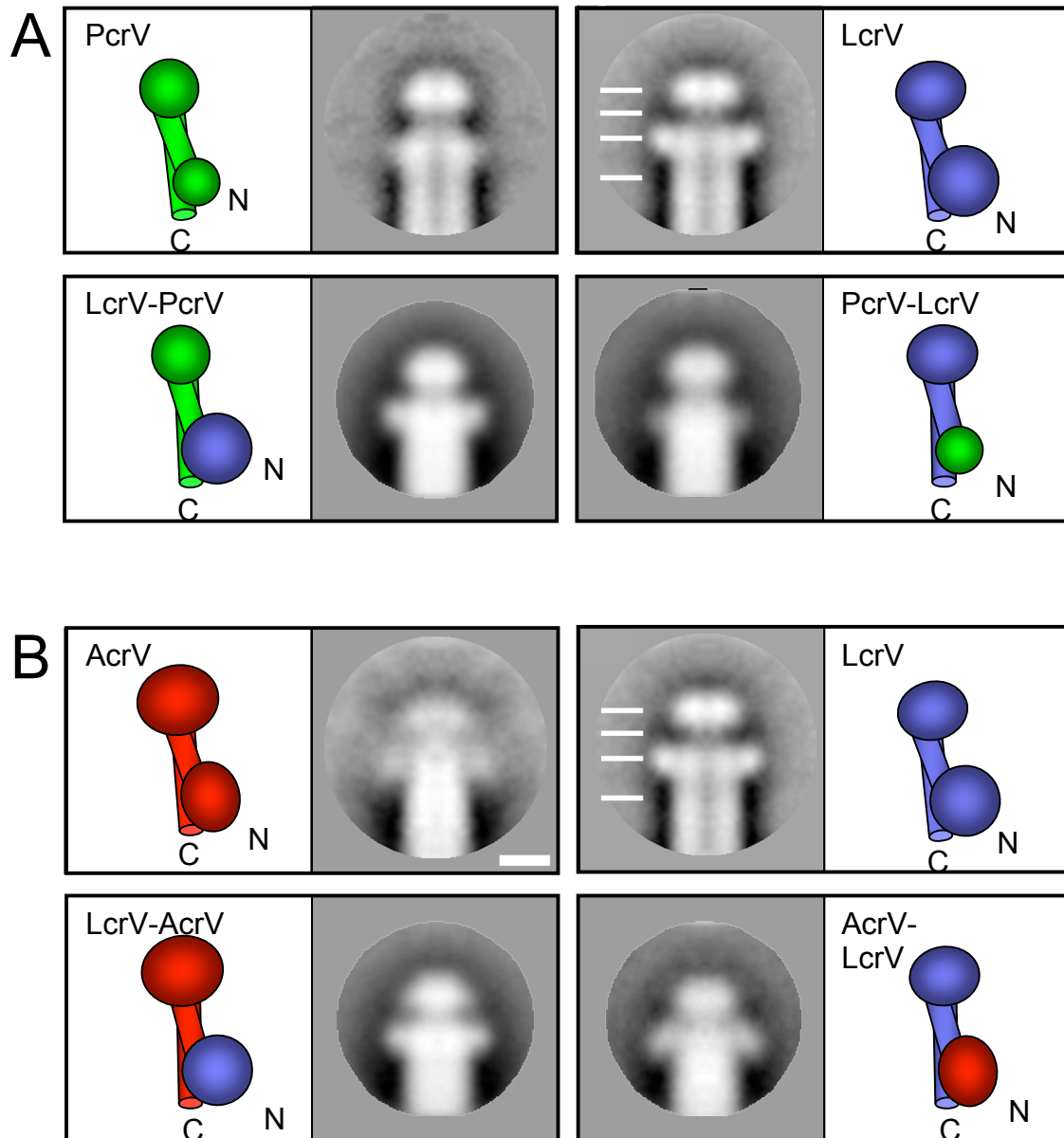


**Fig. 25.** Tip complexes formed by *Y. enterocolitica*  $\Delta$ HOPEMNV complemented with the four hybrid proteins. **(A)** Projection averages of tip complexes formed by wildtype PcrV and LcrV (top) and LcrV-PcrV (H5), PcrV-LcrV (H6) hybrids (bottom). Schematic representations of all proteins are drawn next to the corresponding tip complexes. **(B)** Projection averages of tip complexes formed by wildtype AcrV and LcrV (top) and LcrV-AcrV (H9), AcrV-LcrV (H10) hybrids (bottom). Schematic representations of all proteins are drawn next to the corresponding tip complexes

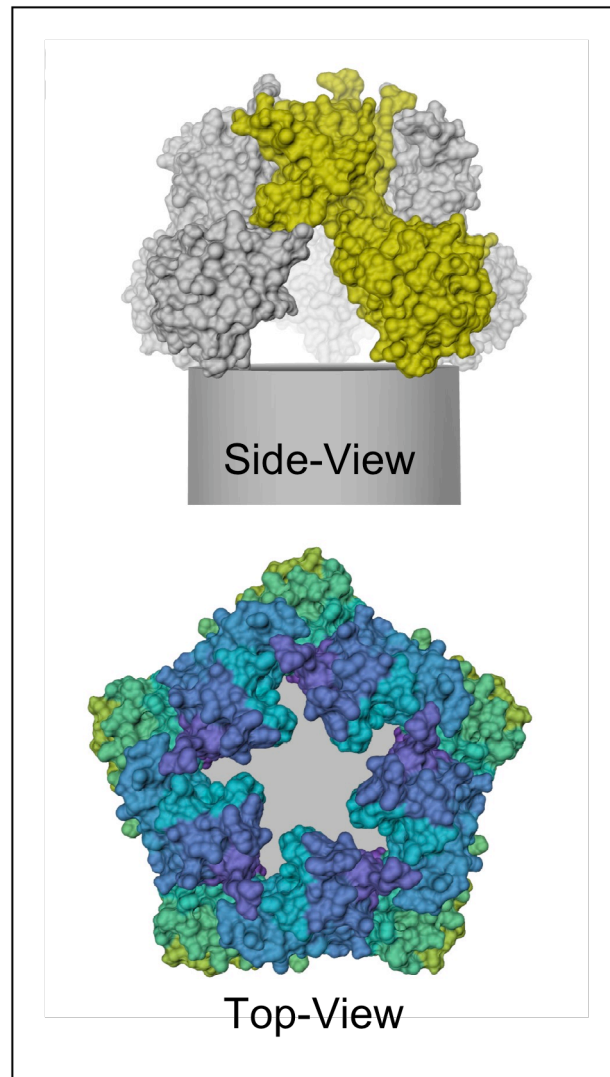


**Fig. 26.** Atomic modeling of the LcrV tip complex on top of the injectisome needle (cylinder). A side-view and a top view are shown.

## Materials and Methods

### Cloning

The *lcrV* sequence was amplified by PCR on pYV40 DNA using primers 3503 and 3504. The PCR products were digested with NdeI and KpnI and cloned into the NdeI and KpnI sites of the vector pLJM3 giving plasmid pPB22 (**Appendix A**). This plasmid encoded a N-terminally *his*-tagged *lcrV* gene under the *yopE* promoter, allowing the expression of His-LcrV in *Y. enterocolitica*.

The FLAG motive was introduced into the *lcrV* gene using overlapping PCR. The first two PCR reactions were performed using the primer pairs 4230/3807 and 4231/3806 for pPB46 or primer pairs 4232/3807 and 4233/3806 for pPB47. Plasmid pMN12 was used as DNA template. The second, overlapping PCR was performed on the PCR products obtained from the first two PCR reactions using primers 3806 and 3807 for both constructs. The PCR products were digested with NcoI and EcoRI and introduced into the NcoI/EcoRI sites of the expression vector pBAD*mycHisA* (Invitrogen), giving plasmid pPB46 or pPB47.

Hybrids between *lcrV*, *pcrV* or *acrV* were generated using overlapping PCR. Individual parts of every hybrid were amplified from the corresponding DNA sequences by PCR with the primer pairs as indicated (**Table 2**). The PCR products were mixed and served as template for the overlapping PCR which was performed with the appropriate primers (**Table 2**). The PCR product was digested with NcoI/EcoRI or AflIII/EcoRI and cloned into the NcoI/EcoRI sites of the expression vector pBAD*mycHisA* (Invitrogen) giving plasmids pPB30, pPB31, pPB34 and pPB35.

Construct		First round of PCR				Overlapping PCR	
		Primers 1	Template 1	Primers 2	Template 2	Primer 1	Primer 2
pPB30	H5	3934/3806	pMN12	3935/3809	pPB24	3806	3807
pPB31	H6	3937/3957	pPB24	3936/3807	pMN12	3957	3807
pPB34	H9	3942/3806	pMN12	3943/3811	pPB25	3806	3811
pPB35	H10	3945/3810	pPB25	3944/3807	pMN12	3810	3807

**Table 2.** Primers used to generate Hybrid H5, H6, H9 and H10. MIPA numbers are indicated.

### Expression test in *E. coli*

To check expression of proteins from the pBAD vector, plasmids were transformed into *E. coli* TOP10 bacteria. Overnight cultures were inoculated to an OD<sub>600</sub> of 0.1 in fresh LB medium containing appropriate antibiotics and grown at 37°C. Expression was induced for 4 h by the addition of 0.2 % arabinose as soon as the cultures reached an OD<sub>600</sub> of 0.6. The bacteria were collected by centrifugation and analyzed by SDS-PAGE followed by Coomassie staining or western blotting.

### Expression and secretion test in *Y. enterocolitica*

*In vitro* secretion was performed as described before by (Mueller, Broz *et al.*, 2005).

### Functional complementation test

Hemolysis assays were performed as described before by (Goure, Broz *et al.*, 2005).

### STEM analysis of Hybrid tip complexes

Needles purification and STEM analysis was done as described before by (Mueller, Broz *et al.*, 2005).

### 3.4.2 Production of antibodies directed against PcrV and AcrV

#### Introduction

To complete the list of tools necessary for the analysis of the tip complex, antibodies against PcrV from *Pseudomonas aeruginosa* and AcrV from *Aeromonas salmonicida* were generated. These antibodies allow the detection of the proteins in western blots, helping the analysis of the hybrids between LcrV/PcrV and LcrV/AcrV. In addition it would be possible to label hybrid tip complexes with anti-LcrV, anti-PcrV or anti-AcrV antibodies, examine them by electron microscopy and thereby determine which parts of these tip complexes are formed by which proteins.

#### Results and Discussion

In order to produce antibodies directed against PcrV and AcrV, the *pcrV* and *acrV* sequences were amplified by PCR on genomic DNA from *Pseudomonas aeruginosa* PAO1 and *Aeromonas salmonicida* JF2267 using the primer pairs MIPA 3808/4250 and MIPA 3810/4251 respectively. The PCR products were digested with NcoI/EcoRI or AflIII/EcoRI and cloned in frame with a C-terminal 6xHis tag into the NcoI/EcoRI sites of the expression vector pBADmycHisA giving plasmids pPB44 and pPB45 (**Appendix A**).

Plasmids pPB44 and pPB45 were transformed into *E. coli* TOP10. Protein expression was induced by the addition of 0.2 % arabinose for 4 h at 37°C. Soluble PcrV-His and AcrV-His proteins were purified on chelating sepharose beads (Amersham Biosciences). Further purification was achieved by size exclusion chromatography on a Superdex 200 preparative column. Rabbits were immunized by 4 injections with a total of 1 mg of either PcrV-His or AcrV-His in 20 mM Phosphate-Buffer, 500 mM NaCl.



### 3.4.3 Determination of the Stoichiometry of needle components

(Mass per length measurements were done by Viola Huschauer and Shirley A. Müller, purified YscF was provided by Isabel Sorg)

#### Introduction

To generate an accurate atomic model of the tip complex it is not only necessary to know the orientation of LcrV, but also how many molecules of LcrV form the tip complex. Therefore we decided to quantify the amount of LcrV and YscF protein in purified needles and calculate the ratio of LcrV:YscF per needle. Together with the known length of the needles and the known mass-per-length value of purified needles it should be possible to estimate the number of LcrV molecules per needle tip complex.

#### Results and Discussion

Dilutions of known amounts of purified YscF and His-LcrV were compared to the YscF and LcrV content in purified needle fractions (**Fig. 27**). Thus the molar ratio of purified wt needles was estimated to be around 1 LcrV to 33 +/- 7 YscF. The mass-per-length value of purified needles was determined to be 21.6 +/- 1.7 kDa/nm, which means 2.3 +/- 0.2 YscF molecules/nm (Viola Huschauer and Shirley Müller, unpublished data). Assuming that the *Y. enterocolitica* needle has a mean length of 55-60 nm, one needle would consist of approximately 127-138 YscF monomers. Thus we can speculate that three to six molecules of LcrV form a needle tip.

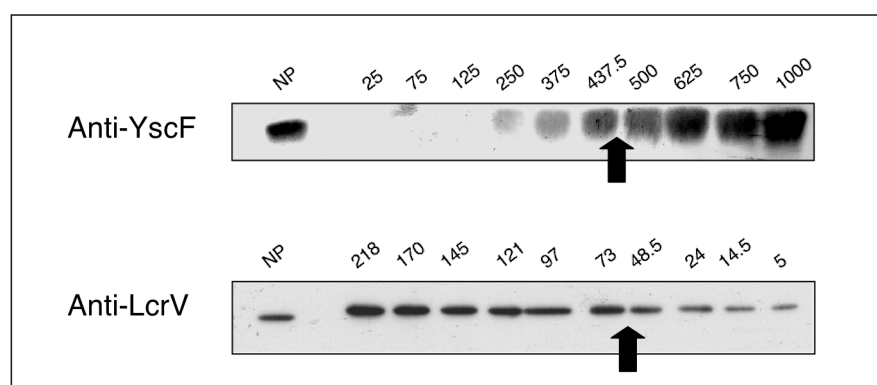


**Fig. 27.** Quantification of the LcrV and YscF content in purified needle fractions. The amount of purified YscF and His-LcrV is indicated in ng of protein. Black arrows indicate where the protein contents of purified needles (NP) match known amounts of purified YscF and LcrV. The quantification was carried out in three independent experiments, giving a molar ratio of 32.3 +/- 7.3 molecules of YscF per molecule of LcrV.

## Materials and Methods

### Protein purification

The LcrV gene was amplified by PCR from the pYV plasmid DNA of the *Y. enterocolitica* strain MRS40, using the primers MIPA 3283 and 3290. The PCR product was digested with NdeI and BamHI, and cloned into the expression vector pET28a (Novagen). A soluble His-LcrV protein was produced in *E. coli* BL21 (DE3) pLysS and purified on chelating sepharose beads (Amersham Biosciences).

YscF was produced as a glutathione S-transferase fusion protein encoded by plasmid pISO66. Expression of the protein was induced by adding 0.2 mM isopropyl- $\beta$ -D-thiogalactopyranoside (final concentration) at an optical density of 0.6. Four hours after induction, cells were collected, lysed by sonication in lysisbuffer (PBS, 1% Triton-X100, 1 mM phenylmethylsulfonylfluoride, 5mM dithiotreitol, protease inhibitor cocktail complete Mini (Roche)), and purified by affinity chromatography with glutathione-Sepharose (Amersham Pharmacia Biotech). Loaded beads were washed five times with PBS at 4°C. YscF was eluted from the beads by thrombin cleavage (thrombin protease 50 units/ml in PBS) for 1 h at room temperature. Thrombin was removed by incubation with benzamidine-Sepharose beads.

### Quantification

Purified needles as well as different amounts of purified His-LcrV and YscF were separated by SDS-PAGE, transferred to nitrocellulose membranes and subjected to western blot analysis with anti-LcrV and anti-YscF antibodies. The intensities of the LcrV and YscF protein bands were analyzed by scanning the films (EPSON PERFECTION 4870 PHOTO, at 300 dpi) and subsequent quantification of the pixel intensities using ImageJ 1.33u (<http://rsb.info.nih.gov/ij/>). The number of molecules of LcrV and YscF in the needle fraction was determined by comparing the intensities of signals in the needle fraction with signals of purified His-LcrV and YscF standards.

### 3.4.4 Estimation of the size of pores made by LcrV and its orthologs

#### Introduction

Recent data, published by Goure, Broz et al. and Mueller, Broz et al. suggested that the tip complex formed by LcrV would act as an assembly platform for the translocation. It was shown that PcrV/AcrV can complement a *Y. enterocolitica lcrV* mutation and form different sized tip complexes. One could therefore hypothesize that such tip complexes would form smaller or bigger pores. This would explain an interesting observation published in 2001. The authors had complemented a *lcrV* mutation with *pcrV* from *P.aeruginosa* and observed that the pore size, measured by osmoprotection, had apparently decreased (Holmstrom *et al.*, 2001).

We decided to use osmoprotection to estimate the size of pores formed by tip complexes made of LcrV, PcrV or AcrV. The principle of osmoprotection is to do a hemolysis assay in the presence of carbohydrates of increasing osmotic diameter. As long the carbohydrates are small enough to pass through the translocation pore, they distribute equally in the red blood cells and the medium and they cannot counteract the osmotic pressure due to hemoglobin in the red blood cells, which leads to hemolysis. Carbohydrates that are bigger than the translocation pore, cannot enter the red blood cells, stay in the medium and counteract the osmotic pressure in the red blood cell, thus preventing hemolysis. This allows to estimate the pore size if the diameter of the carbohydrates is known.

#### Results and Discussion

*Y. enterocolitica*  $\Delta$ HOPEMNV bacteria complemented by LcrV (pPB42), PcrV (pPB24) or AcrV (pPB25) were tested in a hemolysis assay. Different sized carbohydrates ranging from 0.92 to 3.8 nm in diameter were added to the medium (**Table 3**). We observed that PEG 3200 ( $\varnothing$  3.2 nm) protected erythrocytes from hemolysis by pores formed by LcrV or AcrV tip complexes (**Fig. 28**). Carbohydrates smaller than PEG 3000 did not protect the erythrocytes, suggesting that the diameter of the pores formed by LcrV or AcrV tip complexes was between 2.4 and 3.2 nm. The levels of hemolysis caused by *Y. enterocolitica*  $\Delta$ HOPEMNV complemented with PcrV (pPB24) were too low to allow any reliable conclusions on the size of the pore (data not shown).

#### Material and Methods

Hemolysis was done as described as before (Goure, Broz *et al.*, 2005).

Name	Osmotic diameter
Sucrose	0.92 nm
Raffinose	1.14 nm
PEG 400	1.36 nm
PEG 600	1.6 nm
PEG 1000	2 nm
PEG 1500	2.1 nm
Dextrin 15	2.2 nm
PEG 2000	2.4 nm
PEG 3000	3.2 nm
PEG 4000	3.8 nm

**Table 3.** Name and osmotic diameter of the carbohydrates used in this study. Osmotic diameters as reported by Hakansson *et al.*, 1996; Holmstrom, *et al.* 2001; Dacheux *et al.*, 2001; Blocker *et al.*, 1999.

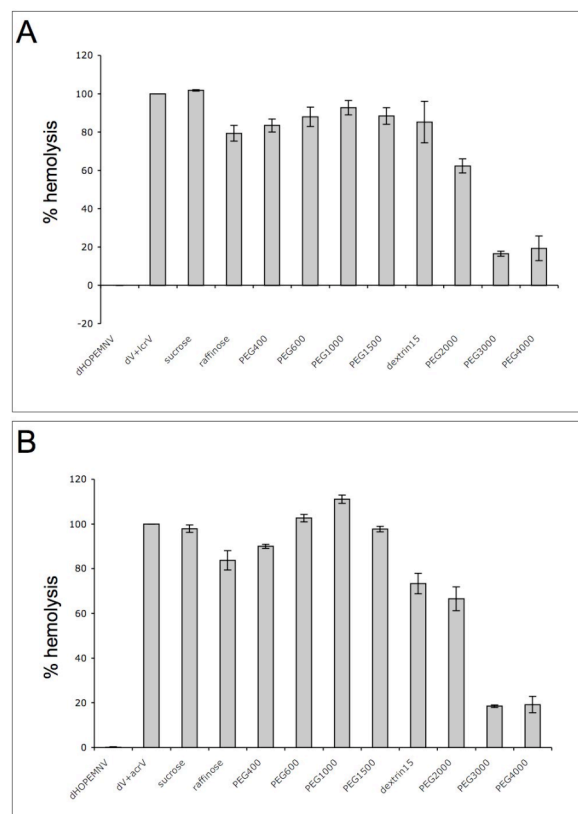


**Fig. 28.** Hemolysis of *Y. enterocolitica* ΔHOPEMNV complemented with (A) pPB42 (LcrV) or (B) pPB25 (AcrV) in the presence of carbohydrates of increasing diameter.

### 3.4.5 The translocators YopB and YopD interact with liposomes *in vitro*

(Freeze Fracture Electron microscopy was done by Mohamed Chami)

#### Introduction

The visualization and analysis of the translocation pore and its component remains one of the burning questions in the field of type III Secretion. So far no convincing images of the pore could be presented. Some very promising data were published by Schoehn et al. in 2003 (Schoehn *et al.*, 2003). The authors expressed and purified the translocators PopB and PopD of *P. aeruginosa* together with their chaperone PcrH. They discovered that upon a shift to acidic pH the chaperone gets partially detached from the translocators, which had been unknown so far. Further they showed that the translocators are able to bind to liposomes at acidic pH. Electron microscopy analysis revealed ring-like structures on and next to the liposomes, suggesting that the translocators oligomerize and form pore-like structures upon contact to membranes. Unfortunately these pictures were far from being convincing and represented a major drawback of the publication. Nevertheless, we decided to use the same strategy to investigate the *Y. enterocolitica* translocators YopB and YopD.

#### Results and Discussion

SycD allows soluble expression of PopB and PopD in *E. coli*

The two hydrophobic translocators of *Y. enterocolitica*, YopB and YopD contain two and one transmembrane domain respectively. It has been reported before that both require an intrabacterial chaperone to be expressed and soluble (Neyt and Cornelis, 1999b; Schoehn *et al.*, 2003). We constructed plasmid pPB14, capable of co-expressing both translocators together with their chaperone SycD, which was cloned with a N-terminal His tag (**Appendix A**). Soluble chaperone-translocator complexes could be produced in *E. coli* and were purified on chelating sepharose beads (**Fig. 29**). The N-terminal His-tag in SycD did not disturb the chaperone/translocator complex formation.

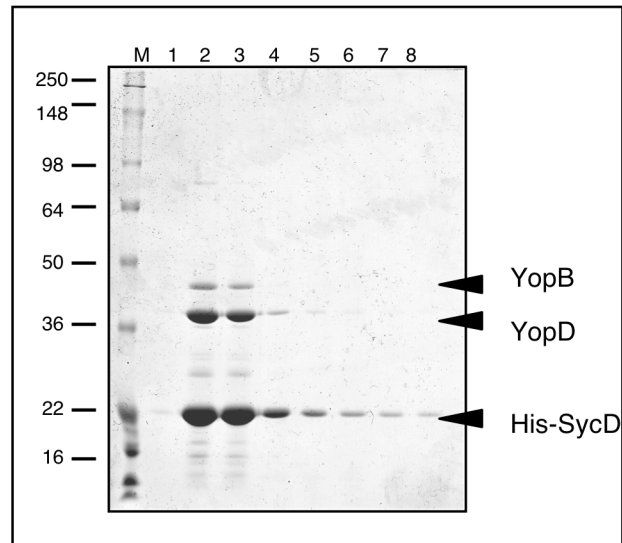


**Fig. 29.** Purification of soluble complexes between His-SycD/YopB and His-SycD/YopD. Lanes 1-8 show purification fractions after elution from chelating sepharose beads with 300 mM Imidazole. YopB and YopD elute mostly in fractions 2 and 3 together with the chaperone SycD. Low levels of the chaperone can still be detected in the following fractions.

### YopB and YopD do not interact with membranes when bound to their chaperone

To test if the translocators are able to interact with membranes, we mixed purified complexes His-SycD/YopB and His-SycD/YopD with artificial liposomes (15% Cholesterol, 25% DOPS and 60% DOPC) at pH 7.4 and separated soluble from membrane bound proteins by floatation in an Opti-Prep gradient (45%-5%). After the centrifugation, control liposomes were visible as a turbid band at the top of the gradient. Liposomes that had been incubated with protein migrated to the same fractions as the control liposomes. Analysis of the gradient revealed that the proteins could only be detected in the lowest fractions of the gradient, indicating that no interaction with the liposomes had occurred (**Fig. 30**).

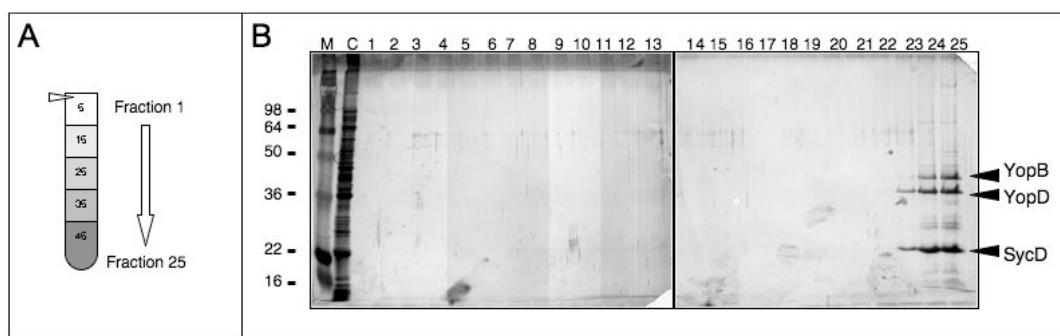


**Fig. 30.** Interaction of the translocators with liposomes in the presence of the chaperone. **(A)** Graph indicating the localization of the liposomes after floatation in the OptiPrep gradient (white arrowhead). **(B)** Fractions (1-25) of the OptiPrep gradient were collected and analyzed by SDS-PAGE followed by Silver staining. The proteins were found in the lowest fractions of the gradient (black arrowheads). Lane 2 shows total cell lysate.

### YopB and YopD interact with membranes upon release from the chaperone

As mentioned before, Schoehn et al. have shown that a change to acidic pH leads to the release of the chaperone PcrH from the translocators PopB/PopD. In this form the translocators can interact with artificial membranes. We decided to use the same approach to study the interaction of YopB and YopD with membranes. Purified complexes His-SycD/YopB and His-SycD/YopD were mixed with liposomes (15% Cholesterol, 25% DOPS and 60% DOPC) and the solution was dialysed against sodium acetate pH 5.0. In this way we would allow the translocators to immediately interact with membranes upon the release from the chaperone.

Visible aggregation and precipitation of the liposomes was observed after the dialysis in the protein/liposome mix, while the control liposome solution remained turbid. The dialysed samples were subjected to gradient floatation to separate the soluble proteins from the liposomes and the membrane bound protein. Again, control liposomes migrated to the top of

the gradient while liposomes that had been incubated with proteins were now found in the middle part of the gradient. This suggested that the overall density of these liposomes had changed due to the interaction with the proteins. The translocators YopB and YopD, as well as traces of the chaperone SycD, could be found in the same fractions as the liposomes (**Fig. 31**). Minor amounts of all three proteins could still be found at the bottom of the gradient. This result indicated that upon pH-triggered release of the YopB and YopD from the chaperone, the translocators were able to interact with artificial membranes. No conclusion could be made concerning the nature of this interaction i.e. whether the proteins were inserted into the membranes or just adhered peripherally to the liposomes. Notably, small amounts of the chaperone SycD were also found in the liposome-containing fractions at acidic pH. This may be due to non-specific association of the chaperone to the liposomes or the membrane bound translocators.

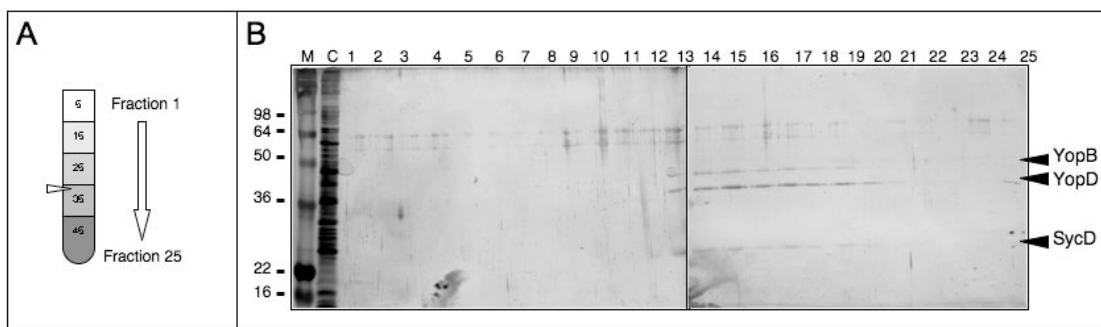


**Fig. 31.** Interaction of the translocators with liposomes after the release from the chaperone by pH-shift. **(A)** Graph indicating the localization of the liposomes after floatation in the OptiPrep gradient (white arrowhead). **(B)** Fractions of the OptiPrep gradient (1-25) were collected and analyzed by SDS-PAGE followed by Silver staining. The proteins migrate in the same fractions as the liposomes (black arrowheads). Lane 2 shows total cell lysate.

#### The role of the lipid composition

Several recent publications suggest that lipid rafts may play an important role during the infection with some bacterial pathogens endowed with a type III Secretion System (Hayward *et al.*, 2005; Schoehn *et al.*, 2003; van der Goot *et al.*, 2004). For *P. aeruginosa*, Schoehn *et al.* reported that the lipid composition of liposomes was important for the *in vitro* interaction with the translocators PopB/PopD. They showed that phosphatidylserine (DOPS) is needed for the association of the translocators with the liposomes, while cholesterol seems to be necessary for the lysis of the liposomes by PopB/PopD. We decided to study the effect of the lipid composition in our *in vitro* assay as well. We have not observed any lysis of liposomes upon interaction with YopB/YopD in our experiments, possibly because the lipid composition of the liposomes used was not adequate. We generated new liposomes with different lipid



compositions (L1-L5, **Table 4**). Proteoliposomes were prepared by dialysis and isolated by floatation. Independently of the lipid composition we observed liposome aggregation after the pH shift. Control liposomes of all compositions (L1-L5) migrated to the top of the gradient after the floatation. Surprisingly L3 and L4 liposomes had also migrated to the top of the gradient, while L1, L2 and L5 liposomes were located in the middle of the gradient (**Fig. 32**). SDS-PAGE and silver staining revealed that in all cases the proteins were associated with liposomes (**Fig. 32, data not shown**). The different migration properties of L3 and L4 (no DOPS) liposomes suggested that the proteins interacted differently with liposomes in the presence/absence of DOPS. In contrast to data published for *P. aeruginosa*, the presence/absence of cholesterol in the liposomes membranes did not have any effect.

	DOPC	DOPS	DOPE	Cholesterol	Sphingomyelin
L1	60%	25%		15%	
L2	25%	25%		25%	25%
L3	60%		25%	15%	
L4	60%		40%		
L5	60%	40%			

**Table 4.** Lipid composition of the different liposomes L1-L5 (w/w).

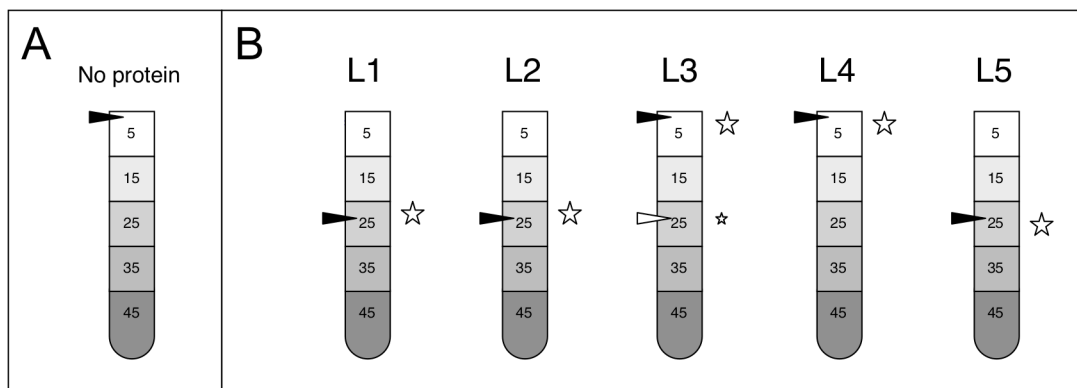


**Fig. 32.** Interaction with liposomes of different compositions. **(A)** Graph indicating the localization of all control liposomes (L1-L5) after floatation in the OptiPrep gradient (black arrowhead). **(B)** Interaction of the translocators with liposomes (L1-L5) after the release from the chaperone by pH-shift. The graphs indicate the localization of the proteoliposomes (L1-L5, Black arrowheads) and the proteins (star). The localization of the protein was determined by SDS-PAGE analysis (data not shown).

### Analysis of liposomes by TEM

Schoehn et al. had prepared proteoliposomes as described above and analyzed them by transmission electron microscopy. They observed that PopB alone, PopD alone and an equimolar mix of both were able to form ring-like structures on and next to the liposomes. These rings had an external diameter of 8 nm and an internal diameter of 4 nm.

We analyzed by TEM proteoliposomes incubated with YopB and YopD. We could not observe any ring-like structures in our samples (data not shown). This was not surprising as membrane proteins are hard to observe by TEM when they are inserted in a membrane.

### Analysis of proteoliposomes by freeze-fracture EM

Freeze fracture electron microscopy is a technique used to study insertion of proteins into membranes. The sample is applied on the grid and shot into liquid propane. The rapid cooling prevents formation of crystalline ice and results in amorphous ice. The frozen sample is split with a blade and the surface is coated with heavy metal (etched). Thus a replica is made. After the sample has been digested away, the replica is examined by EM. We took advantage of this technique to study proteoliposomes with different lipid compositions (L1, L2 and L4) that had been prepared as described before (**Fig. 33**). Control liposomes were well distributed in the sample. They had a diameter ranging from 50-500 nm. In contrast to this the proteoliposomes were aggregated and the size of the liposomes seemed to have decreased. Two distinct populations of proteins could be observed on L1 and L2 liposomes: inserted and membrane surface associated. The inserted proteins had a diameter of 8-10 nm suggesting that they were oligomers; as monomers would be too small to be detected by freeze fracture EM. However, the population did not appear to be homogenous, slightly smaller and bigger complexes could be observed. It was not possible to determine if these particles were pores due to the low resolution of freeze fracture EM. The second population of protein complexes was covering the surface of the liposomes. They may represent pre-insertion forms of the complexes. These might be responsible for the liposome aggregates, as they seemed to tether the liposomes together.

In contrast to this the proteins in the L4 liposome sample formed bigger protein aggregates that could be observed distributed between the liposomes. Such kind of aggregates can be generally observed when precipitated proteins are analyzed by freeze-fracture EM. Occasionally inserted complexes could be found as well, although in very low amounts.

These data suggested that the negatively charged phospholipid DOPS promoted the association of the translocators YopB/YopD with membranes and was required for the insertion of proteins complexes into the liposome membranes. When DOPS was missing, the proteins could not interact with the membranes and tended to aggregate. The insertion of the complexes into the liposome membranes could alter the density of the liposomes, which

would explain the difference in the migration pattern of the different liposomes in the gradient, observed before.

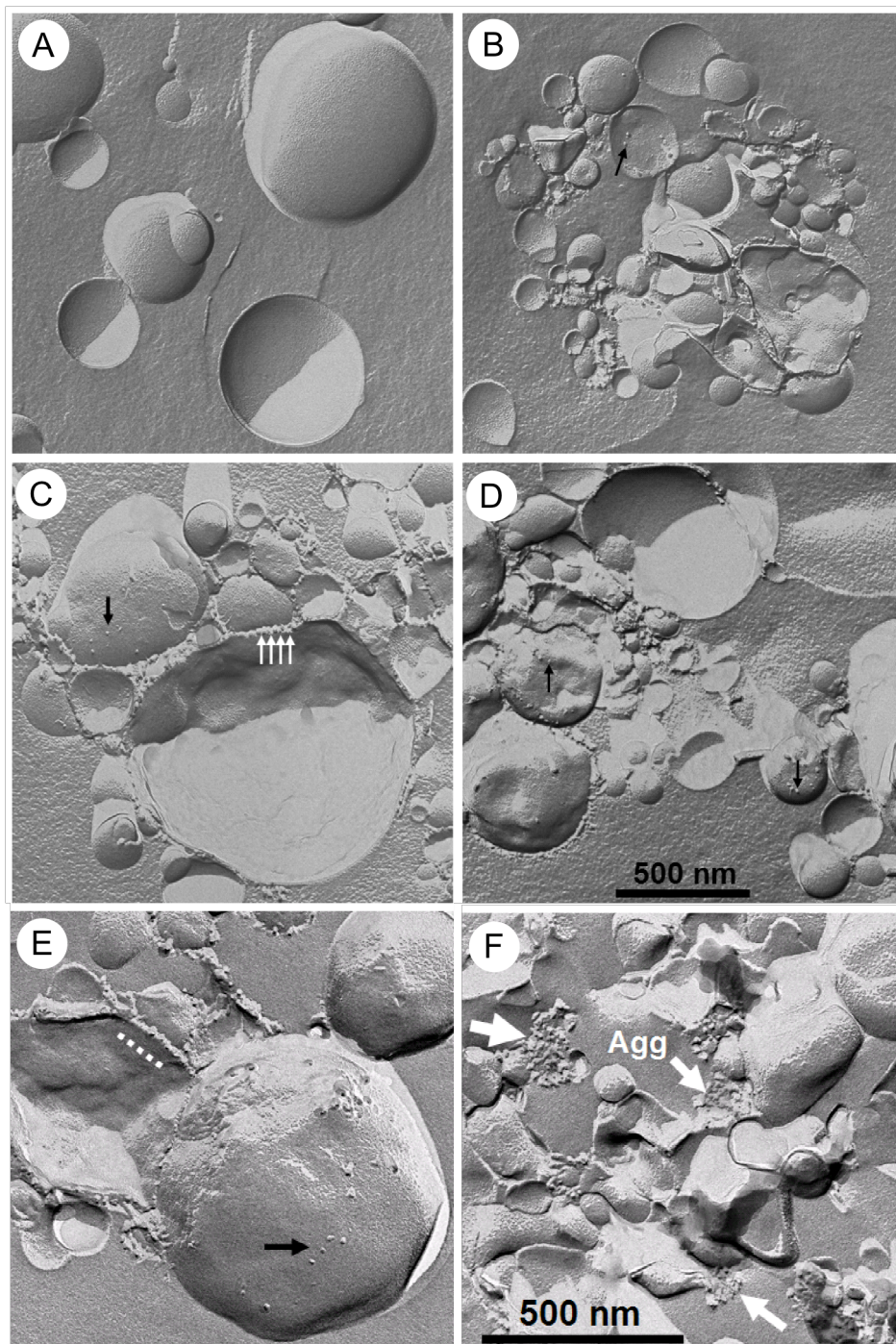


**Fig. 33.** Freeze-fracture EM analysis of proteoliposomes. (A) Control liposomes. (B-D) L1 Proteoliposomes. (E) L2 Proteoliposomes. (F) L4 Proteoliposomes. Black arrows indicate membrane-inserted complexes; white arrows indicate membrane-associated protein. Protein aggregates are indicated. Scale bars: 500 nm. Electron micrographs were provided by M. Chami and A. Engel.

## Materials and Methods

### Construction of the expression vector

A section of the *Y. enterocolitica* translocator operon, containing the genes *sycDyopByopD*, was amplified by PCR on the pYV40 DNA with primers MIPA 3277 and MIPA 3282. The PCR product was digested with BamHI and NdeI and cloned into the BamHI and NdeI sites of the expression vector pET28a (Novagen) giving plasmid pPB14 (**Appendix A**), which allowed co-expression YopB and YopD together with N-terminally 6xHis tagged SycD.

### Protein expression and purification

The plasmid was transformed into *E. coli* BL21 (DE3) pLysS. The bacteria were grown in Luria-Bertani medium. Protein expression was induced by the addition of 1 mM IPTG for 4 h at 37°C. Cells were harvested by centrifugation and lysed by 3 passes in the French pressure cell in binding buffer (20 mM Phosphate, 500 mM NaCl). The supernatant was cleared by centrifugation and the proteins were purified using chelating sepharose beads.

### Liposome preparation

Liposomes containing five distinct ratios of lipids were produced: L1-L5. A film of dried lipids was prepared under Argon flow. The film was solubilized by resuspension in binding buffer (20 mM Phosphate, 500 mM NaCl) containing 3 % Octylglucoside and the detergent was dialysed out to allow formation of the liposomes.

### Preparation of proteoliposomes

400  $\mu$ g of proteins were mixed with 250  $\mu$ l of liposomes. This mix was dialyzed against sodium acetate pH 5.0 for 6 h at room temperature. The solution was adjusted to 45% OptiPrep and transferred to an ultracentrifugation tube. A stepwise gradient from 35-5% OptiPrep was layered on top and centrifugated for 16 h at 150 000 g at 4°C. fractions of 0.5 ml were collected from the top of the gradient. Aliquots were analysed by SDS-PAGE and Silver staining.

### Electron microscopy

Droplets were applied for 1 min to freshly glow-discharged, formvar-carbon coated grids, and negatively stained with 2% (w/v) uranyl acetate. The samples were visualized in a Philips Morgagni 268D electron microscope at an acceleration voltage of 80 kV.

### Freeze fracture electron microscopy

Was done as described by (Chami *et al.*, 2005).

### 3.4.6 Purification of the TTS translocation pore using tagged translocators

#### Introduction

The purification and visualization of the translocation pore remains so far one of the unsolved questions in the field of type III Secretion. Previous attempts focused on the purification of the hydrophobic translocators, which presumably form the translocation pore, and the reconstitution of the pore into artificial membranes *in vitro*. The disadvantage of such an approach is, that, even if it succeeds, it is not possible to prove that the pores formed *in vitro* are exactly the same as the translocation pores formed *in vivo* by the bacteria. To avoid this disadvantage, we decided to purify the translocation pore out of membranes of erythrocytes that were infected with *Y. enterocolitica*, using a tag on one of the translocators. Using this kind of approach we could be sure that the purified pores represent the functional and native translocation pore. The first step of this approach is to insert a tag either in YopB or in YopD. It is crucial that the tagged protein is still functional and thus fully able to complement a mutation in the corresponding gene.

#### Results and Discussion

##### Expression of YopB or YopD in *E. coli*

We constructed vectors pPB1-6, capable of expressing YopB/YopD without a tag or with a His-tag in the amino-or carboxyterminus. Protein expression from these vectors was first tested in *E. coli* TOP10. No overexpression of the recombinant proteins could be detected on Coomassie stained SDS-PAGE (**Fig. 34A**). Western blot analysis revealed that even though all proteins were expressed, the levels remained very low (**Fig. 34A**). To clarify if the protein expression had a detrimental effect on the bacteria, the growth was monitored for 500 minutes after the induction. Constructs expressing YopB lead to a stop in growth or even to lysis of the *E. coli* (**Fig. 34B**). This suggested that YopB had a strong toxic effect on the bacteria. Expression of YopD had a less drastic effect, but still lead to decreased growth (**Fig. 34C**). No toxic effect is observed when they are expressed together with their chaperone SycD, which presumably prevents the interaction with membranes (chapter 3.4.5).

##### Complementation of *yopB/yopD* mutants with tagged-translocators

In order to test if constructs pPB1-6 can complement a deletion of the *yopB/yopD* genes, the plasmids were transformed into *Y. enterocolitica*  $\Delta$ HOPEMNB or  $\Delta$ HOPEMND bacteria and analyzed in a red blood cell hemolysis assay (**Fig. 35**). C-terminally tagged



translocators (pPB1 and pPB4) caused only low levels of hemolysis. This suggested that the C-terminal tag interfered with pore formation. The N-terminally tagged translocators (pPB2 and pPB5), were able complement the respective mutation as well as the untagged proteins (pPB3 and pPB6). This observation was surprising, because it is known for the effector Yops that changes in the aminotermis abolish the secretion. It suggests that the secretion signal of YopB and YopD might be different or localized in another place.

#### Isolation of membranes containing tagged pores

In order to purify pores we need enough starting material i.e. membranes containing translocation pores. To test the yield of tagged translocators, we performed a “large scale” hemolysis experiment. In contrast to a hemolysis experiment done with  $5 \times 10^7$  RBCs the “large scale” hemolysis is done with  $3 \times 10^9$  RBCs. Two strains were analyzed in parallel: *Y. enterocolitica*  $\Delta$ HOPEMN and *Y. enterocolitica*  $\Delta$ HOPEMND complemented with pPB5 (**Fig. 36**). The complemented mutant caused a bit less hemolysis than the  $\Delta$ HOPEMN strain. Membranes of the RBCs were isolated after the infection and the amounts of the translocators YopB and YopD in the membranes were compared. The complemented mutant inserted considerable amounts of translocators into the red blood cell membranes, only slightly less than the  $\Delta$ HOPEMN strain (**Fig. 36**), correlating with the levels of hemolysis. Unfortunately, even though protease inhibitors were added, native YopD as well as His-YopD tended to be degraded (**Fig. 36, black arrowheads**). This degradation might interfere with the purification therefore it is necessary to find a way to avoid it. Nevertheless, if proper upscaling is achieved, this assay should provide enough starting material to start the purification of the native pore via the His-tag in YopD. As an alternative the same attempt can be done using His-tagged YopB.

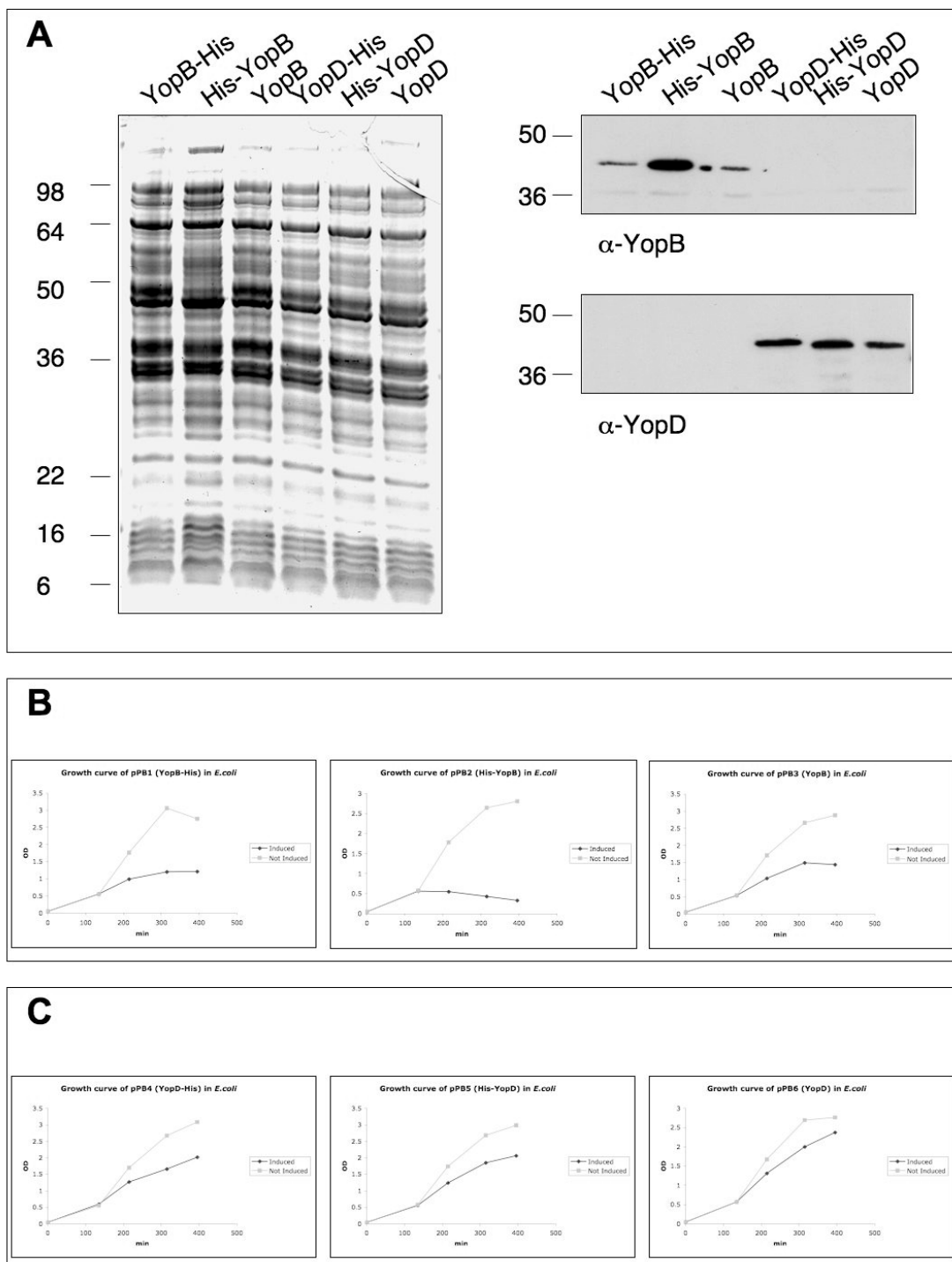


**Fig. 34.** Expression analysis of plasmids pPB1-6 in *E. coli* TOP10 bacteria. **(A)** Coomassie stained SDS-PAGE and western blots of total cell pellets of *E. coli* TOP10 bacteria harboring plasmids pPB1-6 after 4 h of induction with 0.2 % arabinose at 37°C. **(B, C)** Growth curves of *E. coli* TOP10 bacteria harboring plasmids pPB1-6. Bacteria were grown at 37°C and samples were collected up to 500 minutes after induction.

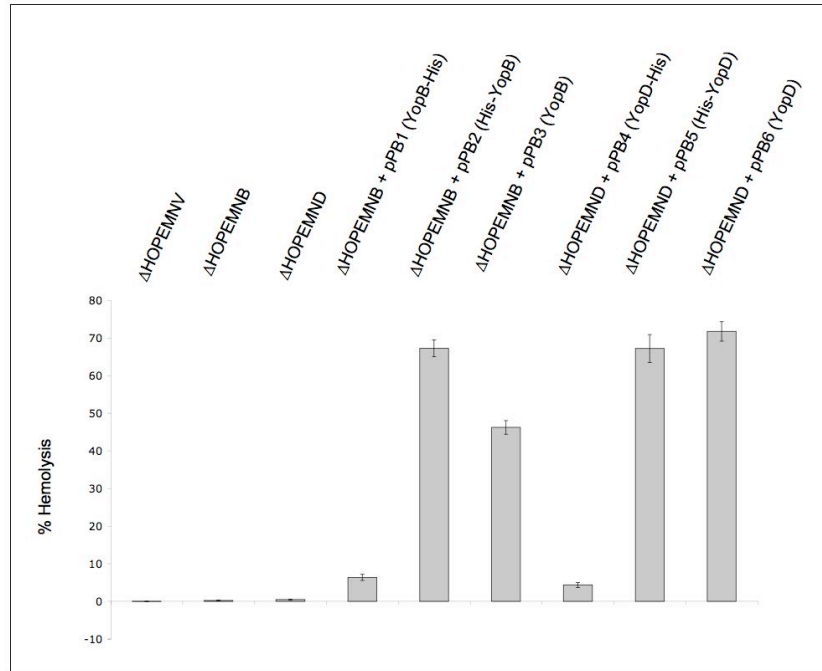


**Fig. 35.** Hemolysis of *Y. enterocolitica* strains ΔHOPEMNV, ΔHOPEMNB, ΔHOPEMND and ΔHOPEMNB/ΔHOPEMND complemented with pPB1-3/pPB4-6 respectively.

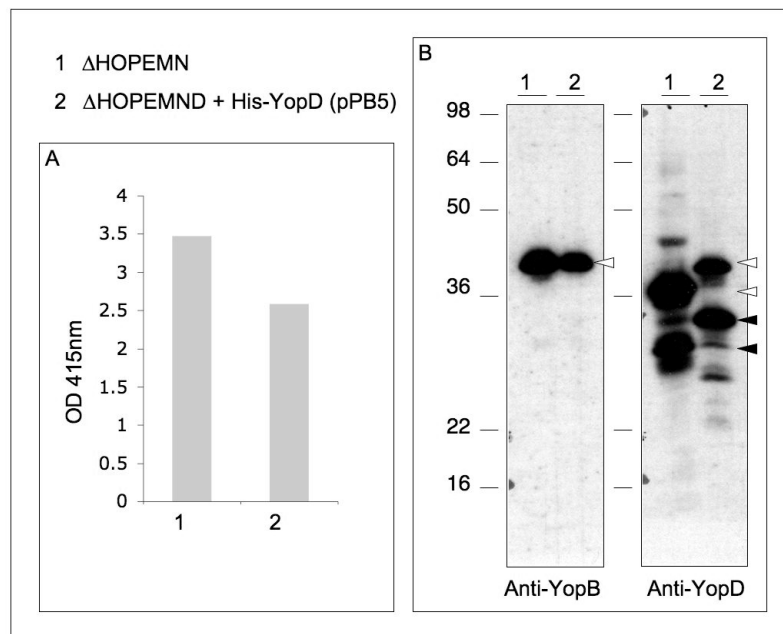


**Fig. 36.** Isolation of red blood cell membranes after infection with *Y. enterocolitica* ΔHOPEMN or ΔHOPEMND complemented with pPB5. **(A)** Hemolysis levels caused by the two strains. **(B)** Western blots of isolated red blood cell membranes probed with anti-YopB and anti-YopD antibodies. Proteins are indicated (white arrowheads); YopB: 41.9 kDa, YopD: 33.7 kDa and His-YopD: 34.5 kDa. Notably, YopD migrates at a higher apparent molecular weight in SDS-PAGE and degradation of YopD can be observed (black arrowhead).



## Material and methods

### Construction of vectors

The *yopB* or *yopD* genes were amplified by PCR on pYV40 DNA. The PCR products were digested with NcoI/PstI or XhoI/PstI and cloned into the NcoI/PstI or XhoI/PstI sites of the expression vector pBADmycHisA (Invitrogen) giving plasmid pPB1-6. These plasmids allowed expression of YopB or YopD with a C-terminal 6xHis-tag, a N-terminally 6xHis-tag or no tag.

### Expression in *E. coli*

The plasmids were transformed into *E. coli* TOP 10 and expression was induced by the addition of 0.2 % Arabinose at 37°C for 4 h. The bacteria were collected and the proteins were separated by SDS-PAGE. To produce the growth-curves, the growth was monitored from 0 to 500 min after induction by measuring the OD<sub>600</sub>.

### Complementation of *yopB/yopD* mutants with tagged-translocators

The plasmids pPB1-3 were transformed into *Y. enterocolitica* ΔHOPEMNB, plasmids pPB4-6 into *Y. enterocolitica* ΔHOPEMND.

To check the functional complementation of the mutations by the different constructs, a red blood cell hemolysis assay was performed as described before (Goure, Broz *et al.*, 2005).

### “Large scale” Hemolysis

Isolation of red blood cells membranes after infection was done as described before (Goure, Broz *et al.*, 2005).

## 4 Discussion

## 4 Discussion

### What are the different roles of the three translocators within the translocon?

Our analysis of the *Y. enterocolitica* type III secretion translocon allows for the first time to understand the function of the three translocators because it shows that the translocon consists of two distinct parts, the tip complex and the actual translocation pore.

The two hydrophobic translocators, YopB and YopD in *Y. enterocolitica*, presumably form the pore in the target cell membrane. Many studies have shown that these proteins interact with membranes and even insert into membranes. *In vitro* in contact with liposomes, they were shown to form oligomeric, pore-like structures, which can even function as channels (Faudry *et al.*, 2006). Pore-formation *in vivo* requires the presence of the tip complex, a structure present at the tip of the injectisome needle, the putative exit point of secreted proteins (Mueller, Broz *et al.*, 2005). This structure is formed by the third translocator (LcrV in *Y. enterocolitica*). We speculate that it assists the hydrophobic translocators to fold correctly and assemble into a functional pore upon secretion (Goure, Broz *et al.*, 2005). We assume that the pore stays connected to the needle via the tip complex. Thus the secretion and the translocation processes are coupled and the bacteria can inject effectors in one step into the target cell.

### How does LcrV help in the pore assembly?

*Yersiniae* deprived of LcrV are no longer hemolytic. Analysis of erythrocytes membranes indicated that *lcrV* mutant bacteria still insert YopB and YopD into the target cell membranes but cannot form a functional pore (Goure, Broz *et al.*, 2005). This suggests that tip complex somehow assists the assembly of the translocation pore.

Due to the size of the needle channel, the secreted proteins have to travel through the needle in a partial unfolded state. The tip complex could help the translocators that emerge at the tip of the needle to fold in a correct way, acting as some sort of extracellular chaperone. Consistent with this, our data show that *lcrV* mutants missing the tip complex insert considerably less translocators into erythrocyte membranes than wildtype bacteria. This suggests that the tip complex could not only ensure proper folding but also the insertion of the translocators into the membrane. In contrast to this, we also demonstrated that *in vitro* YopB and YopD insert into membranes even in the absence of the tip complex. This may be

explained by the fact that *in vitro* the concentration of the proteins is much higher and could force the equilibrium towards insertion.

Another possibility would be that the tip complex could also stabilize or retain the translocators in the membrane, keeping the local concentration of translocators high enough to allow interaction between them and formation of the translocation pore. In the absence of the tip complex the translocators are still inserted but they would easily diffuse or would not be retained in the membrane.

We also speculate that the tip complex provides interaction sites acting as some sort of scaffold for pore assembly. Only on this scaffold a functional pore can be formed and via the tip complex the pore stays connected to the needle. This idea is supported by the fact that the three translocators were reported to interact with each other, suggesting that there is no further mediator between the tip complex and the pore. This theory is contradicted by the observation that *in vitro* purified translocators can also form functional channels (Faudry *et al.*, 2006). But these *in vitro* experiments were done with unnaturally high protein concentrations and do only partially reflect what happens in nature.

## Is the tip complex a conserved feature of all TTSSs?

Based on our results we suggest that the tip complex might be a general feature found in every type III secretion system. It can be assumed that tip complexes similar to the LcrV tip complex of *Yersinia* can be found on injectisome needles from *P. aeruginosa* and *A. salmonicida* because PcrV and AcrV form a tip complex in a *Yersinia lcrV* mutant background (Mueller, Broz *et al.*, 2005). In addition purified needles from *P. aeruginosa* have also a tip complex at one end (C. Gebus and C.A. Mueller, unpublished results).

EspA, the hydrophilic translocator from EPEC could be considered a functional homolog of LcrV. Though EspA is smaller (20.5 kDa) than LcrV (37.6 kDa) and the two proteins do not share significant sequence similarity, EspA has been shown to form a comparable structure, a helical filament at the tip of the injectisome needle. This suggests that in this case the tip complex has evolved to polymerize to a long filament than a short ring.

Recently a sheath-like structure was found to cover the distal end of the injectisome needles from the *S. Typhimurium* SPI-2 TTSS. The protein SseB, which shares homology to EspA from EPEC, is part of this structure. It is not clear yet if this sheet is not just an artifact, because in contrast to the EspA filament of EPEC, there is no need to elongate the SPI-2 needle with a sheet. The needle is already long enough to reach the target cell membrane, when the bacteria were taken up into phagosomes. One possible explanation could be that the sheet protects the needle from the acidic pH in the phagosome, which could destabilize it.

No filament or tip complex has been observed for the needle complexes of *S. flexneri* and *S. Typhimurium* SPI-1, even though they are the best analyzed NCs of all type III secretion systems. It is still possible that the tip complex was either not detected or it was detached and lost during the purification. Only recently it could be shown that IpaD localizes to the distal end of the *S. flexneri* needles (Espina *et al.*, 2006). As IpaD has basically the same function as LcrV, we can speculate that IpaD as well as its homologs SipD from *S. Typhimurium* and BipD from *Burkholderia pseudomallei* would form a similar tip complex. But only STEM analysis of purified needles will show if there is a tip complex and how it looks like.

Taken together, it seems that in every type III secretion system the needle is topped with a distinct structure, be it a tip complex or a filament, which is formed by the hydrophilic translocator.

### **Is the tip complex the connector between the pore and the translocation pore? Is there a need for a connecting structure?**

The concept of type III secretion requires that the translocation pore remains connected to the needle once it is assembled. Indeed no leakage of effectors into the culture medium can be observed during infection (Mota *et al.*, 2005a). Based on our results we assume that the tip complex serves as a connector between the needle and the translocation pore, but so far this was not shown directly. However it is known that LcrV interacts with YopB and YopD, suggesting that there is no other protein in between. Such a protein would be necessary for the translocation, but by now all proteins encoded on the pYV plasmid were mutated and no new translocators were identified.

The situation seems to be clearer for EPEC. Here the bacteria are separated from the enterocytes by the thick glycocalyx layer and the needle is too short to bridge this distance. The EspA filament elongates the needle and allows the bacterium to reach the target cell membrane. Therefore it must serve as a connector between the needle and the translocation pore that is inserted in the target cell membrane. In addition a channel that could serve as a hollow conduit for the effector proteins to the target cell membrane spans the filament. Interestingly, STEM images of *Yersinia* wildtype needles also show that a channel spans all the way through the needle and the tip complex.

The need for a connecting structure seems quite obvious for EPEC, but for *Yersinia* the situation is different because the needle itself is long enough to span the space between the bacterium and the target cell. So, why is the needle not directly connected to the translocation pore? An explanation could be that the tip complex may act as an adaptor between the helical needle and the presumably ring-like translocation pore. Indeed the recently published

modeling of a tip complex on top of a type III secretion needle, suggests that LcrV would continue the helix of the needle (Deane *et al.*, 2006).

### **Are other proteins a part of the tip complex?**

Silver stained SDS-PAGE analysis of purified needles revealed several other major bands beside LcrV, YscF and flagellin. One band was identified as YopD, but we showed that that it is not part of the tip complex. Several minor bands remain to be identified, therefore we cannot completely exclude that some other proteins could be minor components of the needle and the tip complex. Intriguingly, the needles from *lcrV* mutant bacteria are not blunt ended but distinctly pointed. This suggests that a pyramid-like structure could be hidden underneath the tip complex. Several secreted Ysc proteins could be possible candidates for this structure. This structure could even serve as a polymerization cap for needle assembly. A capping protein has been identified for the flagellar filament, but could not be found so far for the needle. The pointed end of the needles might also just be the end of the helix viewed from the side, appearing higher at one side and therefore pointed. This would be in agreement with the modeling presented by (Deane *et al.*, 2006). In addition when STEM images of isolated needle are closely observed the base of the tip complex appears higher at one side (Mueller, Broz *et al.*, 2005). This difference is not visible in the final averages of the tip complex where the base looks even. But due to the averaging such differences disappear and the base seems to be even. This would suggest that LcrV just continues the helix of the needle. In agreement with this we were able to crosslink LcrV and YscF, suggesting a direct interaction.

### **Correlation between pore formation “*in vitro*” and “*in vivo*”**

The analysis and visualization of the translocation pore is one of the major unsolved questions in the field of type III secretion. So far the only promising approaches were done *in vitro* with purified translocator proteins (Schoehn *et al.*, 2003, P. Broz unpublished data). The main drawback of such approaches is that there is no way to validate that the “*in vitro* pore” is the same as the pore formed *in vivo*. Nevertheless these *in vitro* experiments provided interesting results and insights.

To purify the translocators of *Yersinia* or *Pseudomonas*, they have to be expressed together with their native chaperone, that prevents the premature interaction of the translocators and the degradation. When placed at acidic pH, the translocators are partially released from the chaperone and form homo- or heteromeric oligomers. These oligomers are able to bind membranes and also to insert into membranes. They have the appearance of

ring-like structures with an outer diameter of around 8-10 nm and an inner diameter of 4 nm. Furthermore these rings may indeed act as channels as they have been shown to lead to release of fluorescent dyes from liposomes.

All these observations may be related to events occurring *in vivo* during an infection. The secretion machinery removes the chaperone and the translocators are exported. The translocators oligomerize upon secretion and insert into the target cell membrane. *In vitro* they form ring-like structure even before they insert into membranes (Schoehn *et al.*, 2003). Our freeze-fracture analysis also suggests that the oligomeric form exists already before the membranes insertion. But *in vivo* this seems rather unlikely because the needle tip is in close contact to the membrane. The tip complex formed by the third translocator somehow facilitates the oligomerization and pore formation *in vivo*. By acting as a scaffold it also imposes a fixed stoichiometry. Faudry *et al.* (Faudry *et al.*, 2006) speculate that the pH change used *in vitro* to trigger interaction with membranes might mimic the action of the tip complex *in vivo*. Analyzing the hemolytic abilities of IcrV mutant bacteria at acidic pH should validate this explanation.

Another drawback of the “*in vitro* pores”, formed by PopB and PopD, is that they seem to be a mixture of pore-like structures with different sizes, 3.4-6.1 nm in diameter (Faudry *et al.*, 2006). In contrast to this pores formed by *P. aeruginosa in vivo* have a size of 2.8-3.5 nm. Our freeze fracture analysis of proteoliposomes formed by incubation with YopB and YopD, reveals transmembrane particles of varying sizes (P. Broz unpublished data). This suggests that even though the hydrophobic translocators have some intrinsic pore-forming properties that allow them to form pores at high concentration like in these *in vitro* assays, the tip complex is necessary to catalyze this reaction *in vivo* so that the right translocation pore is formed.

## **What is the status of the translocators in the type III secretion hierarchy?**

The localization and the function of the three translocators implicates that they need to have their own status in the secretion hierarchy. The type III secretion hierarchy has never been experimentally established. But it is known that knock out mutations in early substrates that build the outer part of the injectisome, like YscF and YscP, abolish the secretion later substrates. It is assumed that the secreted substrates can be classified into three major classes. First, the early substrates that are essential for the assembly of the secretion apparatus itself. Upon contact with a target cell they should be followed by the hypothetical middle substrates, the translocators. And finally, when the translocation pore is assembled the late substrates, the effector proteins, can be secreted. How the three classes are

distinguished is unknown, but it is possible that they have different secretion signals. Indeed the three translocators seem to have a different secretion signal than the effectors (Fields *et al.*, 1999). We observed that N-terminal tags do not affect the secretion of the translocators, while changes in the N-terminus interfere with the secretion of the effectors.

But there must be some differences between LcrV and the hydrophobic translocators as well. We demonstrated that the LcrV tip complex is already assembled on the needle in non-secreting conditions, before secretion is triggered, and that YopB and YopD are not part of the tip complex. Therefore LcrV must be secreted right after the needle component YscF but before the actual translocation pore components.

How the secretion hierarchy is established is unknown, but it is intriguing that the three translocators are somehow involved in the regulation of type III secretion: LcrV interacts with LcrG, thus controlling effector proteins secretion. SycD the chaperone of both YopB and YopD is also critically involved in the regulation of *yop* gene expression. It is possible that these interactions ensure the secretion of the three translocators at the right time.

### **Is the tip complex involved in the trigger mechanism?**

It has been proposed that type III secretion is triggered by the contact between the needle tip and the target cell (Mota *et al.*, 2005a). It is tempting to hypothesize that the tip complex might be involved in the trigger mechanism. As bacteria do not form pores, the secreted proteins should end up in the culture supernatant. On the contrary, it was shown that *lcrV* mutant do not secrete proteins into the culture supernatant, suggesting that the secretion can't be triggered (DeBord *et al.*, 2001). Recently it was reported that contact with liposomes can trigger the secretion by *S. flexneri* (van der Goot *et al.*, 2004) and IpaD, an ortholog of LcrV, is localized at the tip of the needle in *S. flexneri* (Espina *et al.*, 2006). Therefore it could be therefore possible that the tip complex could sense the presence of membranes and transmit this signal via an unknown mechanism to the machinery, triggering the secretion of the translocators and effectors. Deane *et al.* speculate that the tip complex would sense contact and transmit the signal via intersubunit contacts of the needle to the bacterium (Deane *et al.*, 2006). So far no convincing data could be presented that would support such a model.

The contact between the needle tip and the host membrane alone is not sufficient to trigger effector secretion; another prerequisite is the ability of the bacterium to form the translocation pore. Bacteria deprived of YopB do not secrete effectors into the medium even though they are in contact with eukaryotic cells (L.J. Mota unpublished data). This suggests that the formation of the pore by the tip complex i.e. the opening of a continuous channel between the bacterium and the eukaryotic cytosol leads to the secretion of the effectors and no special signal is required. This scenario would imply that the pore-forming translocators are



localized in the needle or the injectisome, ready to be secreted as soon as the tip reaches a membrane.

## Requirements on membrane side?

As mentioned in the introduction, it has been shown for *Shigella*, *Salmonella* and EPEC that the lipid composition of the membrane is very important. These three pathogens require the presence of cholesterol in the host cell membrane to translocate effectors via the type III secretion system (Hayward *et al.*, 2005). As the translocators insert directly into host cell membrane it was speculated that the formation of the translocation pore could depend on the presence of certain lipids in the host cell membrane. In addition the authors show that purified *Salmonella* SipB and *Shigella* IpaB are cholesterol-binding proteins and that cholesterol is the main binding determinant of purified SipB/IpaB to host cells (Hayward *et al.*, 2005). As cholesterol is a component of lipid rafts it suggests that these pathogens can only assemble the translocation pore in the special lipid environment of lipid rafts.

We were interested if the family of Ysc-type TTSSs (*Yersinia*, *Pseudomonas*) also requires cholesterol for translocation. Our *in vitro* experiments with purified translocators indicated that phosphatidylserine (PS) is necessary for the binding of YopB and YopD to liposomes and also for the insertion of the proteins into membranes. Other lipids like cholesterol and sphingomyelin were not necessary. In addition unpublished data from J. Mota show that when macrophages are depleted from cholesterol, by incubating them with methylcyclodextrin, the infection is not affected.

Data published on *P. aeruginosa* (Faudry *et al.*, 2006; Schoehn *et al.*, 2003) also show that the translocators require negatively charged phospholipids (PS) to bind membranes and insert into membranes. Initially Schoehn *et al.* reported that PS is necessary for the binding to membranes but that cholesterol is required for lysis (insertion of the translocators) of liposomes. But it seems that the authors had observed aggregation of liposomes and misinterpreted this observation as liposomes lysis. Later the same group had to revise their result, as they could not observe liposome lysis any more. Another interesting observation is that purified IpaB from *S. flexneri* leads to the release of Calcein from liposomes that contain negatively charged lipids, but not from liposomes containing positively charged lipids (De Geyter *et al.*, 2000). This suggests that the formation of the type III secretion translocon, in all systems, requires negatively charged phospholipids in the target cell membrane.

Altogether it seems that the requirements on the membrane depend on the type of TTS system that the bacteria have acquired. Ysc-type TTSS are independent of lipid rafts, while they are crucial for others. This may also reflect the different infection strategies of these

pathogens. Some pathogens, like *Yersinia* and *P. aeruginosa*, are extracellular. To avoid phagocytosis by macrophages, they need to act in seconds and inject effector proteins into the macrophage. On the other hand, *Shigella*, *Salmonella* and EPEC invade epithelial cells. They can take their time to find the right spot (lipid raft) to successfully enter their target cells.

## Action of protective antibodies

For decades LcrV has been known to be the major protective antigen against plague infections. Later the same activity was reported for antibodies directed against the V antigens of *P. aeruginosa* and *A. salmonicida*. Only recently it could be shown that antibodies against lpaD, a functional homolog of LcrV, from *S. flexneri* also prevent hemolysis. Antibodies against EspA are found in human maternal milk and were proposed to provide protection against EHEC (Noguera-Obenza *et al.*, 2003).

Our results show that the V-antigens are forming an exposed structure at the tip of the injectisome needle and that antibodies bind specific to this tip complex. It is this binding that affects the action of the tip complex and interferes with the formation of a translocation pore. Further we could show that if LcrV contains a FLAG tag, anti-FLAG antibodies can also interfere with the function of the tip complex. This suggests that it is not a specific motif of LcrV that has to be bound by the antibodies, but that the sheer physical presence of the relatively large antibodies impairs pore formation.

Interestingly we did not observe any protective action with antibodies directed against YscF, the needle subunit. This is in apparent contradiction to reports found in literature that show that vaccination of animals with YscF provides significant protective immune response to plague infections. This contradiction may be explained by the observation that our YscF antibody recognizes only the lower end of the needle. During the assembly and function of the needle this part is never exposed, except when the needles are broken off. One could imagine that antibodies directed against other epitopes of YscF could possibly interfere with the assembly of the needle or the tip complex, which would explain the protective action observed *in vivo*.

## Therapeutic target?

Our work shows that the tip complex is vital for the success of the whole TTS apparatus. At the same time it is the weakest point of the whole system because of its exposed localization. Only antibodies directed against the tip complex can efficiently disturb the system. Therefore the tip complex is probably the best-suited target for new infectives, as these would not even have to pass through the bacterial membranes to block the function of the TTSS. In addition our work has shown that the hemolysis assay is well suited for the study of the function of the translocon and could be adapted for screening of new anti-infectives that specifically target the TTS system system. Further analysis of the tip complex and the crystal structure of LcrV may be used to specifically design molecules that could interfere with the function of the tip complex.

## 5 Outlooks

## 5 Outlooks

To finally understand the translocation process, we will need to understand the function of the tip complex and the translocation pore in detail and also how these structures are connected to the injectisome needle. Therefore it is necessary to determine the interaction sites between the different parts of the translocon and to investigate the structure of the translocation pore. It is also crucial to establish the chronological order of events during the assembly and the function of the injectisome. Here are some questions directly arising from the present study and which would be relevant to address:

-How is the tip complex connected to the translocation pore and the needle? Which domains of LcrV interact with YscF (the needle)? Which domains interact with YopB and YopD (the translocation pore)?

-How many molecules of LcrV form the tip complex (Stoichiometry)?

-Are there other proteins involved? Small, secreted Ysc proteins? What is the pyramid underneath the tip complex?

-What is the composition and structure of the translocation pore? How does the membrane topology of YopB and YopD look like?

-Is the tip complex involved in the trigger mechanism? How is the formation of the pore involved in the trigger mechanism?

-What is the hierarchy of secretion and how is it established? Are the translocators secreted? How are the chaperones involved? What are the export signals of LcrV, YopB and YopD?

-Is LcrG the chaperone of LcrV?

-How are the coiled-coil domains of LcrV involved in polymerization?

## Appendix

## Appendix

### A List of constructs

MIPA number	name		description	vector	resistance
3921	pPB	1	<i>yopB-his</i>	pBAD	Amp
3922	pPB	2	<i>his-yopB</i>	pBAD	Amp
3923	pPB	3	<i>yopB</i>	pBAD	Amp
3924	pPB	4	<i>yopD-his</i>	pBAD	Amp
3925	pPB	5	<i>his-yopD</i>	pBAD	Amp
3926	pPB	6	<i>yopD</i>	pBAD	Amp
3726	pPB	9	<i>lcrVsyncDyopByopD</i>	pET28a	Kan
3727	pPB	10	<i>his-lcrV</i>	pET28a	Kan
3728	pPB	11	<i>his-sycD</i>	pET28a	Kan
3729	pPB	12	<i>his-yopB</i>	pET28a	Kan
3730	pPB	13	<i>his-yopD</i>	pET28a	Kan
3731	pPB	14	<i>his-sycDyopByopD</i>	pET28a	Kan
3732	pPB	15	<i>his-sycDyopB-his</i>	pET28a	Kan
3733	pPB	16	<i>his-sycDyopB-his</i>	pET28a	Kan
3734	pPB	17	<i>his-sycDyopB</i>	pET28a	Kan
3927	pPB	22	<i>his-lcrV</i>	pLJM3	Kan
3841	pPB	24	<i>pcrV</i> of <i>P. aeruginosa</i> PAO1	pBAD	Amp
3842	pPB	25	<i>acrV</i> of <i>A. salmonicida</i> JF2267	pBAD	Amp
3928	pPB	26	H1 (LcrV aa1-124, PcrV aa105-294)	pBAD	Amp
3929	pPB	27	H2 (LcrV aa1-195, PcrV aa174-294)	pBAD	Amp
3930	pPB	28	H3 (PcrV aa1-105, LcrV aa125-329)	pBAD	Amp
3931	pPB	29	H4 (PcrV aa1-174, LcrV aa196-329)	pBAD	Amp
3932	pPB	30	H5 (LcrV aa1-145, PcrV aa124-294)	pBAD	Amp
3933	pPB	31	H6 (PcrV aa1-123, LcrV aa146-329)	pBAD	Amp
3934	pPB	32	H7 (LcrV aa1-181, PcrV aa160-294)	pBAD	Amp
3935	pPB	33	H8 (PcrV aa1-159, LcrV aa182-329)	pBAD	Amp
3936	pPB	34	H9 (LcrV aa1-145, AcrV aa146-361)	pBAD	Amp
3937	pPB	35	H10 (AcrV aa1-143, LcrV aa146-329)	pBAD	Amp
3938	pPB	36	H11 (LcrV aa1-181, AcrV aa180-361)	pBAD	Amp
3939	pPB	37	H12 (AcrV aa1-179, LcrV aa182-329)	pBAD	Amp
3940	pPB	38	H13 (LcrV aa1-181, PcrV aa160-233, LcrV aa268-329)	pBAD	Amp
3941	pPB	39	H14 (PcrV aa1-159, LcrV aa182-267, PcrV aa234-294)	pBAD	Amp
3942	pPB	40	H15 (LcrV aa1-181, AcrV aa180-300, LcrV aa301-361)	pBAD	Amp
3943	pPB	41	H16 (AcrV aa1-179, LcrV aa182-267, AcrV aa301-361)	pBAD	Amp
3944	pPB	42	<i>lcrV</i>	pBAD	Amp
3945	pPB	43	<i>lcrV</i> del aa218-243	pBAD	Amp
3946	pPB	44	<i>pcrV-his</i>	pBAD	Amp
3947	pPB	45	<i>acrV-his</i>	pBAD	Amp
3948	pPB	46	LcrV with FLAG tag between aa227-228	pBAD	Amp
3949	pPB	47	LcrV with FLAG tag replacing aa226-233	pBAD	Amp
3950	pPB	48	His-LcrV aa1-156 (his-G1)	pBAD	Amp

3951	pPB	49	His-LcrV aa1-192 (his-G1A1)	pBAD	Amp
3952	pPB	50	His-LcrV aa1-289 (his-G1A1G2)	pBAD	Amp
3953	pPB	51	His-LcrV aa1-329 (his-G1A1G2A2)	pBAD	Amp
3954	pPB	52	His-LcrV aa193-289 (his-G2)	pBAD	Amp
3955	pPB	53	His-LcrV aa193-329 (his-G2A2)	pBAD	Amp
3956	pPB	54	His-LcrV aa157-329 (his-A1G2A2)	pBAD	Amp
3957	pPB	55	His-LcrV aa290-329 (his-A2)	pBAD	Amp
3958	pPB	56	His-LcrV aa157-192 (his-A1)	pBAD	Amp
3959	pPB	57	His-LcrV aa157-289 (his-A1G2)	pBAD	Amp
3960	pPB	58	<i>his-lcrV</i>	pBAD	Amp
3961	pPB	59	<i>his-pcrV</i>	pBAD	Amp
3962	pPB	60	<i>his-acrV</i>	pBAD	Amp
3963	pPB	61	His-H5	pBAD	Amp
3964	pPB	62	His-H6	pBAD	Amp
3965	pPB	63	His-H9	pBAD	Amp
3966	pPB	64	His-H10	pBAD	Amp



## B References

- Allmond, L.R., Karaca, T.J., Nguyen, V.N., Nguyen, T., Wiener-Kronish, J.P., and Sawa, T. (2003) Protein binding between PcrG-PcrV and PcrH-PopB/PopD encoded by the pcrGVH-popBD operon of the *Pseudomonas aeruginosa* type III secretion system. *Infect Immun* **71**: 2230-2233.
- Anderson, D.M., Ramamurthi, K.S., Tam, C., and Schneewind, O. (2002) YopD and LcrH regulate expression of *Yersinia enterocolitica* YopQ by a posttranscriptional mechanism and bind to yopQ RNA. *J Bacteriol* **184**: 1287-1295.
- Bergman, T., Hakansson, S., Forsberg, A., Norlander, L., Macellaro, A., Backman, A., Bolin, I., and Wolf-Watz, H. (1991) Analysis of the V antigen lcrGVH-yopBD operon of *Yersinia pseudotuberculosis*: evidence for a regulatory role of LcrH and LcrV. *J Bacteriol* **173**: 1607-1616.
- Blocker, A., Gounon, P., Larquet, E., Niebuhr, K., Cabiaux, V., Parsot, C., and Sansonetti, P. (1999) The tripartite type III secretin of *Shigella flexneri* inserts lpaB and lpaC into host membranes. *J Cell Biol* **147**: 683-693.
- Blocker, A., Jouihri, N., Larquet, E., Gounon, P., Ebel, F., Parsot, C., Sansonetti, P., and Allaoui, A. (2001) Structure and composition of the *Shigella flexneri* "needle complex", a part of its type III secretin. *Mol Microbiol* **39**: 652-663.
- Boland, A., Sory, M.P., Iriarte, M., Kerbouch, C., Wattiau, P., and Cornelis, G.R. (1996) Status of YopM and YopN in the *Yersinia* Yop virulon: YopM of *Y. enterocolitica* is internalized inside the cytosol of PU5-1.8 macrophages by the YopB, D, N delivery apparatus. *Embo J* **15**: 5191-5201.
- Broms, J.E., Forslund, A.L., Forsberg, A., and Francis, M.S. (2003) Dissection of homologous translocon operons reveals a distinct role for YopD in type III secretion by *Yersinia pseudotuberculosis*. *Microbiology* **149**: 2615-2626.
- Burrows, T.W. (1956) An antigen determining virulence in *Pasteurella pestis*. *Nature* **177**: 426-427.
- Buttner, D., and Bonas, U. (2002) Port of entry--the type III secretion translocon. *Trends Microbiol* **10**: 186-192.
- Chakravorty, D., Rohde, M., Jager, L., Deiwick, J., and Hensel, M. (2005) Formation of a novel surface structure encoded by *Salmonella* Pathogenicity Island 2. *Embo J* **24**: 2043-2052.
- Chami, M., Guilvout, I., Gregorini, M., Remigy, H.W., Muller, S.A., Valerio, M., Engel, A., Pugsley, A.P., and Bayan, N. (2005) Structural insights into the secretin PulD and its trypsin-resistant core. *J Biol Chem* **280**: 37732-37741.
- Chen, Y., Smith, M.R., Thirumalai, K., and Zychlinsky, A. (1996) A bacterial invasin induces macrophage apoptosis by binding directly to ICE. *Embo J* **15**: 3853-3860.
- Chiu, H.J., and Syu, W.J. (2005) Functional analysis of EspB from enterohaemorrhagic *Escherichia coli*. *Microbiology* **151**: 3277-3286.
- Cordes, F.S., Komoriya, K., Larquet, E., Yang, S., Egelman, E.H., Blocker, A., and Lea, S.M. (2003) Helical structure of the needle of the type III secretion system of *Shigella flexneri*. *J Biol Chem* **278**: 17103-17107.
- Dacheux, D., Goure, J., Chabert, J., Usson, Y., and Attree, I. (2001) Pore-forming activity of type III system-secreted proteins leads to oncosis of *Pseudomonas aeruginosa*-infected macrophages. *Mol Microbiol* **40**: 76-85.
- Daniell, S.J., Takahashi, N., Wilson, R., Friedberg, D., Rosenshine, I., Booy, F.P., Shaw, R.K., Knutton, S., Frankel, G., and Aizawa, S. (2001) The filamentous type III secretion translocon of enteropathogenic *Escherichia coli*. *Cell Microbiol* **3**: 865-871.
- Daniell, S.J., Kocsis, E., Morris, E., Knutton, S., Booy, F.P., and Frankel, G. (2003) 3D structure of EspA filaments from enteropathogenic *Escherichia coli*. *Mol Microbiol* **49**: 301-308.
- Darwin, K.H., and Miller, V.L. (2001) Type III secretion chaperone-dependent regulation: activation of virulence genes by SicA and InvF in *Salmonella typhimurium*. *Embo J* **20**: 1850-1862.
- De Geyter, C., Wattiez, R., Sansonetti, P., Falmagne, P., Ruyschaert, J.M., Parsot, C., and Cabiaux, V. (2000) Characterization of the interaction of lpaB and lpaD, proteins required for entry of *Shigella flexneri* into epithelial cells, with a lipid membrane. *Eur J Biochem* **267**: 5769-5776.
- Deane, J.E., Roversi, P., Cordes, F.S., Johnson, S., Kenjale, R., Daniell, S., Booy, F., Picking, W.D., Picking, W.L., Blocker, A.J., and Lea, S.M. (2006) Molecular model of a type III secretion system needle: Implications for host-cell sensing. *Proc Natl Acad Sci U S A* **103**: 12529-12533.
- DeBord, K.L., Lee, V.T., and Schneewind, O. (2001) Roles of LcrG and LcrV during type III targeting of effector Yops by *Yersinia enterocolitica*. *J Bacteriol* **183**: 4588-4598.
- Derewenda, U., Mateja, A., Devedjiev, Y., Rutzahn, K.M., Evdokimov, A.G., Derewenda, Z.S., and Waugh, D.S. (2004) The structure of *Yersinia pestis* V-antigen, an essential virulence factor and mediator of immunity against plague. *Structure* **12**: 301-306.

- Edqvist, P.J., Broms, J.E., Betts, H.J., Forsberg, A., Pallen, M.J., and Francis, M.S. (2006) Tetratricopeptide repeats in the type III secretion chaperone, LcrH: their role in substrate binding and secretion. *Mol Microbiol* **59**: 31-44.
- Espina, M., Olive, A.J., Kenjale, R., Moore, D.S., Ausar, S.F., Kaminski, R.W., Oaks, E.V., Middaugh, C.R., Picking, W.D., and Picking, W.L. (2006) IpaD localizes to the tip of the type III secretion system needle of *Shigella flexneri*. *Infect Immun* **74**: 4391-4400.
- Faudry, E., Vernier, G., Neumann, E., Forge, V., and Attree, I. (2006) Synergistic pore formation by type III toxin translocators of *Pseudomonas aeruginosa*. *Biochemistry* **45**: 8117-8123.
- Fields, K.A., Nilles, M.L., Cowan, C., and Straley, S.C. (1999) Virulence role of V antigen of *Yersinia pestis* at the bacterial surface. *Infect Immun* **67**: 5395-5408.
- Francis, M.S., and Wolf-Watz, H. (1998) YopD of *Yersinia pseudotuberculosis* is translocated into the cytosol of HeLa epithelial cells: evidence of a structural domain necessary for translocation. *Mol Microbiol* **29**: 799-813.
- Francis, M.S., Aili, M., Wiklund, M.L., and Wolf-Watz, H. (2000) A study of the YopD-lcrH interaction from *Yersinia pseudotuberculosis* reveals a role for hydrophobic residues within the amphipathic domain of YopD. *Mol Microbiol* **38**: 85-102.
- Frithz-Lindsten, E., Holmstrom, A., Jacobsson, L., Soltani, M., Olsson, J., Rosqvist, R., and Forsberg, A. (1998) Functional conservation of the effector protein translocators PopB/YopB and PopD/YopD of *Pseudomonas aeruginosa* and *Yersinia pseudotuberculosis*. *Mol Microbiol* **29**: 1155-1165.
- Garcia-del Portillo, F., Pucciarelli, M.G., Jefferies, W.A., and Finlay, B.B. (1994) *Salmonella typhimurium* induces selective aggregation and internalization of host cell surface proteins during invasion of epithelial cells. *J Cell Sci* **107 ( Pt 7)**: 2005-2020.
- Garner, M.J., Hayward, R.D., and Koronakis, V. (2002) The *Salmonella* pathogenicity island 1 secretion system directs cellular cholesterol redistribution during mammalian cell entry and intracellular trafficking. *Cell Microbiol* **4**: 153-165.
- Goure, J., Pastor, A., Faudry, E., Chabert, J., Dessen, A., and Attree, I. (2004) The V antigen of *Pseudomonas aeruginosa* is required for assembly of the functional PopB/PopD translocation pore in host cell membranes. *Infect Immun* **72**: 4741-4750.
- Goure, J., Broz, P., Attree, O., Cornelis, G.R., and Attree, I. (2005) Protective anti-V antibodies inhibit *Pseudomonas* and *Yersinia* translocon assembly within host membranes. *J Infect Dis* **192**: 218-225.
- Hakansson, S., Bergman, T., Vanooteghem, J.C., Cornelis, G., and Wolf-Watz, H. (1993) YopB and YopD constitute a novel class of *Yersinia* Yop proteins. *Infect Immun* **61**: 71-80.
- Hakansson, S., Schesser, K., Persson, C., Galyov, E.E., Rosqvist, R., Homble, F., and Wolf-Watz, H. (1996) The YopB protein of *Yersinia pseudotuberculosis* is essential for the translocation of Yop effector proteins across the target cell plasma membrane and displays a contact-dependent membrane disrupting activity. *Embo J* **15**: 5812-5823.
- Hayward, R.D., and Koronakis, V. (1999) Direct nucleation and bundling of actin by the SipC protein of invasive *Salmonella*. *Embo J* **18**: 4926-4934.
- Hayward, R.D., McGhie, E.J., and Koronakis, V. (2000) Membrane fusion activity of purified SipB, a *Salmonella* surface protein essential for mammalian cell invasion. *Mol Microbiol* **37**: 727-739.
- Hayward, R.D., Cain, R.J., McGhie, E.J., Phillips, N., Garner, M.J., and Koronakis, V. (2005) Cholesterol binding by the bacterial type III translocon is essential for virulence effector delivery into mammalian cells. *Mol Microbiol* **56**: 590-603.
- Hersh, D., Monack, D.M., Smith, M.R., Ghorri, N., Falkow, S., and Zychlinsky, A. (1999) The *Salmonella* invasin SipB induces macrophage apoptosis by binding to caspase-1. *Proc Natl Acad Sci U S A* **96**: 2396-2401.
- Hilbi, H., Moss, J.E., Hersh, D., Chen, Y., Arondel, J., Banerjee, S., Flavell, R.A., Yuan, J., Sansonetti, P.J., and Zychlinsky, A. (1998) *Shigella*-induced apoptosis is dependent on caspase-1 which binds to IpaB. *J Biol Chem* **273**: 32895-32900.
- Hobbie, S., Chen, L.M., Davis, R.J., and Galan, J.E. (1997) Involvement of mitogen-activated protein kinase pathways in the nuclear responses and cytokine production induced by *Salmonella typhimurium* in cultured intestinal epithelial cells. *J Immunol* **159**: 5550-5559.
- Hoiczky, E., and Blobel, G. (2001) Polymerization of a single protein of the pathogen *Yersinia enterocolitica* into needles punctures eukaryotic cells. *Proc Natl Acad Sci U S A* **98**: 4669-4674.
- Holmstrom, A., Olsson, J., Cherepanov, P., Maier, E., Nordfelth, R., Pettersson, J., Benz, R., Wolf-Watz, H., and Forsberg, A. (2001) LcrV is a channel size-determining component of the Yop effector translocon of *Yersinia*. *Mol Microbiol* **39**: 620-632.
- Hume, P.J., McGhie, E.J., Hayward, R.D., and Koronakis, V. (2003) The purified *Shigella* IpaB and *Salmonella* SipB translocators share biochemical properties and membrane topology. *Mol Microbiol* **49**: 425-439.

- Ide, T., Laarmann, S., Greune, L., Schillers, H., Oberleithner, H., and Schmidt, M.A. (2001) Characterization of translocation pores inserted into plasma membranes by type III-secreted Esp proteins of enteropathogenic *Escherichia coli*. *Cell Microbiol* **3**: 669-679.
- Journet, L., Agrain, C., Broz, P., and Cornelis, G.R. (2003) The needle length of bacterial injectisomes is determined by a molecular ruler. *Science* **302**: 1757-1760.
- Kaniga, K., Tucker, S., Trollinger, D., and Galan, J.E. (1995) Homologs of the *Shigella* IpaB and IpaC invasins are required for *Salmonella typhimurium* entry into cultured epithelial cells. *J Bacteriol* **177**: 3965-3971.
- Kimbrough, T.G., and Miller, S.I. (2000) Contribution of *Salmonella typhimurium* type III secretion components to needle complex formation. *Proc Natl Acad Sci U S A* **97**: 11008-11013.
- Knutton, S., Rosenshine, I., Pallen, M.J., Nisan, I., Neves, B.C., Bain, C., Wolff, C., Dougan, G., and Frankel, G. (1998) A novel EspA-associated surface organelle of enteropathogenic *Escherichia coli* involved in protein translocation into epithelial cells. *Embo J* **17**: 2166-2176.
- Kubori, T., Matsushima, Y., Nakamura, D., Uralil, J., Lara-Tejero, M., Sukhan, A., Galan, J.E., and Aizawa, S.I. (1998) Supramolecular structure of the *Salmonella typhimurium* type III protein secretion system. *Science* **280**: 602-605.
- Lafont, F., Tran Van Nhieu, G., Hanada, K., Sansonetti, P., and van der Goot, F.G. (2002) Initial steps of *Shigella* infection depend on the cholesterol/sphingolipid raft-mediated CD44-IpaB interaction. *Embo J* **21**: 4449-4457.
- Lafont, F., and van der Goot, F.G. (2005) Oiling the key hole. *Mol Microbiol* **56**: 575-577.
- Lawton, D.G., Longstaff, C., Wallace, B.A., Hill, J., Leary, S.E., Titball, R.W., and Brown, K.A. (2002) Interactions of the type III secretion pathway proteins LcrV and LcrG from *Yersinia pestis* are mediated by coiled-coil domains. *J Biol Chem* **277**: 38714-38722.
- Lawton, W.D., Erdman, R.L., and Surgalla, M.J. (1963) Biosynthesis and Purification of V and W Antigens in *Pasteurella Pestis*. *Tech Manuscr US Army Biol Lab* **21**: 1-15.
- Lee, V.T., Tam, C., and Schneewind, O. (2000) LcrV, a substrate for *Yersinia enterocolitica* type III secretion, is required for toxin targeting into the cytosol of HeLa cells. *J Biol Chem* **275**: 36869-36875.
- Marenne, M.N., Journet, L., Mota, L.J., and Cornelis, G.R. (2003) Genetic analysis of the formation of the Ysc-Yop translocation pore in macrophages by *Yersinia enterocolitica*: role of LcrV, YscF and YopN. *Microb Pathog* **35**: 243-258.
- Marlovits, T.C., Kubori, T., Sukhan, A., Thomas, D.R., Galan, J.E., and Unger, V.M. (2004) Structural insights into the assembly of the type III secretion needle complex. *Science* **306**: 1040-1042.
- Matson, J.S., and Nilles, M.L. (2001) LcrG-LcrV interaction is required for control of Yops secretion in *Yersinia pestis*. *J Bacteriol* **183**: 5082-5091.
- Mavris, M., Page, A.L., Tournabize, R., Demers, B., Sansonetti, P., and Parsot, C. (2002) Regulation of transcription by the activity of the *Shigella flexneri* type III secretion apparatus. *Mol Microbiol* **43**: 1543-1553.
- Menard, R., Sansonetti, P., Parsot, C., and Vasselon, T. (1994) Extracellular association and cytoplasmic partitioning of the IpaB and IpaC invasins of *S. flexneri*. *Cell* **79**: 515-525.
- Michiels, T., Wattiau, P., Bresseur, R., Ruyschaert, J.M., and Cornelis, G. (1990) Secretion of Yop proteins by *Yersiniae*. *Infect Immun* **58**: 2840-2849.
- Miki, T., Okada, N., Shimada, Y., and Danbara, H. (2004) Characterization of *Salmonella* pathogenicity island 1 type III secretion-dependent hemolytic activity in *Salmonella enterica* serovar Typhimurium. *Microb Pathog* **37**: 65-72.
- Mimori, Y., Yamashita, I., Murata, K., Fujiyoshi, Y., Yonekura, K., Toyoshima, C., and Namba, K. (1995) The structure of the R-type straight flagellar filament of *Salmonella* at 9 Å resolution by electron cryomicroscopy. *J Mol Biol* **249**: 69-87.
- Morita-Ishihara, T., Ogawa, M., Sagara, H., Yoshida, M., Katayama, E., and Sasakawa, C. (2006) *Shigella* Spa33 is an essential C-ring component of type III secretion machinery. *J Biol Chem* **281**: 599-607.
- Mota, L.J., Journet, L., Sorg, I., Agrain, C., and Cornelis, G.R. (2005a) Bacterial injectisomes: needle length does matter. *Science* **307**: 1278.
- Mota, L.J., Sorg, I., and Cornelis, G.R. (2005b) Type III secretion: the bacteria-eukaryotic cell express. *FEMS Microbiol Lett* **252**: 1-10.
- Mueller, C.A., Broz, P., Muller, S.A., Ringler, P., Erne-Brand, F., Sorg, I., Kuhn, M., Engel, A., and Cornelis, G.R. (2005) The V-antigen of *Yersinia* forms a distinct structure at the tip of injectosome needles. *Science* **310**: 674-676.
- Neves, B.C., Mundy, R., Petrovska, L., Dougan, G., Knutton, S., and Frankel, G. (2003) CesD2 of enteropathogenic *Escherichia coli* is a second chaperone for the type III secretion translocator protein EspD. *Infect Immun* **71**: 2130-2141.
- Neyt, C., and Cornelis, G.R. (1999a) Insertion of a Yop translocation pore into the macrophage plasma membrane by *Yersinia enterocolitica*: requirement for translocators YopB and YopD, but not LcrG. *Mol Microbiol* **33**: 971-981.

- Neyt, C., and Cornelis, G.R. (1999b) Role of SycD, the chaperone of the Yersinia Yop translocators YopB and YopD. *Mol Microbiol* **31**: 143-156.
- Nikolaus, T., Deiwick, J., Rappl, C., Freeman, J.A., Schroder, W., Miller, S.I., and Hensel, M. (2001) SseBCD proteins are secreted by the type III secretion system of Salmonella pathogenicity island 2 and function as a translocon. *J Bacteriol* **183**: 6036-6045.
- Nilles, M.L., Williams, A.W., Skrzypek, E., and Straley, S.C. (1997) Yersinia pestis LcrV forms a stable complex with LcrG and may have a secretion-related regulatory role in the low-Ca<sup>2+</sup> response. *J Bacteriol* **179**: 1307-1316.
- Nilles, M.L., Fields, K.A., and Straley, S.C. (1998) The V antigen of Yersinia pestis regulates Yop vectorial targeting as well as Yop secretion through effects on YopB and LcrG. *J Bacteriol* **180**: 3410-3420.
- Noguera-Obenza, M., Ochoa, T.J., Gomez, H.F., Guerrero, M.L., Herrera-Insua, I., Morrow, A.L., Ruiz-Palacios, G., Pickering, L.K., Guzman, C.A., and Cleary, T.G. (2003) Human milk secretory antibodies against attaching and effacing Escherichia coli antigens. *Emerg Infect Dis* **9**: 545-551.
- Ogino, T., Ohno, R., Sekiya, K., Kuwae, A., Matsuzawa, T., Nonaka, T., Fukuda, H., Imajoh-Ohmi, S., and Abe, A. (2006) Assembly of the type III secretion apparatus of enteropathogenic Escherichia coli. *J Bacteriol* **188**: 2801-2811.
- Page, A.L., Fromont-Racine, M., Sansonetti, P., Legrain, P., and Parsot, C. (2001) Characterization of the interaction partners of secreted proteins and chaperones of Shigella flexneri. *Mol Microbiol* **42**: 1133-1145.
- Pallen, M.J., Francis, M.S., and Futterer, K. (2003) Tetratricopeptide-like repeats in type-III-secretion chaperones and regulators. *FEMS Microbiol Lett* **223**: 53-60.
- Parsot, C., Hamiaux, C., and Page, A.L. (2003) The various and varying roles of specific chaperones in type III secretion systems. *Curr Opin Microbiol* **6**: 7-14.
- Perry, R.D., Harmon, P.A., Bowmer, W.S., and Straley, S.C. (1986) A low-Ca<sup>2+</sup> response operon encodes the V antigen of Yersinia pestis. *Infect Immun* **54**: 428-434.
- Pettersson, J., Holmstrom, A., Hill, J., Leary, S., Frithz-Lindsten, E., von Euler-Matell, A., Carlsson, E., Titball, R., Forsberg, A., and Wolf-Watz, H. (1999) The V-antigen of Yersinia is surface exposed before target cell contact and involved in virulence protein translocation. *Mol Microbiol* **32**: 961-976.
- Picking, W.L., Nishioka, H., Hearn, P.D., Baxter, M.A., Harrington, A.T., Blocker, A., and Picking, W.D. (2005) IpaD of Shigella flexneri is independently required for regulation of Ipa protein secretion and efficient insertion of IpaB and IpaC into host membranes. *Infect Immun* **73**: 1432-1440.
- Price, S.B., Leung, K.Y., Barve, S.S., and Straley, S.C. (1989) Molecular analysis of lcrGVH, the V antigen operon of Yersinia pestis. *J Bacteriol* **171**: 5646-5653.
- Price, S.B., Cowan, C., Perry, R.D., and Straley, S.C. (1991) The Yersinia pestis V antigen is a regulatory protein necessary for Ca<sup>2+</sup>-dependent growth and maximal expression of low-Ca<sup>2+</sup> response virulence genes. *J Bacteriol* **173**: 2649-2657.
- Rosqvist, R., Forsberg, A., and Wolf-Watz, H. (1991) Intracellular targeting of the Yersinia YopE cytotoxin in mammalian cells induces actin microfilament disruption. *Infect Immun* **59**: 4562-4569.
- Rosqvist, R., Magnusson, K.E., and Wolf-Watz, H. (1994) Target cell contact triggers expression and polarized transfer of Yersinia YopE cytotoxin into mammalian cells. *Embo J* **13**: 964-972.
- Sarker, M.R., Neyt, C., Stainier, I., and Cornelis, G.R. (1998a) The Yersinia Yop virulon: LcrV is required for extrusion of the translocators YopB and YopD. *J Bacteriol* **180**: 1207-1214.
- Sarker, M.R., Sory, M.P., Boyd, A.P., Iriarte, M., and Cornelis, G.R. (1998b) LcrG is required for efficient translocation of Yersinia Yop effector proteins into eukaryotic cells. *Infect Immun* **66**: 2976-2979.
- Schoehn, G., Di Guilmi, A.M., Lemaire, D., Attree, I., Weissenhorn, W., and Dessen, A. (2003) Oligomerization of type III secretion proteins PopB and PopD precedes pore formation in Pseudomonas. *Embo J* **22**: 4957-4967.
- Sekiya, K., Ohishi, M., Ogino, T., Tamano, K., Sasakawa, C., and Abe, A. (2001) Supermolecular structure of the enteropathogenic Escherichia coli type III secretion system and its direct interaction with the EspA-sheath-like structure. *Proc Natl Acad Sci U S A* **98**: 11638-11643.
- Shaw, R.K., Daniell, S., Ebel, F., Frankel, G., and Knutton, S. (2001) EspA filament-mediated protein translocation into red blood cells. *Cell Microbiol* **3**: 213-222.
- Skrzypek, E., and Straley, S.C. (1993) LcrG, a secreted protein involved in negative regulation of the low-calcium response in Yersinia pestis. *J Bacteriol* **175**: 3520-3528.
- Skrzypek, E., and Straley, S.C. (1995) Differential effects of deletions in lcrV on secretion of V antigen, regulation of the low-Ca<sup>2+</sup> response, and virulence of Yersinia pestis. *J Bacteriol* **177**: 2530-2542.
- Sory, M.P., and Cornelis, G.R. (1994) Translocation of a hybrid YopE-adenylate cyclase from Yersinia enterocolitica into HeLa cells. *Mol Microbiol* **14**: 583-594.



- Tamano, K., Aizawa, S., Katayama, E., Nonaka, T., Imajoh-Ohmi, S., Kuwae, A., Nagai, S., and Sasakawa, C. (2000) Supramolecular structure of the Shigella type III secretion machinery: the needle part is changeable in length and essential for delivery of effectors. *Embo J* **19**: 3876-3887.
- Tardy, F., Homble, F., Neyt, C., Wattiez, R., Cornelis, G.R., Ruyschaert, J.M., and Cabiiaux, V. (1999) Yersinia enterocolitica type III secretion-translocation system: channel formation by secreted Yops. *Embo J* **18**: 6793-6799.
- Taylor, K.A., O'Connell, C.B., Luther, P.W., and Donnenberg, M.S. (1998) The EspB protein of enteropathogenic Escherichia coli is targeted to the cytoplasm of infected HeLa cells. *Infect Immun* **66**: 5501-5507.
- Taylor, K.A., Luther, P.W., and Donnenberg, M.S. (1999) Expression of the EspB protein of enteropathogenic Escherichia coli within HeLa cells affects stress fibers and cellular morphology. *Infect Immun* **67**: 120-125.
- Tran Van Nhieu, G., Ben-Ze'ev, A., and Sansonetti, P.J. (1997) Modulation of bacterial entry into epithelial cells by association between vinculin and the Shigella IpaA invasin. *Embo J* **16**: 2717-2729.
- Tran Van Nhieu, G., Caron, E., Hall, A., and Sansonetti, P.J. (1999) IpaC induces actin polymerization and filopodia formation during Shigella entry into epithelial cells. *Embo J* **18**: 3249-3262.
- Tucker, S.C., and Galan, J.E. (2000) Complex function for SicA, a Salmonella enterica serovar typhimurium type III secretion-associated chaperone. *J Bacteriol* **182**: 2262-2268.
- Turbyfill, K.R., Mertz, J.A., Mallett, C.P., and Oaks, E.V. (1998) Identification of epitope and surface-exposed domains of Shigella flexneri invasion plasmid antigen D (IpaD). *Infect Immun* **66**: 1999-2006.
- van der Goot, F.G., Tran van Nhieu, G., Allaoui, A., Sansonetti, P., and Lafont, F. (2004) Rafts can trigger contact-mediated secretion of bacterial effectors via a lipid-based mechanism. *J Biol Chem* **279**: 47792-47798.
- Wainwright, L.A., and Kaper, J.B. (1998) EspB and EspD require a specific chaperone for proper secretion from enteropathogenic Escherichia coli. *Mol Microbiol* **27**: 1247-1260.
- Walker, K.A., and Miller, V.L. (2004) Regulation of the Ysa type III secretion system of Yersinia enterocolitica by YsaE/SycB and YsrS/YsrR. *J Bacteriol* **186**: 4056-4066.
- Wattiau, P., Bernier, B., Deslee, P., Michiels, T., and Cornelis, G.R. (1994) Individual chaperones required for Yop secretion by Yersinia. *Proc Natl Acad Sci U S A* **91**: 10493-10497.
- West, N.P., Sansonetti, P., Mounier, J., Exley, R.M., Parsot, C., Guadagnini, S., Prevost, M.C., Prochnicka-Chalufour, A., Delepierre, M., Tanguy, M., and Tang, C.M. (2005) Optimization of virulence functions through glucosylation of Shigella LPS. *Science* **307**: 1313-1317.
- Wolff, C., Nisan, I., Hanski, E., Frankel, G., and Rosenshine, I. (1998) Protein translocation into host epithelial cells by infecting enteropathogenic Escherichia coli. *Mol Microbiol* **28**: 143-155.
- Yip, C.K., Finlay, B.B., and Strynadka, N.C. (2005) Structural characterization of a type III secretion system filament protein in complex with its chaperone. *Nat Struct Mol Biol* **12**: 75-81.
- Zobiack, N., Rescher, U., Laarmann, S., Michgehl, S., Schmidt, M.A., and Gerke, V. (2002) Cell-surface attachment of pedestal-forming enteropathogenic E. coli induces a clustering of raft components and a recruitment of annexin 2. *J Cell Sci* **115**: 91-98.
- Zurawski, D.V., and Stein, M.A. (2004) The SPI2-encoded SseA chaperone has discrete domains required for SseB stabilization and export, and binds within the C-terminus of SseB and SseD. *Microbiology* **150**: 2055-2068.

## C Acknowledgments

**Prof. Dr. Guy Cornelis** thank you for your continuous support and your enthusiasm about my project. I am grateful for your trust in my abilities and your advice whenever the project was in a difficult phase. You had always time to discuss and to share your broad knowledge with me.

**Catherine Müller** thank you for the excellent and successful collaboration that we had. I had a lot of fun working and discussing with you, developing new “working hypotheses” for the tip complex. I hope we will continue like this and finish another great story.

**Dr. Luis Jaime Mota** and **Dr. Isabel Sorg** thank you both for discussions, the time you took to help me with my project and all the practical help with experiments in the lab.

**Marina Kuhn** thank you for your friendship and all the support you gave me during my diploma and the PhD.

I would also like to thank all the past and present members of the lab for the nice atmosphere, all the laughs and the help you provided: Marlise Amstutz, Emilie Clément, Dr. Geertrui Denecker, Andreas Diepold, Dr. Gottfried Eisner, Dr. Mario Feldmann, Chantal Fiechter, Franziska Fischer, Viola Huschauer, Dr. Laure Journet, Michel Letzelter, Silke Lützelschwab, Yvonne Lussi, Manuela Mally, Kerstin Maylandt, Salome Meyer, Cécile Pfaff, Dr. Nadine Schracke, Dr. Hwain Shin, Jaqueline Stalder, Dr. Paul Troisfontaines and Steffi Wagner.

**Prof. Dr. Andreas Engel** thank you for your support and your interest in type III secretion systems. I appreciate all the time you took to discuss with us and provide input for the project.

**Dr. Shirley Müller**, **Dr. Philippe Ringler** and **Françoise Erne-Brand** thank you for the wonderful microscopy work you did. It was a pleasure to work with you and I hope you are still motivated to see some more “needles” in the future.

**Dr. Myriam Duckely** and **Kitaru Suda** thank you for the knowledge you shared about membrane proteins and for the time you took to help me with my experiments.

Thanks to all the present and former members of the 4<sup>th</sup> floor for the nice and professional atmosphere.

**Markus Dürrenberger**, **Vesna Oliveri** and **Ursula Sauder** thank you for providing the ZMB facilities.

**Dr. Ina Attree** and **Dr. Julien Gouré** thank you for the great collaboration we had and the knowledge and motivation you shared with me. I had a lot of fun in Grenoble and learned all the secrets of “hemolysis”.

Last but not least, I would like to thank my family and especially my girlfriend Daniela for their support during my PhD and for all their encouragement. Without your help I would have not made it.

## Curriculum vitae

### Personal information

Surname/ First name **BROZ Petr**  
Address Rixheimerstrasse 16, 4055 Basel  
Telephone 076 477 43 49  
E-mail petr.broz@stud.unibas.ch  
Nationality Swiss  
Date and place of birth 30.12.1977 in Prague / CZ



### Occupational field

**Molecular Microbiologist**

### Education and work experience

Dates	December 2002 to now
Title of qualification awarded	<b>PhD, mark 5.5</b> magna cum laude
Principal subjects	Molecular Microbiology/ Microbial Pathogenesis
Name and address of employer	Department of Microbiology, Biozentrum, University of Basel, 50-70 Klingelbergstrasse, 4056 Basel, Switzerland
Supervisor	Prof. Dr. Guy Cornelis
Subject	<i>Functional and structural characterization of the Yersinia enterocolitica type III secretion translocon</i>
Dates	September 1997 to October 2002
Title of qualification awarded	<b>Diplom für Biologie II, mark: 5.5</b>
Name and type of organisation providing education and training	University of Basel, Switzerland
Minor Subject	Molecular Microbiology/ Microbial Pathogenesis
Dates	1993 to 1996
Title of qualification awarded	<b>Certificate of Matura type B (latin)</b>

### Technical skills

Molecular Biology	Cloning, DNA purification and analysis, Allelic exchange in bacteria
Biochemistry	Protein expression and purification, HPLC, Protein analysis (SDS-PAGE, Western blot, Co-Immunoprecipitation, Overlay, pull-down techniques), Lipid vesicle preparation, Gradient centrifugation
Cell biology	Cell culture, transfection, cell infection assays, Immunofluorescence
Other	Electron microscopy, Immunogold labelling, TLC of lipids

## Teaching experience

Dates	Activity
December 2003 to Juli 2004	Supervision of trainee
2002-2006 (one week per year)	Teaching assistantship in practical courses at the Biozentrum der Universität Basel
October 2003 to March 2004	Tutoring of first semester biology students (certificate)

## Publications

**Broz P.\***, Mueller C.A.\*, Müller S.A., Ringler P., Erne-Brand F., Sorg I., Kuhn M., Engel A., and Cornelis G.R. (2005). The V-antigen of *Yersinia* Forms a Distinct Structure at the Tip of Injectisome Needles. **Science** 310: 674-676

*\*These authors contributed equally to the work*

**Broz P.\***, Goure J.\*, Attree O., Cornelis G.R., and Attree I. (2005). Protective Anti-V Antibodies Inhibit *Pseudomonas* and *Yersinia* Translocon Assembly within Host Membranes. **Journal of Infectious Diseases** 192:218-25

*\*These authors contributed equally to the work*

Journet L., Agrain C., **Broz P.**, and Cornelis G.R. (2003). The Needle Length of Bacterial Injectisomes is Determined by a Molecular Ruler. **Science** 302: 1757-60.

## Posters

**Broz P.**, Mueller C.A., Müller S.A., Engel A., and Cornelis G.R. (2006). The V-antigen of *Yersinia* Forms a Distinct Structure at the Tip of Injectisome Needles. **Frontiers in Bio-Imaging 2006**, Basel, Switzerland, 12/05-13/05.

Mueller C.A., **Broz P.**, Müller S.A., Engel A., and Cornelis G.R. (2006). The V-antigen of *Yersinia* Forms a Distinct Structure at the Tip of Injectisome Needles. **Swiss Society of Microbiology (SSM) Congress**, Lausanne, Switzerland, 07/03-08/03.

**Broz P.**, Mueller C.A., Müller S.A., Engel A., and Cornelis G.R. (2005). The V-antigen of *Yersinia* Forms a Distinct Structure at the Tip of Injectisome Needles. **7<sup>th</sup> International EMBL PhD Symposium**, EMBL Heidelberg, Germany, 01-03/12. *Awarded 1st poster prize.*

**Broz P.**, Goure J., Chami M., Attree I., and Cornelis G.R. (2005) Protective anti-LcrV antibodies inhibit *Yersinia enterocolitica* translocon assembly within host membranes (2005. **Swiss Society of Microbiology (SSM) Congress**, Geneva, Switzerland, 31/03-01/04.

Journet L., Agrain C., **Broz P.**, and Cornelis G.R. (2004). The needle length of bacterial injectisomes is determined by a molecular ruler. **Swiss Society of Microbiology (SSM) Congress**, Lugano, Switzerland. *Awarded 1st poster prize.*

**Broz P.**, Cornelis G.R. (2003). Characterization of the YopBD translocation pore of *Yersinia enterocolitica*. **EMBO Lecture Course, Cellular and molecular biology of membranes**, Cargèse, Corsica, France, 09/06-21/06.



## Talks

**Broz P.**, Mueller C.A., Müller S.A., Ringler P., Erne-Brand F., Sorg I., Kuhn M., Engel A., and Cornelis, G.R. (2005). Protein V, the Protective Antigen Against Plague, is Located at the Tip of the Injectisome. **Biozentrum Symposium 2005**, St. Chrischona, Switzerland, 21/10/2005

**Broz P.**, Journet L., Agrain C., and Cornelis, G.R. (2004). YscP. The key component of the *Yersinia enterocolitica* Injectisome. **Vth Workshop on Pore-forming Toxins**, Mainz, Germany, 11/10/2004

**Broz P.**, and Cornelis, G.R. (2004). Biochemical Analysis of the Translocators YopB and YopD in *Yersinia enterocolitica*. CEA, Grenoble, France, 23/9/2004

## Language skills

German	Native speaker
English	Fluent
French	Good knowledge
Czech	Mother tongue, fluent

## Additional experience

Dates	Activity
January 2000 to June 2000	Offiziersschule der Schweizerischen Armee in Dailly / VS
Juli 2000 to September 2000	Praktischer Dienst bei Fest RS 259 in Mels / SG

## Interests

sports (Karate, hiking)  
travelling, foreign cultures  
books, cinema

## References

**Professor Guy R. Cornelis**

Biozentrum, University of Basel  
Klingelbergstrasse 50/70  
4056 Basel  
Switzerland  
guy.cornelis@unibas.ch

**Dr. Luis Jaime Mota**

Centre for Molecular Microbiology and Infection, Division of Investigative Sciences  
Flowers Building, South Kensington Campus  
Imperial College London, London SW7 2AZ  
England  
j.mota@imperial.ac.uk

**Dr. Laure Journet**

ESBS UMR 7175  
Récepteurs et Protéines Membranaires  
Bd Sebastien Brand  
BP 10413  
67412 Illkirch CEDEX  
France  
journet@esbs.u-strasbg.fr